Inaugural dissertation

for

obtaining the doctoral degree

of the

Combined Faculty of Mathematics, Engineering and Natural Sciences

of the

Ruprecht - Karls - University

Heidelberg

Presented by

M.Sc. Nicole Yue Ling Giebel

born in: Usingen, Germany

Oral examination: 25th November 2022

Regulation of Wnt signalling by the deubiquitinase USP42 in adult stem cells and colorectal cancer

Referees:

Dr. Sergio Perez Acebrón

Prof. Dr. Thomas Holstein

Zusammenfassung

Der Wnt/β-catenin Signalweg ist essentiell für die Erhaltung von Stammzellen und Gewebehomöostase. Eine Fehlregulierung der Mechanismen kann zu Krankheiten führen, zum Beispiel zu verschiedenen Tumorerkrankungen. Zwei der wichtigsten negativen Wnt-Regulatoren in Stammzellen sind die E3-Ubiquitin-Protein-Ligasen ZNRF3 (Zinc And Ring Finger 3) und RNF43 (Ring Finger Protein 43). In gesunden Zellen ubiquitinieren sie die Wnt-Rezeptoren Frizzled und LRP5/6 (LDL receptor related protein 5/6), wodurch es zu deren Abbau kommt und dadurch der Wnt-Signalweg inhibiert wird. Da ZNRF3/RNF43 oft in Wnt-assoziierten Tumorzellen mutiert sind, wuchs das Interesse an der Forschung ihrer Regulationsmechanismen in den letzten Jahren an. Es ist bereits bekannt, dass die Interaktion mit R-spondin und LGR4/5/6 (Leucine Rich Repeat Containing G Protein-Coupled Receptor 4/5/6), der Aktivität von ZNRF3/RNF43 entgegenwirkt. Diese führt zur Auto-ubiquitinierung von ZNRF3/RNF43 und zu deren Internalisierung. Jedoch ist noch nicht erforscht, wie sie an der Plasmamembran stabilisiert werden. Im Rahmen dieses Projekts, erforschte ich die Rolle der Deubiquitinase USP42 als ein neuer ZNRF3/RNF43-Regulator, welcher die Auto-ubiquitinierung von ZNRF3/RNF43 wieder aufhebt. Mithilfe verschiedener Zellkulturtechniken und molekularbiologischer Methoden untersuchte ich die zugrunde liegenden Wirkmechanismen der Wnt-Inhibierung durch USP42. Durch meine durchgeführten Experimente konnte ich zeigen, dass USP42 ZNRF3/RNF43 deubiquitiniert und an der Plasmamembran stabilisiert, was wiederum zu einem erhöhten Frizzled- und LRP5/6-Proteinumsatz führt. Vor allem ist dieser Effekt von USP42 unabhängig von seiner Funktion in der frühen Stressantwort durch den p53-Signalwegs. Des Weiteren untersuchte ich die Rolle von USP42 in der Stammzellerneuerung und Tumorentwicklung. Dafür generierte ich Usp42 Knockout Dünndarm-Organoide der Maus. Der Verlust von Usp42 verbesserte die Überlebensrate der Organoide unter Entzug der Wachstumsfaktoren Wnt und R-spondin1.

Zusammen mit meinem Kollegen Anchel und unseren Kollaboratoren an der Genomics Core Facility (EMBL Heidelberg), konnte ich einen Eindruck darüber gewinnen, wie der Mangel an USP42 zu der Entwicklung und dem Fortschreiten von Tumorerkrangungen beiträgt. Zudem generierte ich eine HCT116 USP42 Knockout-Zelllinie, um die Auswirkungen des Verlusts von USP42 auf den Darmkrebs zu untersuchen. Zusammengefasst weisen meine Ergebnisse darauf hin, dass USP42 eine Hürde für die Proliferation und die epitheliale-mesenchymale Transition von Darmkrebs-Zellen darstellt.

Insgesamt liefert meine Arbeit eine neue Rolle von USP42 als negativer Regulator des Wnt-Signalwegs durch ZNR3/RNF43, unabhängig von seiner Funktion im p53-Signalweg.

.

Summary

The canonical Wnt signalling pathway is required for stem cell maintenance and tissue homeostasis, and its misregulation can lead to cancer. Two important negative regulators of Wnt signalling in stem cells are the E3 ubiquitin-protein ligases ZNRF3 and RNF43, which target the Wnt receptors Frizzled and LRP5/6 to degradation. Since ZNRF3/RNF43 are often mutated in Wnt-associated cancers, research on how they are regulated has gained more attention in recent years. It has been shown that binding to R-spondin and LGR4/5/6 antagonises ZNRF3/RNF43, leading to their auto-ubiquitination and internalisation. However, how ZNRF3/RNF43 are stabilised at the plasma membrane remains unknown. In this project, I identified the deubiquitinase USP42 as a novel negative regulator of Wnt signaling. Using different cell culture techniques and methods in molecular biology, I showed that USP42 interacts with and deubiquitinates ZNRF3/RNF43 at the plasma membrane. I also found that USP42 prevents the internalisation of ZNRF3/RNF43 upon binding to R-spondin and LGR, thereby inducing clearance of the Wnt receptors Frizzled and LRP5/6. Furthermore, I investigated the USP42 roles in adult stem cells and cancer cells by generating Usp42 knockout mouse intestinal organoids and colorectal cancer cell lines. First, I found that loss of Usp42 promoted survival upon Wnt and R-spondin withdrawal in mouse intestinal stem cells, thereby phenocopying RNF43/ZNRF3 double knockout. Second, together with my colleague Anchel and our collaborators from the Genomics Core Facility (EMBL Heidelberg), I identified that USP42 functions as a roadblock for proliferation and epithelial-to-mesenchymal transition in colorectal cancer cells. In conclusion, my work uncovered a new role for USP42 in Wnt signalling as a regulator of ZNRF3/RNF43 with relevance in tissue homeostasis and cancer.

Contents

Abbreviations

APC	Adenomatous polyposis coli
ATP	Adenosine triphosphate
BMP	Bone morphogenetic protein
BSA	Bovine Serum albumin
CK1α	Casein kinase 1
Co-IP	Co-Immunoprecipitation
CRISPR/Cas9	Clustered regularly interspaced short palindromic repeats/caspase 9
DIR	Dishevelled interacting region
DMEM	Dulbecco's modified Eagle's medium
DMSO	Dimethyl sulfoxide
DNA	Deoxyribonucleic acid
Dnase	Deoxyribonuclease
dNTP	Deoxynucleotide triphosphate
DTT	Dithiothreitol
DUB	Deubiquitinating enzyme
Dvl	Dishevelled
EDTA	Ethylene glycol tetraacetate
EGF	Epidermal growth factor
EMT	epithelial-mesenchymal transition
FACS	Fluorescence activated cell sorting
FGF	Fibroblast growth factor
Fzd	Frizzled
GFP	Green fluorescent protein
GSK3β	Glycogen synthase kinase 3
HCT116	Human colorectal carcinoma cell line
HEK293T	Human embryonic kidney cell line
HRP	Horseradish peroxidase
KO	Knockout
LGR	Leucine-rich repeat containing G protein coupled receptor
LRP	Low density lipoprotein receptor-related protein
NLS	Nuclear localisation signal
PCP	Planar cell polarity
qRT-PCR	Quantitative real-time polymerase chain reaction
RNF43	Ring finger protein 43
RSPO	R-spondin
RT	Room temperature
SD	Standard deviation
SDS-PAGE	Sodium dodecylsulfate polyacrylamide gel electrophoresis
sgRNA	Single guide RNA
siRNA	Small interfering RNA
TEMED	Tetramethyl ethylene diamine
TGF	Transforming growth factor

USP42	Ubiquitin specific peptidase 42
WT	Wild-type
ZNRF3	Zinc and ring finger 3

1. Introduction

1.1 Wnt signalling pathways

The Wnt/β-catenin signalling pathway is highly conserved pathway which plays an important role in embryonic development and stem cell homeostasis (Holstein 2012, Niehrs 2010). Misregulation of this pathway leads to different diseases, including neurodegenerative diseases such as Alzheimer's disease and Parkinson, Wnt-associated cancers (e.g. colorectal cancer) and bone defects (MacDonald 2009, Inestrosa and Arenas 2010, Nusse and Clevers 2012, Massink 2015, Bond 2016, Zhan *et al.* 2017, Matsumoto 2020, Salem 2020).

In the 1980s, the first Wnt ligand was discovered and was thought to induce mammary tumours (Nusse and Varmus 1982). Currently, there are 19 Wnt proteins known, which are categorised into 12 subfamilies (Niehrs 2012). Wnt proteins have a molecular weight of around 40 kDa, are rich in cysteins and are modified with lipids, such as the mono-unsaturated fatty acid palmitoleic acid, and n-glycosylation (Tanaka *et al.* 2002, Willert *et al.* 2003, Takada *et al.* 2006). These lipids are important for Wnt signalling and secretion (Willert *et al.* 2003). Wnt proteins mature in the endoplasmic reticulum and are modified by Porcupine, so that they can be secreted by binding to Evi/Wls (Kadowaki 1996, Bartscherer 2006, Herr *et al.* 2012). Because their post-translational modification make them hydrophobic, they are shuttled as cargo in extracellular vesicles, such as exosomes, or through cytonemes (Gross *et al.* 2012, Stanganello 2016). Once they are secreted, they can then bind to different Wnt receptors: Frizzled (Fzd), low-density lipoprotein receptors (LRP) or the receptor tyrosine kinase-like orphan receptor (ROR) (Najdi 2012, Niehrs 2012, Voloshanenko 2017). Depending on which Wnt receptor complex the Wnt ligand is binding to, it can activate either the canonical Wnt/β-catenin signalling pathway or the non-canonical planar cell polarity (PCP) and Wnt/Calcium pathway.

1.1.1 Wnt/β-catenin signalling pathway

The Wnt receptors Frizzled and LRP5/6 form a heterodimeric complex at the cell surface and bind canonical Wnt ligands, such as Wnt1, Wnt3, Wnt3a, Wnt7a/b, Wnt8a/b and Wnt10a/b (Najdi 2012). Frizzled proteins consist of a 7-transmembrane domain and have a cysteine-rich domain at its extracellular N-terminal (Bhanot *et al.* 1996). In the Wnt off state β-catenin binds to the scaffold proteins adenomatous polyposis coli (APC) and Axis inhibition protein 1 (Axin). There, it is phosphorylated by the serine/threonine kinases casein kinase 1α (CK1α) and the glycogen synthase kinase 3β (GSK3β) and ubiquitinated by Skp1-Cullin-F-box protein (SCF) β-TrCP in the cytoplasm, followed by proteasomal degradation (Winston *et al.* 1998, Liu *et al.* 1999).

Binding of Wnt ligands leads to the recruitment of the β-catenin destruction complex to the membrane and β-catenin ubiquitination is inhibited (Liu *et al.* 2002). Then, β-catenin accumulates in the cytoplasm and translocated to the nucleus where it forms a complex with TCF/LEF to activate transcription of Wnt target genes, for example LGR5/GPR49, DKK and c-myc (He 1998, Niida *et al.* 2004, Barker *et al.* 2007, Doumpas *et al.* 2019).

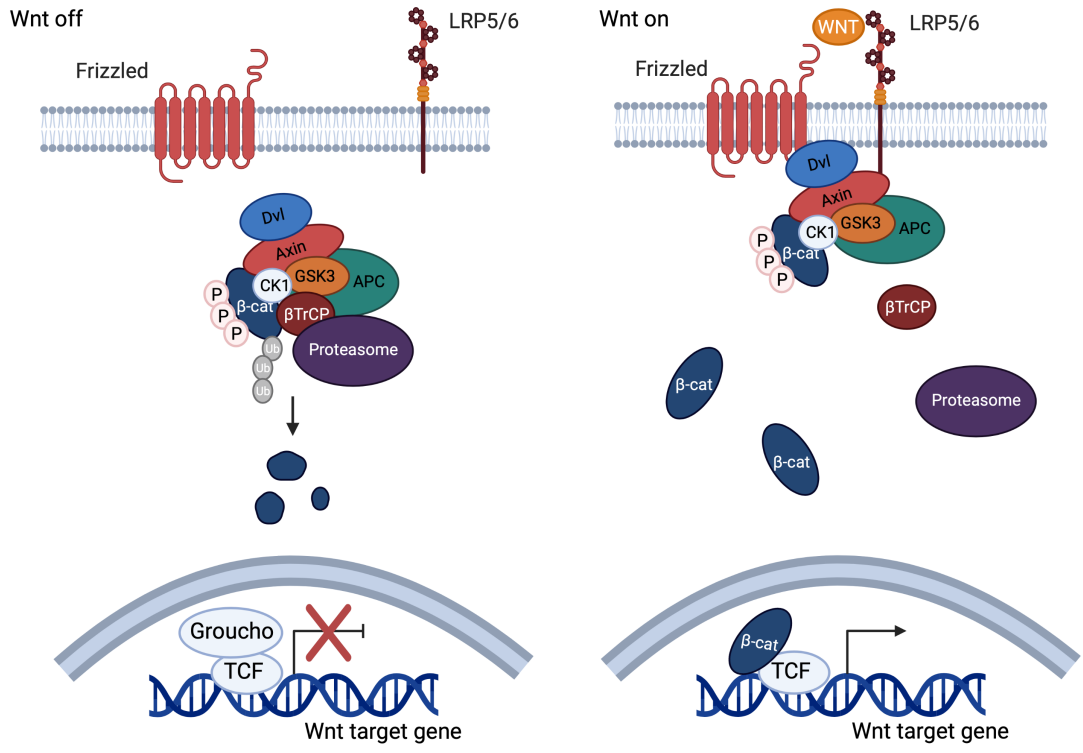

Figure 1.1: The canonical Wnt signalling pathway.
In the Wnt off state, β-catenin is phosphorylated by CK1 α and GSK3 β. Then, β-TrCP detects the phosphorylated β-catenin and ubiquitinates it, so that it will get degraded by the proteasome. When Wnt ligands bind to the Wnt receptor complex, the β-catenin destruction complex is bound to them at the membrane. β-catenin is not ubiquitinated anymore and accumulates in the cytoplasm, until it gets shuttled to the nucleus, where it activates the transcription of Wnt target genes. (Made with BioRender.)

1.1.2 β-catenin independent Wnt signalling

Besides the canonical Wnt signalling pathway, there are also two non-canonical Wnt pathways, which are the Wnt/PCP and the Wnt/Calcium pathway. They do not require β-catenin for signal transduction.

1.1.2.1 Wnt/PCP signalling

The Wnt/Planar cell polarity pathway is important for embryogenesis, epithelial polarisation, asymmetric cell division and migration (Humphries 2018). Planar cell polarity works through the asymmetric distribution of the PCP core group. This group consists of Frizzled, Vangl, Fmi/Celsr, Dishevelled, Prickle and Diego (Goodrich *et al.* 2011). They divide into two subgroups and position themselves on the opposite sides of a cell. Wnt5a is one of the non-canonical Wnt ligands which can active Wnt/PCP signalling (Gao 2011). Instead of binding to LRP5/6 as in the canonical Wnt signalling pathway, the Frizzled receptor binds to either ROR2 or inactive tyrosine-protein kinase 7 (PTK7). Subsequently, Dishevelled is recruited and activates downstream cascades (Nomachi *et al.* 2008). Abberant Wnt-PCP signalling increases cell motility an aggressiveness of metastatic melanoma and gastric cancer (Weeraratna *et al.* 2002, Kurayoshi 2006).

1.1.2.2 Wnt/Calcium signalling

The Wnt/Calcium is activated by Wnt ligands binding to the G-protein-coupled receptor Frizzled, together with the coreceptor Ror1/2 (Koval *et al.* 2011, Ho *et al.* 2012). This leads to the production of 1,4,5-tri-phosphate (IP3) and 1,2-diacylglycerol

(DAG) through the enzyme phospholipase C (PLC, De 2011). After forming a complex with Dishevelled and Axin, GSK3 phosphorylates Ror2 (De 2011). Then, IP3 releases Calcium^{2+} from the endoplasmic reticulum, which activates DAG (Slusarski *et al.* 1997, Kühl *et al.* 2000). This event leads to protein kinase C (PKC) activation and its downstream transcription factors NFκB and CREB (Sheldahl 1999).

1.1.3 Wnt signalling and its regulation in tissue homeostasis and disease

1.1.3.1 Wnt signalling in small intestine and tissue homeostasis

The canonical Wnt signalling pathway plays an important role in development and stem cell homeostasis (Koo *et al.* 2012). One of tissues depending on Wnt signalling for stem cell renewal is the intestinal stem cell niche. It is constantly renewed by stem cells localised in the intestinal crypts, whereas the more differentiated cells form the villus. The intestine is composed of different types of cells, including Lgr5+ stem cells and Paneth cells in the crypts, a transit amplifying zone and the villus containing enterocytes, tuft cells which are responsible for the immune reaction and enteroendocrine cells (Figure 1.2, Spit *et al.* 2018, Schneider *et al.* 2019, Beumer *et al.* 2020).

The transit amplifying cells originate from intestinal stem cells at the bottom of the crypt and differentiate to the epithelial cells of the villus (Barker *et al.* 2007). Throughout the villus and the intestinal crypt, there are several gradients of active signalling pathways (Madison *et al.* 2005, Barker *et al.* 2007, Shyer *et al.* 2015). The strongest Wnt signalling is found at the bottom of the intestinal crypt, together with BMP antagonists (Haramis *et al* 2004, Kosinski *et al.* 2007). The growth factors EGF and Wnt, as well the BMP antagonists Gremlin1 and Noggin, are produced by the subepithelial mesenchyme cells and inhibit BMP-dependent differentiation (Shyer *et al.* 2015). In addition, Paneth cells also secrete Wnt ligands, Notch and EGF (Tian *et al. 2015*). Contrary, BMP signalling increases towards the tip of the villi, as well as the Hedgehog signalling pathway (McCarthy *et al.* 2020). Together, the crosstalk between the pathways regulate tissue homeostasis.

The intestinal stem cells niche requires the growth factors Wnt and R-spondins (Park *et al.* 2018). R-spondins stabilise the Wnt receptors Frizzled and LRP5/6 by forming a

complex with LGR4/5/6 together with ZNRF3/RNF43 which are highly expressed at the bottom of the crypts (Farin *et al.* 2012, Hao *et al.* 2012, Chen *et al.* 2013). ZNRF3 and its paralogue RNF43 are E3 ubiquitin-protein ligases which ubiquitinate the Wnt receptors Frizzled and LRP5/6 (Figure 1.3). For the interaction with Frizzled receptors, they are recruited by Dishevelled (Jiang *et al.* 2015). Upon ubiquitination through ZNRF3/RNF43, the Wnt receptors get internalised via ubiquitin-mediated endocytosis and degraded by the lysosome (Hao *et al.* 2012, Koo *et al.* 2012). When ZNRF3/RNF43 bind to R-spondin and LGR4/5/6, they auto-ubiquitinate and get internalised (Figure 1.4, (Kazanskaya *et al.* 2004 and 2008, Carmon *et al.* 2011, de Lau *et al.* 2011, Glinka *et al.* 2011 Xie *et al.* 2013, Zebisch and Jones 2015).

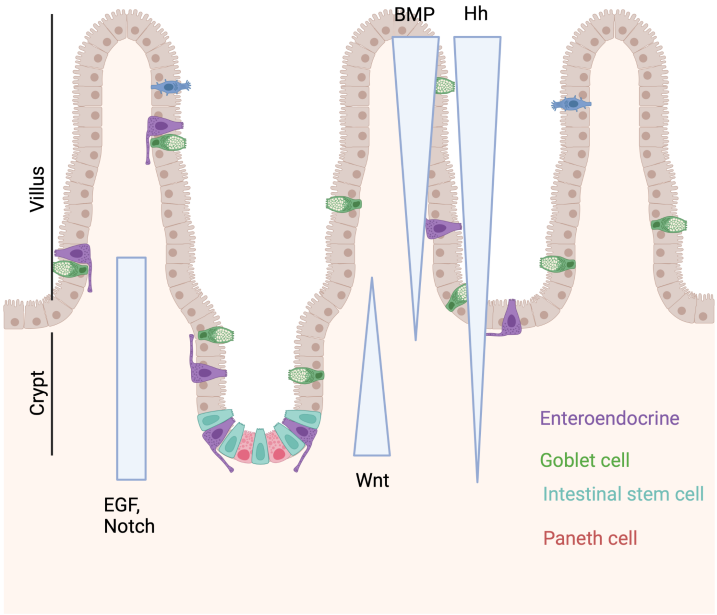

Figure 1.2: Scheme of the intestinal structure.
Indicated are the gradients of active signalling pathways and the different cells of the intestine. EGF and Notch signalling remain stable throughout the crypts and the transit amplifying zone. Since Paneth cells and subepithelial mesenchymal cells secrete Wnt, Wnt signalling peaks at the bottom of intestinal crypts. On the contrary, BMP signalling gradient is highest at the tip of the intestinal villi. (Made with BioRender.)

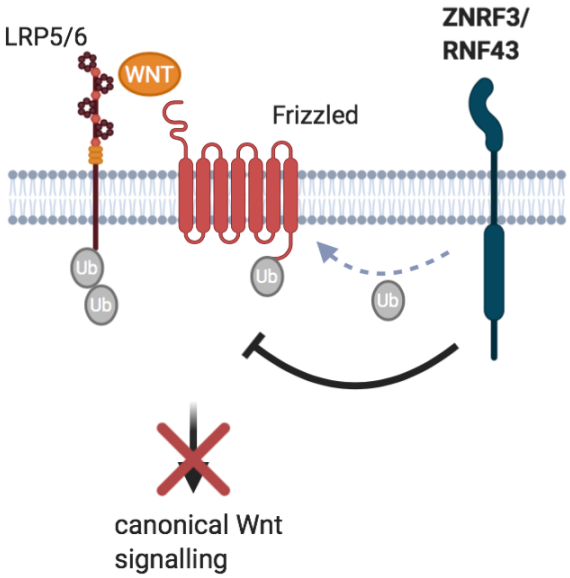

Figure 1.3: ZNRF3/RNF43 ubiquitinate the Wnt receptors Frizzled and LRP5/6.
ZNRF3/RNF43 are E3 ubiquitin-protein ligases that ubiquitinate the Wnt receptors Frizzled and LRP5/6. This leads to the internalisation of LRP5/6 and Frizzled, thereby Wnt signalling is inhibited. (Made with BioRender.)

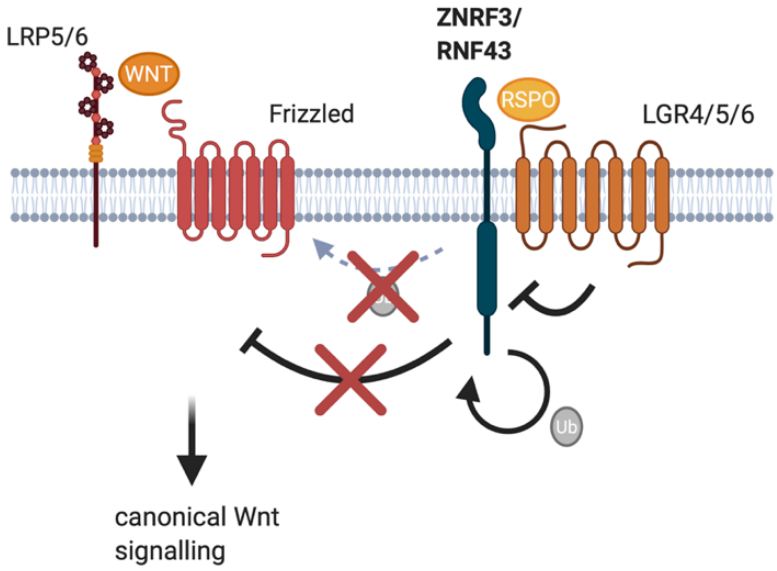

Figure 1.4: R-spondin and LGR antagonise ZNRF3/RNF43 in Wnt signalling.
Upon binding to R-spondin and LGR4/5/6, ZNRF3/RNF43 auto-ubiquitinate and get internalised. Thus, the Wnt receptors Frizzled and LRP5/6 are stabilised and Wnt signalling is potentiated. (Made with BioRender.)

1.1.3.2 Canonical Wnt Signalling in Cancer

Aberrant Wnt signalling has been detected in several types of cancer. This is caused by mutations in genes encoding for proteins of the Wnt signalling pathway, which may lead to impaired functions, the inactivation or amplification of a protein. Many cancer types show an increased Wnt/β-catenin activity. This is achieved by mutations enhancing positive Wnt regulators, such as β-catenin or R-spondin (Morin *et al.* 1997, Seshagiri *et al.* 2012, Han *et al.* 2017), or down regulating negative Wnt regulators involved in the β-catenin destruction complex or the regulation at the receptor level. Negative regulators often mutated in cancer are for example APC and Axin2 in colorectal cancer (Morin *et al.* 1997, Liu *et al.* 2000), Axin1 in hepatocellular carcinoma (Satoh *et al.* 2000) and ZNRF3/RNF43 in gastric and colorectal cancer (Koo *et al.* 2012, Nanki *et* al 2018). They promote cell proliferation and survival of the indicated cancers.

In *silico* analysis (cBioPortal MSKCC, Nat Med 2017) of Wnt genes mutated across several cancer types has revealed that colorectal cancer harbours 84% of alterations, followed by Small Bowel Cancer (45%), Ampullary Cancer (43%) and Adrenocortical Carcinoma (32%). The genes analysed were APC, AXIN1, AXIN2, DVL2, GSK3B, CTNNB1 (β-catenin) and RNF43.

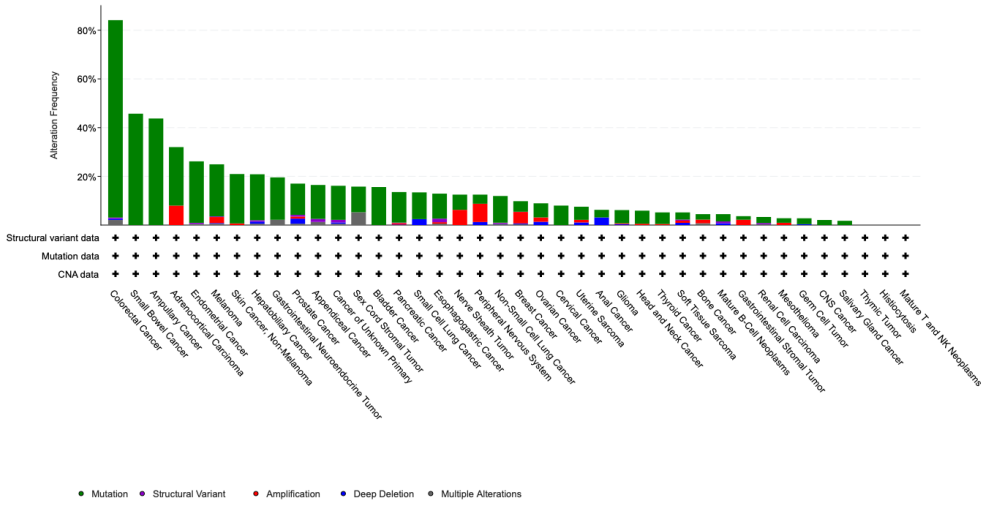

Figure 1.5: Proteins of the Wnt signalling pathway are mutated in different types of cancer.

cBioPortal analysis of the genes encoding for APC, Axin1/2, Dishevelled 2, GSK3, β-catenin and RNF43 in different cancer types.

1.2 Ubiquitination

Ubiquitin is a small molecule, consisting of 76 amino acids, which acts as a tag in the reversible post-translational modification of proteins (Schnell and Hicke 2003). Depending on which type of ubiquitination is marking a protein, the target can either get degraded by the proteasome or lysosome, change its activity, subcellular localisation and interaction affinity. The ubiquitin molecule is covalently bound to the lysine residues of a substrate protein. During this process, there are three common types of enzymes required. First, the E1 ubiquitin-activating enzyme acts as a catalyst in binding ubiquitin dependent on ATP (Pickart 2001). Then, the activated ubiquitin is transferred to the E2 ubiquitin-conjugating enzyme, before it gets ligated to the substrate by the E3 ubiquitin-protein ligase.

There are different types of ubiquitinations, such as mono- or poly-ubiquitination. Monoubiquitylation is thought to regulate processes associated with DNA repair, endocytosis or membrane trafficking (Ikeda and Dikic 2008). On the other hand, polyubiquitination is defined by the formation of ubiquitin chains on the substrate molecule. These chains usually start with a mono-ubiquitination of the substrate and are elongated by binding of an ubiquitin molecule to one of the 7 N-terminal lysine (K) residues K6, K11, K27, K29, K33, K48, K63 or M1 (reviewed in Haglund *et al.* 2003, Kim *et al.* 2007). Hence, K48-ubiquitin chains target proteins for proteasomal degradation (Finley *et al.* 1994). Regarding the composition of ubiquitin chains, there are the homotypic chains formed by linking ubiquitin molecules by the same type of lysine residue (reviewed in Haglund *et al.* 2003). Then, there are also mixed chains with linkages between different lysine residues and generating branching of the ubiquitin chains. Finally, the ubiquitin chains can also incorporate ubiquitin-like modifiers, such as SUMO or NEDD8 (Kamitani *et al.* 1997, van Wijk *et al.* 2011).

There are three types of E3 ubiquitin ligases, which differ by the mechanism of ubiquitination. Really interesting new gene (RING) E3 ligases bring their substrate close to the E2 ligase and can directly transfer the ubiquitin to its substrate (Ozkan *et al.* 2005), whereas Homologous to E6AP C-Terminus (HECT) and RING between RING

(RBR) type E3 ligases take the ubiquitin from the E2 ligase, before tagging its substrate (Huibregste *et al.* 1995, Scheffner *et al.* 1995, Wenzel *et al.* 2011).

1.2.1 Ubiquitination regulating protein stability in Wnt signalling

There are numerous ways to regulate signalling pathways by post-translational modifications. One common mechanism is ubiquitination, which is reversible upon interacting with the substrate-specific deubiquitinating enzyme (DUB) (Takahashi *et al.* 2020). Different ubiquitinating enzymes have been identified to interact and ubiquitinate Wnt signalling components. Here, interactions between canonical Wnt proteins and E3 ligases leading to protein destabilisation and degradation will be listed (Figure 1.6).

Frizzled and LRP: It has been shown that the Wnt receptors LRP5/6 and Frizzled are ubiquitinated by the RING-type E3 ligases ZNRF3 and RNF43 (Hao *et al.* 2012, Koo *et al.* 2012).

APC: The β-catenin destruction complex component APC is targeted by the E3 ligase RNF61, which is also known as the Makorin Ring Finger Protein 1 (MKRN1, Lee *et al.* 2018). Lee *et al.* 2018 demonstrate that MKRN1 binds to APC's Armadillo repeats.

Axin: Four E3 ubiquitin ligases have been identified which target Axin for proteasomal degradation. RNF146 is known to ubiquitinate previously poly-ADP-ribosylated (PARsylated) Axin (Callow *et al.* 2011, Zhang *et al.* 2011). Axin1/2 are PARsylated by the tankyrases TNKS1/2 (Huang *et al.* 2009). Also, the Seven in absentia homolog 1/2 (Siah1/2) ubiquitinate Axin by binding to the VxP motif of the GSK3-binding domain of Axin. Hence, the interaction between Siah and Axin can be prevented by the binding of GSK3 to Axin (Huang *et al.* 2009). These ubiquitination mechanisms lead to Axin degradation and therefore promote Wnt signalling. Then, there is the HECT-type ubiquitin ligase Smad ubiquitination regulatory factor 1 (Smurt1), which does not induce proteolytic degradation of Axin (Fei *et al.* 2013). Instead, it negatively regulates Wnt signalling by inhibiting the binding to LRP5/6.

CK1: CK1α is bound at its N-terminal and ubiquitinated by CUL4-RBX1-DDB1-CRBN (CRL4, Krönke *et al.* 2015).

Dvl: Several E3 ligases have been reported to target Dishevelled for degradation. Dishevelled is ubiquitinated by the RING-type E3 ubiquitin ligase membrane-associated RING-CH2 (March2) in *Xenopus*, which leads to lysosomal degradation of Dishevelled (Lee *et al.* 2018a). RING type E3 ligase Malin ubiquitinates Dishevelled 2 with K48- and K63- linked ubiquitin (Sharma *et al.* 2012). It is then degraded by the proteasome and by autophagy. Dishevelled 3 is ubiquitinated by the Cullin 3 ubiquitin ligase complex, together with Kelch-like 12 (KLHL12, Angers *et al.* 2006). Then, the HECT-containing NEDD4-like ubiquitin ligase ITCH ubiquitinates previously phosphorylated Dishevelled 1-3, which leads to the proteasomal degradation of Dishevelled (Wei *et al.* 2012). ITCH interacts with the DEP region of Dishevelled. NEDD4L also targets Dishevelled 2 for proteasomal degradation by linking ubiquitin K6, K27 and K29 (Ding *et al.* 2013).

GSK3: GSK3 has been shown to be ubiquitinated by Tumour Necrosis Factor (TNF) receptor-associated factor 6 (TRAF6, Ko *et al.* 2015). Ko *et al.* 2015 report that the N-terminal of GSK3 is required for the interaction with TRAF6.

β-catenin: Phosphorylation of β-catenin by CK1 and GSK3 leads to its ubiquitination and proteasomal degradation by β-TrCP (Liu *et al.* 1999). It has also been reported that Siah1 targets β-catenin at its Armadillo repeats for proteasomal degradation, which can be prevented by transducin beta-like 1 (TBL1, Dimitrova *et al.* 2010).

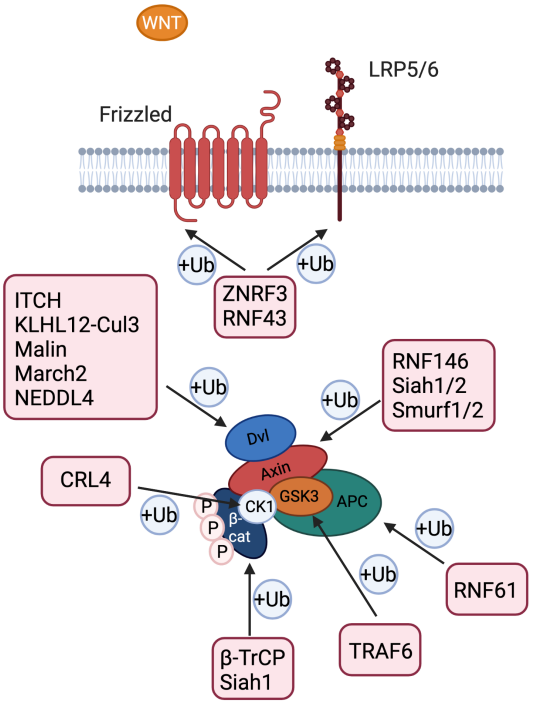

Figure 1.6: E3 ligases targeting canonical Wnt proteins for degradation.
Indicated with the red boxes are the known E3 ubiquitin ligases that target the components of the Wnt signalling pathway for proteasomal, lysosomal or autophagic degradation. They tag their substrate with different types of ubiquitin, such as mono-ubiquitination or the formation of ubiquitin chains. (Made with BioRender.)

1.2.2 ZNRF3 and RNF43

ZNRF3 and its paralogue RNF43 are E3 ubiquitin-protein ligases, which are known to ubiquitinate the Wnt receptors Frizzled and LRP5/6 and are antagonised by binding to the R-spondin/LGR complex (Peng *et al.* 2013, Zebisch *et al.* 2013). They belong to the family of RING-finger E3 ligases, containing an enzymatic RING-domain. The structures of ZNRF3 and RNF43 share similarities. Their genes encode an extracellular protease associated (PA) domain, a transmembrane domain and a Dishevelled interacting region (Jiang *et al.* 2015). They also contain a signal peptide, which translocates them to the cell membrane. It has been shown that the PA domain of RNF43 binds to R-spondin/LGR, but is not required for the inhibition of

canonical Wnt signalling in human cells (Radaszkiewicz and Bryja 2020). Also, they are targeted for degradation by SCF-β-TrCP (Ci *et al.* 2018).

ZNRF3 and RNF43 have been reported to play an important role in liver zonation by inhibiting hepatocyte proliferation (Planas-Paz *et al.* 2016, Annunziato *et al.* 2022), in oligodendrocyte maturation (Niu *et al.* 2021, Sun *et al.* 2021, reviewed in Annunziato *et al.* 2022) and in adrenal homeostasis (Basham *et al.* 2018). Hao *et al.* 2012 showed that loss of ZNRF3 can lead to impaired eye development and body axis duplication.

ZNRF3 is often mutated in adrenal cancers (Assié *et al.* 2014), liver (Belenguer *et al.* 2022) and thyroid cancer (Qiu *et al.* 2016), whereas RNF43 is mutated in colorectal cancer (Figure 1.7, Koo *et al.* 2012 and 2015, Giannakis *et al.* 2014), pancreatic (Jiang *et al.* 2013), endometrial (Giannakis *et al.* 2014), liver (Belenguer *et al.* 2022) and stomach cancer (Wang *et al.* 2014, Neumeyer *et al.* 2019). RNF43 has been reported to inhibit non-canonical Wnt5 signalling by ubiquitinating the receptor VANGL2 and negatively regulates ROR1/2 protein levels at the surface (Radaszkiewicz *et al.* 2021). This inhibits invasion of melanoma cells. In addition, RNF43 has been shown to ubiquitinate phosphorylated E-cadherin, thereby promoting epithelial-mesenchymal-transition (EMT) in lung adenocarcinoma (Zhang *et al.* 2019).

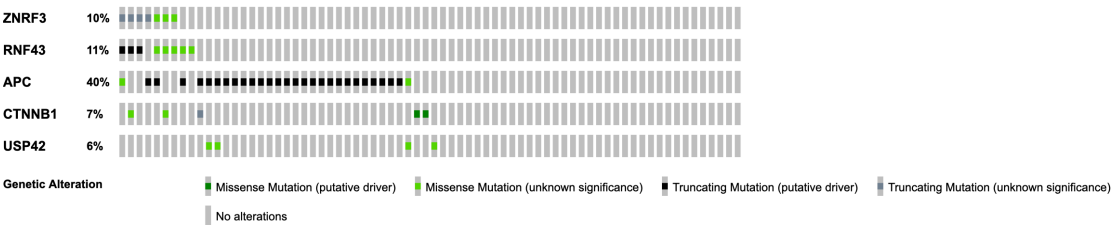

Figure 1.7: The negative Wnt signalling regulators APC, ZNRF3 and RNF43 are highly mutated in colorectal cancer.
cBioPortal analysis of mutations in the genes encoding for ZNRF3, RNF43, APC, β-catenin and USP42 in colorectal cancer (Genentech, Nature 2012).

1.3 Deubiquitinating enzymes

Deubiquitinating enzymes (DUB) are proteases that can reverse the ubiquitination of their substrate proteins. They are classified in two subfamilies: A) Cysteine proteases, B) Metallo-proteases. The first class consists of 7 types of deubiquitinating enzymes: 1) Ubiquitin-specific proteases (USP), ubiquitin C-terminal

hydrolase (UCH), ovarian tumor protease (OTU), Machado-Joseph disease (MDJ), MIU-containing novel DUB (MINDY), monocyte chemoattractant protein-induced protein-1 (MCPIP1) (reviewed in Harrigan *et al.* 2017).

The different types of deubiquitinating enzymes differ from catalytic and binding domains, as well as their affinity to cleave different ubiquitination links.
For example, MINDY deubiquitinating enzymes are selective for deubiquitinating K48-linked polyubiquitin chains (Rehman *et al.* 2016).

1.3.1 Deubiquitinating enzymes in canonical Wnt signalling

While ubiquitination by E3 ligases often leads to protein degradation, deubiquitination can reverse this effect and stabilise their substrate protein. Recent research has identified several deubiquitinating enzymes stabilising canonical Wnt proteins (Figure 1.8).

Frizzled: Frizzled has been shown to be deubiquitinated by and stabilised upon the interaction with USP6 and USP8 (Mukai *et al.* 2010, Madan *et al.* 2016, Chaugule *et al.* 2021). Non-functional deubiquitination of Frizzled by USP8 results in defects in skeletogenesis, in particular the differentiation from osteoprogenitors to osteoblasts (Chaugule *et al.* 2021).

LRP5/6: Ubiquitination of Lysin-1403 of LRP6 has been shown to stabilise and protect it from degradation in the endoplasmic reticulum (Abrami *et al.* 2008). By exiting the endoplasmic reticulum, the deubiquitination of this residue is required. Perrody *et al.* 2016 have found that USP19 is the deubiquitinating enzyme involved in this step.

APC: USP15 associated with the COP9 signalosome has been shown to stabilise APC (Huang *et al.* 2009b). They found that the COP9 signalosome recruits the β-catenin destruction complex, cullin-RING ubiquitin ligases and the proteasome to form a supercomplex and promote β-catenin degradation.

Axin: USP7 is the deubiquitinase which stabilises Axin, thereby inhibiting Wnt signalling (Ji *et al.* 2019). They bind through interaction with the TRAF region of Axin.

Dishevelled: CYLD has been shown to cleave K63 ubiquitin from the DIX domain of Dishevelled (Tauriello *et al.* 2010). Also, it has been revealed that USP14 deubiquitinates Dishevelled by interacting with its C-terminal regulatory domain of ubiquitination (Jung *et al.* 2013). Another deubiquitinase found to stabilise Dishevelled is USP4 (Zhou *et al.* 2016). They found that USP4 removes K63 from Dishevelled and impairs osteoblast differentiation. Finally, it has also been discovered that USP9X positively regulates canonical Wnt signalling by deubiquitinating Dishevelled 2 (Nielsen *et al.* 2019).

β-catenin: For β-catenin, six deubiquitinases have been found to interact with and to stabilise it: USP2a (Kim *et al.* 2018), USP4 (Yun *et al.* 2015), USP7 (Ma *et al.* 2014), USP9X (Yang *et al.* 2016), USP20 (Wu *et al.* 2018) and USP47 (Shi *et al.* 2015).

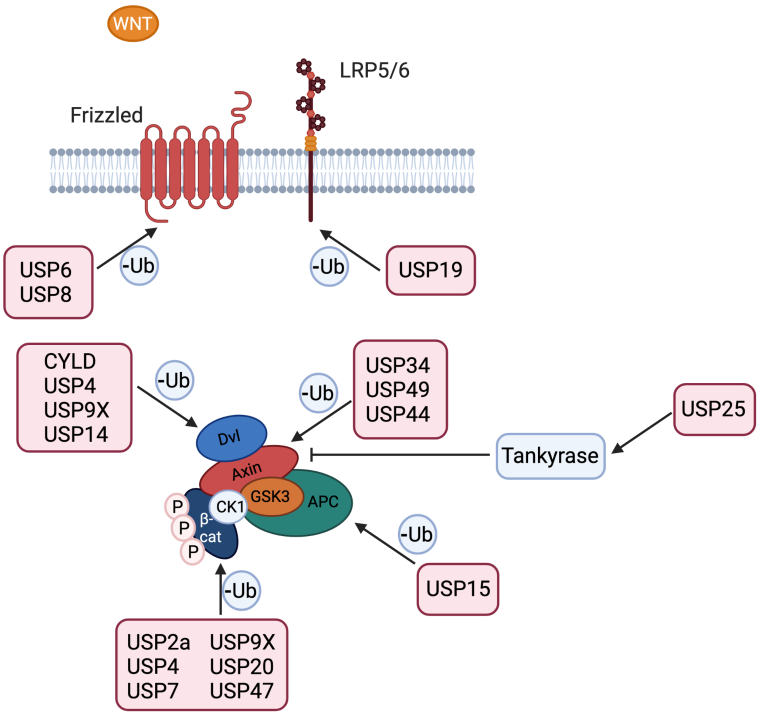

Figure 1.8: Deubiquitinating enzymes in canonical Wnt signalling
Here, known deubiquitinases stabilising the canonical Wnt components are indicated in the pink boxes. Deubiquitinating enzymes cleave one or more ubiquitin tags from their substrate. (Made with BioRender.)

1.3.2 USP42

Ubiquitin specific peptidase 42 is a deubiquitinating enzyme, which belongs to the DUB family USP. The protein structure consists of a conserved USP domain ranging from the residues 111 to 412 for its enzymatic activity, and it also contains predicted monopartite nuclear localisation signals (NLS) at its C-terminal for the import into the nucleus (Figure 1.9 and 1.10). Concerning the subcellular localisation, USP42 is mainly expressed in the nucleus (about 80-90%), whereas its cytosolic protein level is around 10-20% (Hock *et al.* 2014). In the human body, high USP42 protein levels are equally distributed throughout different tissues (https://v15.proteinatlas.org/ENSG00000106346-USP42/tissue). In contrast, the RNA level in the testis is 5 fold higher than in any other tissue as USP42 has been reported to play an important role in spermatogenesis (Kim *et al.* 2007).

Figure 1.9: The USP domain of USP42 is conserved throughout different species.
Multiple sequence alignment of USP42 in the frog species *Xenopus laevis* and *Xenopus tropicalis*, zebrafish (*Danio rerio*), human and mouse (from top to bottom line). The sequence encoding the USP domain is marked in green and the level of conservation is indicated below the lines: An asterisk * shows fully conserved residues, the colon : shows conservation between groups of high similarity, and the

period . shows conservation between groups of a weaker similarity according to Clustal Omega.

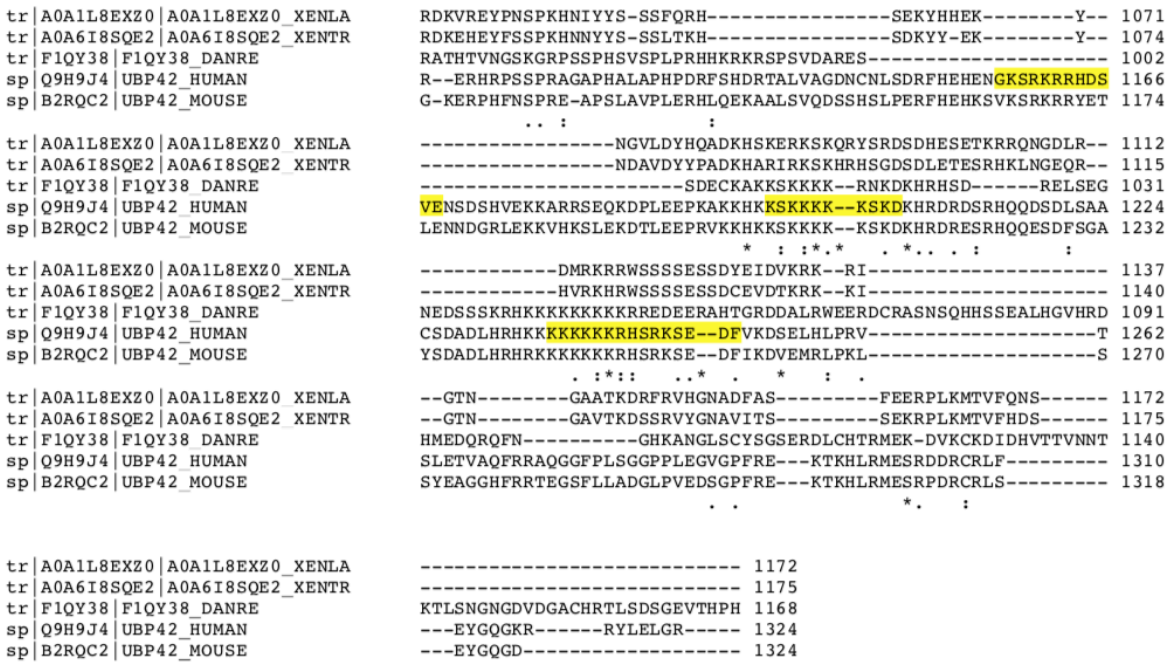

Figure 1.10: The NLS of USP42 is only partially throughout different species.
Multiple sequence alignment of USP42 in frogs (*Xenopus laevis* and *Xenopus tropicalis*), zebrafish (*Danio rerio*), human and mouse (from top to bottom line). The predicted human NLS sequences are marked in yellow. The level of conservation is indicated as followed: An asterisk * shows fully conserved residues, a colon : shows conservation between groups of high similarity, and a period . shows conservation between groups of a weaker similarity according to Clustal Omega.

Known functions of USP42 include the deubiquitination and stabilisation of p53 in the early stress response (Hock *et al.* 2011), as well as Histone 2B (H2B) in the nucleus to enhance transcription (Hock *et al.* 2014). It has recently been reported that USP42 interacts with the proteins of the spliceosome and drives nuclear speckle formation in non-small-cell lung cancer (Liu *et al.* 2021). Regarding the nuclear speckles, USP42 has been shown to facilitate DNA repair at double strand breaks, by recruiting BRCA1 and resolving R-loops (DNA-RNA hybrid structures regulating homologous recombination) together with DHX9 (Matsui *et al.* 2020). So far, USP42 has been reported to promote cancer progression, such as in gastric cancer and non-

small-cell lung cancer and acute myeloid leukemia (Paulsson *et al.* 2006, Ji *et al.* 2014, Zagaria *et al.* 2014, Hou *et al.* 2016, Liu *et al.* 2021).

1.4 Aims of the PhD project

Wnt signalling is a master regulator of adult stem cell homeostasis, and its misregulation is associated with many diseases, including colorectal cancer. The activity of canonical Wnt signalling is primary modulated by ubiquitination. A siRNA screen using Wnt reporter assays revealed the deubiquitinase USP42 as a negative regulator of Wnt signalling.

In this project, I aimed to identify the interaction partners of USP42 in canonical Wnt signalling. I wanted to elucidate the molecular mechanism and functions underlying the negative regulation of Wnt signalling by USP42, as well as its crosstalk with other signalling pathways in adult stem cells and colorectal cancer.

2. Material and Methods

2.1 List of Materials

Cell lines

Cell line	Information	Source	Number
HEK293T		ATCC	CRL-3216
HCT116		ATCC	CCL-247
H1703		ATCC	CRL-5889
L-cells control	Parental	ATCC	CRL-2648
L-cells Wnt3a	Stably transfected with Wnt3a	ATCC	CRL-2647

Cell culture

Product	Company	Product number
DMEM	gibco	41966052
RPMI 1640	gibco	11875093
DMEM/F12	gibco	11320033
DPBS	gibco	14190169
0.05% Trypsin-EDTA, phenol red	Thermo	25300054
100x Sodium Pyruvate	Thermo	11360070
HEPES	gibco	15630080
GlutaMAX	gibco	35050061
Penicillin/Streptomycin	Thermo	15140122
IntestiCult Intestinal Organoid Growth Medium	Stemcell Technologies	6005
Gentle Cell Dissociation Reagent	Stemcell Technologies	100-0485

Corning® Matrigel® Growth Factor Reduced (GFR) Basement Membrane Matrix, Phenol Red-free, LDEV-free, 10 mL	Corning	356231
X-tremeGENE™ 9 DNA Transfection Reagent	Roche/Sigma	6365787001
Opti-MEM	Gibco	51985026
DharmaFECT 1	Horizon	T-2001-03
Lipofectamine RNAiMAX	Thermo	13778150
5x siRNA buffer	Horizon	B-002000-UB-100

Organoid media according to Merenda *et al.* 2017

	Advanced DMEM/F12 +++
Advanced DMEM/F12	500 ml
GlutaMAX (100x)	5 ml
HEPES 1M (100x)	5 ml

For 20 ml each:

Component	**WENR + Nic**	**ENR**	**EN + CHIR + Y-276332**	**EN + CHIR + Y-276332 + DMSO**
Advanced DMEM/F12 +++	7.2 ml	17.4 ml	19.1 ml	18.9 ml
B27 supplement (50x)	400 µl	400 µl	400 µl	400 µl
N2 supplement (100x)	200 µl	200 µl	200 µl	200 µl
n-Acetylcysteine (500 mM)	50 µl	50 µl	50 µl	50 µl
Mouse EGF (100 µg/ml)	10 µl	10 µl	10 µl	10 µl
Mouse Noggin	20 µl	20 µl	20 µl	20 µl
R-spondin 1 CM	2 ml	2 ml	-	-
Wnt3a CM (5-fold activity)	10 ml	-	-	-
Nicotinamide (1M)	200 µl	-	200 µl	200 µl

CHIR (10 mM)	-	-	10 µl	10 µl
Y-276332 (10 mM)	-	-	20 µl	20 µl
DMSO	-	-	-	250 µl

Animals

Female mouse:

Name: <CD1>BAT-lacZ(1302)

Label #11643

Code: R

Date of birth: 16th June 2020

Genotype: +/T

Primary Antibodies

Antibody	Host species	Dilution	Supplier	Cat. No.
USP42	Rb	IF, IHC 1:200	Sigma	HPA006752
FLAG M2	Mo	WB 1:5000	Sigma	F1804
V5	Mo	WB 1:5000	Invitrogen	R960-25
α-Tubulin (clone DM 1A)	Mo	WB 1:5000	Sigma	T9026
β-Catenin	Mo	IF 1:200 WB 1:2000	BD	610153 (61054 10/2019)
HA 3F10	Rt	WB 1:5000	Sigma	00000011867423001
Axin 1-3	Rb	WB 1:2000	Niehrs lab	-
GSK3β	Mo	WB 1:2000	BD	610202
LRP6 (C5C7)	Rb	WB 1:1000	Cell Signalling	13113S
HA	Mo	WB 1:2000	Sigma	H3663
GFP (ChIP Grade)	Rb	WB 1:5000	Abcam	ab290
γ- tubulin	Mo	IF 1:500	Sigma	T5326

FLAG	Rb	WB 1:500	Invitrogen	PA1-984B
Ki67	Rb	IHC 1:200	Abcam	ab15580
E-cadherin	Rb	IF 1:200	Abcam	ab40772
Lysozym EC 3.2.1.17 (anti-human)	Rb	IHC 1:200	Dako	A0099

Secondary Antibodies

Antibody	Host species	Dilution	Supplier	Cat. No.
Mouse AF488	Donkey	IF, IHC 1:500	Thermo	A21202
Mouse AF594	Donkey	IF, IHC 1:500	Thermo	A21203
Rabbit AF488	Donkey	IF, IHC 1:500	Thermo	A21206
Rabbit AF594	Donkey	IF, IHC 1:500	Thermo	A21207
Mouse IgG HRP	Goat	WB 1:5000	Millipore	AP308P
Rabbit IgG HRP	Goat	WB 1:5000	Millipore	AP307P
Rat IgG HRP	Goat	WB 1:8000	Millipore	AP136P

Enzymes

Enzyme	Company	Product number
Q5 polymerase	NEB	M0491S
T4 DNA Ligase	NEB	M0202S
FastDigest BpiI (BbsI)	Thermo	FD1014
T4 DNA PNK	NEB	M0201L
T7 ligase	NEB	M0318L
Exonuclease	Cambio	E3101K
EcoRI-HF	NEB	R3101S
BglII	NEB	R0144S

Proteomics

Product	Supplier	Product number
Protein A Agarose beads	Millipore	16-125

Halt Protease & Phosphatase Inhibitor Cocktail (100x)	Thermo	1861284

Consumables

Product	Supplier	Product number
Electroporation Cuvettes	BioRad	1652086
48-well organoid plates	Sarstedt	83.3923.500
96-well flat bottom white polysterol plate	Greiner	655083
Nitrocellulose membrane (0.2 µm pores)	GE Healthcare	10600001
Superfrost plus microscope slides	Thermo	J1800AMNZ
Coverslips (round)	Thermo	P232.1
Coverslips (rectangular)	Roth	H878.2
Liquid Blocker Pen	Thermo	NC9827128
Tissue-Tek OCT Compound	Sakura	4583

Buffers and solutions

Buffer/solution	Composition
Blocking solution (IF)	2% Horse serum in PBS + 0.1% Triton X-100
Blocking solution (IHC)	2 % Horse serum in PBS 0.1% Triton X-100
Blocking solution (organoids)	10 % Horse serum in PBS 0.1% Triton X-100
10x Cryo antigen retrieval buffer	Sodium citrate (29.4 g) in 1 l MilliQ water, pH 6
Blocking solution (WB)	5 % Milk powder in TBST
Freezing medium	10 % DMSO in FBS

10x Laemmli running buffer	1.92 M glycerol 1 % SDS 0.25 M Tris in 1 l ddH_2O, pH 8.3
NuPAGE MOPS SDS running buffer	50 mM MOPS 50 mM Tris base 0.1% SDS 1 mM EDTA pH 7.7
10x Transfer buffer (Laemmli)	29.3 g Glycine, 200 mL of 0.5 M EDTA at pH 8.0, 58.2 g Tris Base, up to total of 1 L with ddH_2O 200 ml Methanol/l are added to 1x transfer buffer.
Transfer buffer (NuPAGE)	25 mM Bicine 25 mM Bis-Tris (free base) 1 mM EDTA pH 7.2
20x TBS	48.4 g Tris base 160g NaCl Dissolve in 900 mL water pH to 7.6 with HCl and adjust to 1l volume
TBS-T	TBS + 0.1% Tween 20
Sodium citrate buffer (10x)	29.4g Sodium citrate, 1 l MilliQ H2O, adjust pH to 6
PFA	4% PFA in PBS
WB lysis buffer (2% NP-40)	PBS

	2% NP-40 10 mM β-Mercaptoethanol 2 mM EDTA 1x Protease Inhibitor Cocktail
Co-IP lysis buffer	20 mM Tris-HCl, pH 7.5 150 mM NaCl 1% Triton X-100 1 mM EDTA 1x Protease & Phosphatase Inhibitor Cocktail
4x Laemmli buffer:	12.5 ml Solution C 5 ml Glycerol 1.0 g SDS 2.5 ml β-Merkaptoethanol 0.5 mg Bromphenolblue up to 25 ml with ddH_2O
Solution B (SDS-PAGE)	0.4 % SDS 1.5 M Tris up to total of 1 l with ddH_2O at pH 8.8
Solution C (SDS-PAGE)	0.5 M Tris 0.4 % SDS up to 1 l a ddH_2O pH 6.8 with conc. HCl
Ub lysis buffer	50 mM Tris-HCl, pH 7.5 150 mM NaCl 1% Triton X-100 1 mM EDTA

	1x Protease & Phosphatase Inhibitor Cocktail
Wash buffer IF	0.01% Triton X-100 in PBS
Permeabilisation buffer IF	0.02% Triton X-100 in PBS
50x TAE buffer	Tris free base 242 g Disodium EDTA 18.61 g Glacial Acetic Acid 57.1 ml ddH2O to 1 l
P/RlucA (pH 8)	200 mM Tris HCl 15mM $MgSO_4$ 0,1 mM EDTA
P/RlucB (pH 5)	25 mM $Na_4P_2O_7$ 10mM NaAc 15 mM EDTA 500 mM Na_2SO_4 500 mM NaCl
5x Topflash lysis buffer	125 mM Tris-phosphate (pH 7.8) 10 mM DTT 10 mM EDTA 50% Glycerol 5% Triton-X-100
2x HBS (pH 7)	50 mM HEPES 10 mM KCl 280 mM NaCl 10 mM Na_2HPO_4 0.1% w/v dextrose (D-glucose)

Commercial Kits

Kit	Company	Product number
Wizard® SV Gel and PCR Clean-Up System	Promega	A9282
Duolink® PLA Starter Kit Mouse/Rabbit	Merck	DUO92102

SNAP-Surface® 549	NEB	S9112S
Clarity Max ECL solution	BioRad	1705062
QIAprep Spin Miniprep Kit	QIAGEN	27106X4
Midori Green Advance DNA Stain	Nippongenetics	MG04
GeneRuler 1 kb Plus DNA Ladder	Thermo	SM1331
4x NuPAGE sample buffer	novex	NP0008
PageRuler Prestained Protein Ladder	Thermo	26616
Mynox Gold 2 Treatments	Minerva	10-1001

Technical Equipment

Equipment	**Manufacturer**
Nikon Eclipse Ti2	Nikon
Binocular microscope (SMZ25)	Nikon
Cell culture incubator	Thermo
Cell culture hood	Thermo
Centrifuge cell culture	Eppendorf
Centrifuge cooled	Heraeus
Centrifuge (Falcon tubes)	Beckmann
Centrifuge (main lab)	Thermo
Cryostat	Thermo
INTAS ECL Chemocam Imager	INTAS
INTAS UV-System	INTAS
Thermocycler	BioRad
NEPA21 Electroporator	NEPA GENE
Tecan Plate reader	Infinite M1000

Computer Software and tools

Software	Provider
Fiji ImageJ 2.0.0-rc-67/1.52e	
NIS Elements Microscope Imaging Software	Nikon Instruments
GraphPad Prism 8	GraphPad Software
Tecan i-control 1.10.4.0	Tecan
cBioPortal	**Colorectal Adenocarcinoma (TCGA, PanCancer Atlas)** Colorectal Adenocarcinoma (Genentech, Nature 2012) **MSK-IMPACT Clinical Sequencing Cohort (MSKCC, Nat Med 2017)**
BioRender	https://biorender.com
cNLS mapper (NLS prediction tool)	http://nls-mapper.iab.keio.ac.jp/cgi-bin/NLS_Mapper_form.cgi
Clustal Omega	https://www.ebi.ac.uk/Tools/msa/clustalo/
Protein Atlas	https://v15.proteinatlas.org/ENSG00000106346-USP42/tissue

2.2 Methods

Cell culture

HEK293T cells, L-cells control and stably transfected with Wnt3a (obtained from ATCC) were cultured in DMEM (Gibco) supplemented with 10% FBS and 1% Penicillin/Streptomycin, at 37°C with 5% CO_2.

HCT116, RKO and H1703 cells (ATCC) were subcultured in RPMI (Gibco) medium, also supplemented with 10% FBS, 1% Sodium Pyruvate and 1% Penicillin/Streptomycin, at 37°C with 5% CO_2. ZNRF3/RNF43 double knockout cells, as well as their parental cell line were a kind gift from MM Maurice lab (Spit *et al.* 2020, UMC Utrecht). HEK293T

sgAPC and sgUSP42_11 were transfected by Oksana Voloshanenko from the Boutros group (DKFZ, Heidelberg).

Mouse intestinal organoids were kindly provided by the Pereira lab (COS, Heidelberg).

Passaging of cell lines

The cell lines were passaged thrice a week, in a 1:5 ratio during the week days and 1:10 over the weekend. The adherent cells were cultivated in 10 ml cell culture medium in T75 cell culture flasks. Before passaging the cells, they were inspected under the microscope, if they were growing healthily or for potential contaminations. All cell culture media, PBS and Trypsin-EDTA were warmed to 37 °C in the water bath. For passaging, the medium was aspirated and the cells were rinsed with 10 ml DPBS. After taking off the PBS, 5 ml Trypsin-EDTA was added to the cells without washing the cells away. The Trypsin-EDTA was immediately aspirated and the cells were incubated at RT until they detached from the bottom of the flask. Then, the cells were resuspended in 10 ml medium and split 1:5 or 1:10 into a new flask, together with fresh medium.

Passaging of organoids

The mouse intestinal organoids are split every 7-10 days. Prior to passaging the organoids, the density and growth stage of the organoids were examined under the microscope. Usually, the organoids were split in a ratio of 1:3 and the required amount of Matrigel was thawed on ice. In contrast to the cell culture media, the intestinal organoid medium was only warmed to RT, instead of the water bath. In addition, the organoid culture plate was warmed to 37 °C in the incubator for 30 minutes.

For passaging, the organoid medium was carefully taken off with a P1000 pipette without disrupting the Matrigel dome. Afterwards, 250 µl of Gentle Cell Dissociation Reagent was added to each well and incubated for 1 minute. Then, the Matrigel domes were disrupted with a P1000 pipette by pipetting the cell dissociation reagent up and down for 15-20 times per well. The disrupted Matrigel dome mixtures were collected in a 15 ml Falcon tube. For rinsing the wells, 500 µl of Gentle Cell

Dissociation Reagent was added to the first well of the organoid culture plate and the bottom of the well was washed to collect all the organoids. The whole solution was then transferred to the next well to repeat the washing process. Finally, the mixture was added to the other organoids in the 15 ml Falcon tube and incubated for 5 minutes at RT. After incubation, DPBS was added (up to 12 ml) to the organoids in the dissociation reagent and the Falcon tube was centrifuged at 300 x g for 3 minutes. The supernatant was carefully discarded first with a 10 ml, then with the P1000 pipette, without aspirating the cell pellet. For the final wash, the dissociated organoids were resuspended in 10 ml of pure (advanced) DMEM F12 and centrifuged at 300 x g for 3 minutes. Again, the supernatant was discarded and the organoid fragments were resuspended in a 1:2 mix of Matrigel and Advanced DMEM F12 medium. 30 µl of the mixture was seeded as Matrigel domes in the center of each well. Before adding the IntestiCult Intestinal Organoid Growth Medium, the Matrigel domes had to solidify for at least 10-15 minutes in the incubator. At last, 250 µl of IntestiCult Intestinal Organoid Growth Medium was added to the wells.

Freezing and thawing of cell lines and organoids

For freezing the cells and organoids, they were washed and dissociated as described above. After resuspending the cells in full cell culture medium, they were transferred into a 15 ml Falcon tube and cetrifuged at 300 x g for 4 minutes. The supernatant was aspirated and the cell pellet was resuspended in 2 ml freezing medium (FBS supplemented with 10 % DMSO). One confluent T75 flask was divided into two cryotubes containing 1 ml of the cell slurry each. Regarding the organoids, 3-4 wells were combined in each cryotube with 1 ml freezing medium. The tubes were cooled in a Mr. Frosty at -70 °C overnight, before getting transferred into the liquid nitrogen storage.

Plasmids and constructs

pEGFP-FLAG-USP42 WT and pEGFP-FLAG-USP42 C120A plasmids originate from KH Vousden lab (Hock *et al.* 2011). Wnt1, hLRP6, mFzd8, xDvl-GFP, Dvl1, xb-catenin, ZNRF3-HA, V5-hLGR4, hRSPO1-DC-AP (RSPO1), hRSPO2-DC-AP (RSPO2), hRSPO3-DC-AP (RSPO3), mRSPO4-AP (RSPO4), TOPflash and Renilla plasmids (Glinka et al, 2011;

Berger et al, 2017; Chang et al, 2020) were gifted to our lab by C Niehrs. BK Koo kindly provided us with the 2gRNA CRISPR concatemer vector and RNF43-FLAG-HA constructs (Koo et al, 2012; Merenda et al, 2017). The SNAP-Frizzled5 and Frizzled5-V5 were given to us by MM Maurice. FLAG-HA-USP39 (#22581), 3xFLAG-DVL2 (#24802) and p53 reporter PG13-luc (#16442), hSpCas9 (#42230), eSpCas9-ATP1A1-dual-gRNA (#86613) plasmids were ordered from Addgene. I generated the USP42 (together with Ana García del Arco) and ZNRF3 truncation mutants by PCR by deleting USP42 ΔN (deletion of N-terminal, Δ1–111), USP42 ΔC (excluding the C-terminal Δ412–1315), USP42 ΔNLS (predicted monopartite nuclear localisation signal, Δ1160–1246), ZNRF3 ΔRING (Δ293–334), ZNRF3 ΔLinker (D335–345) and ZNRF3 ΔDIR (Δ346–528). Also, I removed the FLAG-tag from the pEGFP-FLAG-USP42, as well as the HA-tag from RNF43-FLAG-HA plasmids by PCR.

Plasmids were amplified by transformation into chemocompetent cells (XL1-Blue) and purified with the QIAprep Spin Miniprep Kit.

Generating USP42 and ZNRF3 truncation mutants

The USP42 truncation mutants were generated by PCR using the pEGFP-FLAG-USP42 plasmid as the template: USP42ΔN (N-terminal, Δ1-111), USP42ΔC (C-terminal Δ412-1315), USP42ΔNLS (predicted monopartite nuclear localization signal, Δ1160-1246).

Table 2.2.1: Primers for generating the USP42 truncation mutants

Construct	Forward primer	Reverse primer	Tm [°C]
ΔN-terminal	CAATACCTGTTTTGCCAATGCAG	CTTATCGTCGTCATCCTTGTAATCCAT	65
ΔNLS	TGACTCGAGATCCACCGGAT	TCCATTTTCGTGTTCGTGAA	63
ΔC-terminal	TGACTCGAGATCCACCGGAT	GGACCTGATATAAAAGAGCACAT	63

ZNRF3 truncation mutants were generated by PCR according to Jiang *et. al* 2015 using the ZNRF3-HA plasmid as the template: ZNRF3ΔRING (Δ293-334), ZNRF3Δlinker (Δ335-345) and ZNRF3ΔDIR (Δ346-528).

Table 2.2.2: Primers for generating the ZNRF3 truncation mutants

Construct	Forward primer	Reverse primer	Tm [°C]
ΔRING	CACAACATCATAGAACAAAAGGGAAACC	GTCGGACGTGGAGCTGCTGCT	67
Δlinker	GCGGTGTGTGTGGAGACC	CCGACAGTGGGGGCAGGTGT	70
ΔDIR	TTCAGCTGCTATCACGGCCACC	GCTTGGGTTTCCCTTTTGTTCTATGATGT	70

The primers were ordered with a phosphorylation and the stock solutions (100 µM) were diluted in nuclease-free water to a final concentration of 10 µM.

The following components were mixed together for the PCR reaction mix (25 µl per sample):

Component	25 µl reaction	Final concentration
Q5 Reaction Buffer (5x)	5 µl	1x
10 mM dNTPs	0.5 µl	200 µM
Forward primer (10 µM)	1.25 µl	0.5 µM
Reverse primer (10 µM)	1.25 µl	0.5 µM
1-2 ng Template DNA	1 µl	
Q5 High-Fidelity DNA Polymerase	0.25 µl	0.02 U/µl
Q5 High GC Enhancer (5x)	5 µl	1x
Nuclease-free water	to 25 µl	

The following settings were used for the PCR reaction in the thermocycler:

Step	Temperature [°C]	Time
Initial denaturation	98	30 seconds
35 Cycles	98	10 seconds
	indicated Tm of the primers	30 seconds
	72	30 seconds/kb + 30 seconds
Final extension	72	2 minutes
Hold	4	

Afterwards, the PCR reactions were run on a 1% agarose gel supplemented with Midori Green Advance in TAE buffer and imaged in an INTAS UV-System. The respective bands were cut out and transferred into a 1.5 ml Eppendorf tube. Then, the gel slices were dissolved in an appropriate amount of Membrane Binding Solution and the PCR products were purified with the Wizard SV Gel and PCR Clean-Up System. Finally, the ligation reaction (20 µl) was prepared by mixing the following components:

Component	20 µl reaction
T4 DNA Ligase Buffer (10x)	2 µl
DNA	50 ng
T4 DNA Ligase	1 µl
Nuclease-free water	to 20 µl

The ligation mix was incubated at 16 °C overnight, followed by a 10 minute heat inactivation step at 65 °C, before getting transformed into chemocompetent cells

(XL1-Blue).

Removing the FLAG-tag from pEGFP-FLAG-USP42 and the HA-tag from RNF43-FLAG-HA

For the ubiquitination assays, the FLAG-tag had to be removed from the pEGFP-FLAG-USP42 construct, as well as the HA-tag from the RNF43-FLAG-HA construct. Also, the HA-tag was exchanged from the ZNRF3-HA with a FLAG-tag. The constructs were generated by PCR as described for the truncation mutants.

Construct	Forward Primer	Reverse Primer	Tm [°C]
pEGFP-USP42	GTACCATG	TTCTAGAGGATCCTTCTGTTCGCTCCT	68
ZNRF3-FLAG	GATGACGACAAGTAAGATATCCAGCACA	GTCTTTGTAGTCGGCTCCCGGGCTGCTGCT	68
RNF43-FLAG	TGATCGAGTCTAGAGGGCCCGTTT	CTTGTCATCGTCGTCCTTGTAGTCTGCTCCAGC	69

Transfection of plasmids

For the sample preparation of some experiments, such as reporter assays and western blots, plasmids were transfected into the cells with the transfection reagent X-tremeGENE 9. Therefore, the total amount of plasmid DNA to be transfected was calculated and a master mix of X-tremeGENE and Opti-MEM was prepared. In general, 3 µl X-tremeGENE was used for 1 µg plasmid DNA and it was mixed with Opti-MEM in a ratio of 1:20. Then, the plasmid DNA was prepared for each sample. Afterwards, the required volume of X-tremeGENE and Opti-MEM mix was added to each sample and incubated for 15 minutes at RT. Finally, the transfection solution was mixed with cell culture medium (e.g. for 96-well: 50 µl/well, or 6-well: 200 µl/well) and the required amount was added to the cells.

Small interfering RNA (siRNA)

Table 2.2.3: siRNA transfected into the cells

siRNA	Company	Product number
siRNA Universal negative control	Sigma	SIC001-10NMOL
siUSP42 **(CAGUCUACCUCGAACGCAU)**	Sigma	SASI_Hs01_00078970
siRNA USP42 siGENOME Human USP42 (84132) siRNA - Set of 4	Dharmacon	D-006089-02-0002
siRNA USP42 ON-TARGETplus Set of 4 upgrade siRNA J-006089-06	Dharmacon	LU-006089-00-0002 set of 4
siTP53	Sigma	
siAPC	Sigma	
siLRP6	Sigma	

siRNA stocks were ordered dry and dissolved in 1x siRNA buffer with nuclease-free water to a stock of 20 µM.

Transfection of siRNA

For the sample preparation of reporter assays or western blot, siRNA was transfected into the cells one day prior to transfection with plasmid DNA.

HEK293T cells were transfected with siRNA using the transfection reagent DharmaFECT 1 on the same day as the seeding of the cells. Here, it was important to use cell culture medium without antibiotics during the transfection with siRNA. First, the siRNA was diluted to a 500 nM stock in siRNA buffer and they were transfected in a final concentration of 50 nM following the DharmaFECT 1 manufacturer's protocol. For example, in a 96-well plate 10 µl of 500 nM siRNA solution was mixed with 0.2 µl DharmaFECT 1 and 20 µl pure DMEM (without antibiotics or FBS) per

well. The mix is incubated for 15 minutes at RT. Finally, 70 µl per well of cell slurry containing 15,000 cells/well was added to each well. They were incubated in the siRNA containing medium overnight. Before transfecting them with plasmid DNA, the medium was changed to DMEM++ 4 hours before the planned transfection.

For transfecting siRNA into HCT116 cells, the transfection reagent Lipofectamine RNAiMAX was used according to the manufacturer's protocol. In contrast to the transfection with DharmaFECT 1, the siRNA is not diluted to a 500 nM stock and is used in a final concentration of 75 nM.

Production of Wnt3a conditioned medium

L-cells control and stably transfected with Wnt3a were used to harvest control and Wnt3a conditioned media. Therefore, they were seeded 1:10 in 10 ml DMEM++ medium onto Ø10 cm petri dishes. The cells were grown for 4 days until they were almost confluent. The medium of fraction #1 was collected in 50 ml Falcon tubes and centrifuged at 300 x g for 4 minutes to sediment the dead cells. Subsequently, the supernatant was transferred into glass bottles and the Wnt3a activity was tested in a Wnt reporter assay. The glass bottles were stored at 4 °C. For fraction #2, 10 ml of fresh DMEM++ medium was added to the cells and they were grown for 3 more days. The medium was collected and processed as fraction #1.

Production of R-spondin conditioned medium

R-spondin1-4 conditioned media were produced by transiently transfecting HEK293T cells with 15 µg (per 10 cm dish) of the respective plasmid with calcium phosphate transfection. Therefore, for each plate 62 µl of a 2 M $CaCl_2$ solution was prepared with 438 µl of ultrapure water together with the plasmid DNA. Then, 2x HBS is slowly dropped into the tube and incubated for 20 minutes at RT. The transfection solution was carefully dropped into the plates containing 90% confluent cells in 10 ml of DMEM++. After 5-7 hours, the medium was exchanged for each plate. 24 hours later, the media were harvested and centrifuged at 300 x g to get rid of dead cells. Finally, the media were tested (1:50) in a Wnt reporter assay in combination with Wnt3a

(1:5) to test the their efficiency to enhance canonical Wnt signalling.

Generating USP42 knockout cell lines

The gRNA for the human USP42 knockout cell lines were designed with the following site: http://www.e-crisp.org/E-CRISP/

gRNA	Top/bottom oligo	Sequence 5' – 3'
hUSP42 #1	Top	CACCGAATCAGCCTGGCAGCTCCG
	Bottom	AAACCGGAGCTGCCAGGCTGATTC
hUSP42 #2	Top	CACCGATGCAGGTTCTGCCAGCTG
	Bottom	AAACCAGCTGGCAGAACCTGCATC

These gRNA were cloned into the eSpCas9(1.1)_No_FLAG_ATP1A1_G3_Dual_sgRNA vector (Addgene #86613). First, the oligo stocks were dissolved in nuclease-free water to a final concentration of 100 µM. 2 µl of 1 M Tris pH 8 was added to the oligos to a final concentration of 20 mM. Then, the oligos are annealed at 95 °C for 5 minutes and slowly cooled down to RT over a duration of 1 hour. In parallel, 1 µg vector DNA is digested with Bbs1 and purified with the Wizard PCR Clean-Up System. Then, the annealed oligos are diluted 1:100 (1 mM) in ultrapure water. 2 µl of diluted oligos are ligated with 1 µl purified cut plasmid in a 10 µl ligation reaction. After ligation, 7 µl of the ligation mix is transformed into chemocompetent bacteria. The plasmid DNA was isolated from the growing colonies, amplified and sequenced (by Eurofins Genomics).

Prior to electroporation, the cells were detached and resuspended in Opti-MEM. Ideally, 1-5 x 10^6 cells per cuvette are optimal. The required amount of cells were concentrated in 50 µl Opti-MEM per electroporation and added to the prepared plasmid DNA in an Eppendorf tube (105 µl in total). Before electroporation, the impedance value was measured, which should be between 0.03 and 0.55 kΩ. The

value was adjusted by adding either Opti-MEM or more cell slurry to the cuvette. Together with the ATP1A1 template, 5 µg of each of the positive gRNA plasmids were then electroporated into HEK293T cells and HCT116 cells with the following settings:

Poring Pulse					
Voltage [V]	**Length [ms]**	**Interval [ms]**	**No.**	**D. Rate [%]**	**Polarity**
150	5	50	2	10	+
Transfer Pulse					
Voltage [V]	**Length [ms]**	**Interval [ms]**	**No.**	**D. Rate [%]**	**Polarity**
20	50	50	5	40	+/-

Subsequently, the cells were rescued with full growth medium and seeded onto a Ø10 cm cell culture dish. Three days after electroporation, the cells were treated with 0.5 µM ouabain for selecting positive clones.

Regarding the HEK293T cells, a positive clone was used for the experiments. On the contrary, the HCT116 USP42 knockout cells were used in bulk because of their genetic variance, as recommended by Prof. Boutros.

In addition, Oksana Voloshanenko cloned the same gRNA into the pX459 plasmid and transfected them into HEK293T cells for 48 hours. The cells were selected with puromycin for 1-2 days, until all control cells were dead. Finally, the cells were allowed to recover for 3-4 days.

Generating Usp42 knockout mouse intestinal organoids

As for the USP42 knockout cell lines, the gRNA for Usp42 was designed with the http://www.e-crisp.org/E-CRISP/ site.

gRNA	Top/bottom oligo	Sequence 5' – 3'
mUsp42 #1	Top	CACCGGGACACAGGCTCTGCCAGCTGGT
	Bottom	TAAAACCAGCTGGCAGAGCCTGTGTCCC
mUsp42 #2	Top	ACCGGGAGACCGCCTCACAACTGCCG
	Bottom	AAAACGGCAGTTGTGAGGCGGTCTCC

They were cloned into the 2 gRNA CRISPR-concatemer following the protocol from Merenda *et al.* 2017.

Therefore, the oligos were phosphorylated and annealed by the following reaction:

Component	Volume
Top oligo (10 µM)	1 µl per gRNA
Bottom oligo (10 µM)	1 µl per gRNA
T4 DNA ligase buffer (10x)	2 µl
T4 DNA PNK	1 µl
Nuclease-free water	to 20 µl

The reaction was run in a thermocycler at 37 °C for 30 minutes, then 95 °C for 5 minutes and finally slowly ramped down to 25 °C at 0.3 °C/minute. After the annealing was done, the reaction was held at 4 °C.

For the BbsI shuffling reaction, the following reaction was assembled on ice:

Component	Amount
2 gRNA CRISPR-concatemer vector	100 ng
Annealed oligo mix	10 µl
FastDigest Buffer (10x)	1 µl
DTT (10 mM)	1 µl
ATP (10 mM)	1 µl
BbsI	1 µl
T7 ligase	1 µl
Nuclease-free water	To 20 µl

The BbsI shuffling reaction was run with the following program in a thermocycler:

Cycles	Temperature [°C]	Time [min]
25	37	5
25	21	5
Hold	37	15
Hold	4	forever

To remove the remaining linear DNA, the ligation reaction was treated with DNA exonuclease at 37 °C for 30 minutes, followed by a heat inactivation step at 70 °C for 30 minutes. Then, 2 µl of the mix was transformed into chemocompetent bacteria.

Component	Amount

Ligation mix	11 µl
Exonuclease buffer (10x)	1.5 µl
ATP (10 mM)	1.5 µl
DNA exonuclease	1 µl
Nuclease-free water	To 15 µl

After the single colonies were grown in LB medium, the plasmid DNA was isolated and positive clones were determined with restriction digestions. First, the presence of the concatemers are confirmed by a digestion with 10 U EcoRI and 5 U BglII in a 10 µl reaction for 3 hours at 37 °C. The digested 2 gRNA-concatemer is supposed to give a band at 800 bp on a 1% agarose gel. The second restriction digestion is run with 5 U BbsI at 37 °C for 3 hours. The positive plasmids should not be cut by the restriction enzyme, as the cassette containing the cutting site was replaced by the gRNA.

Positive clones were confirmed by sequencing.

Before electroporation, the mouse intestinal organoids had to be prepared. On day 0 the organoids were split in a high density (1:2 ratio) and grown in the WENR + Nic medium. For each sample, 6 wells were used for an electroporation. The control organoids were transfected with the hSpCas9 and the empty CRIPR-concatemer vector. Also, a sample electroporated with GFP is included to observe the efficiency of the electroporation. On day 2 (48 hours before electroporation) the medium was exchanged to the EN + CHIR + Y-276332 without antibiotics. Then, on day 3, the medium was changed to the EN + CHIR + Y-276332 + DMSO medium.

On the day of electroporation (day 4), the Matrigel domes were broken by pipetting up and down with a P1000 pipette. The organoids were transferred to a 15 ml Falcon tube and mechanically disrupted by using a P200 pipette. After centrifugation at 600 x g for 5 minutes, the supernatant was discarded and the organoid fragments were treated with Trypsin-EDTA at 37 °C for 5 minutes. The dissociation was closely

monitored, until the fragments had a size of 8-10 cells. This reaction was terminated by adding full growth medium. The cells were centrifuged at 500 x g for 3 minutes and resuspended in 1 ml Opti-MEM to determine the amount of cells. For each electroporation, 1-5 x 10^6 were used and concentrated in 50 µl of Opti-MEM. The 2 gRNA CRISPR-concatemer was mixed with the same amount of hSpCas9 plasmid and diluted to a volume of 55 µl. The organoid fragments were mixed with the DNA in the electroporation cuvette and the resistance was measured as for the knockout cell lines. Then, the electroporation was performed with the following settings:

Poring Pulse					
Voltage [V]	**Length [ms]**	**Interval [ms]**	**No.**	**D. Rate [%]**	**Polarity**
175	5	50	2	10	+
Transfer Pulse					
Voltage [V]	**Length [ms]**	**Interval [ms]**	**No.**	**D. Rate [%]**	**Polarity**
20	50	50	5	40	+/-

Subsequently, 400 µl of Opti-MEM + Y-27632 were added to the cuvette and the whole mix was transferred to a 1.5 ml Eppendorf tube to let the cells recover for 30 minutes at RT. Then, the tubes were centrifuged at 400 x g for 3 minutes and the cells were resuspended in a mix of Matrigel and Advanced DMEM F12 medium. 20 µl Matrigel domes were seeded into each well. After the Matrigel domes were solidified, the domes were covered with EN + CHIR + Y-27632 + DMSO medium. On the following day, the medium was exchanged to EN + CHIR + Y-27632 medium and the transfection efficiency was examined by GFP expression under the fluorescent microscope. Every 2 days the medium is exchanged until day 9, where the medium changes to WENR + Nic + Y-27632. The ROCK inhibitor Y-27632 can be removed on day 19. The knockout organoids were selected for 2 passages by a reduction of Wnt3a and R-spondin conditioned medium, as described for other negative Wnt

regulators (Merenda *et al.* 2017).

Reporter assays

Topflash dual-luciferase reporter assay (Wnt reporter assay)

10,000 HEK293T cells per well (of a 96-well plate) were seeded on day 0, if indicated also with siRNA as described above. 24 hours after seeding the cells, they were transfected with 50 ng in total of plasmid DNA, using the X-tremeGENE 9 transfection protocol.

Plasmid	Amount per well [ng]
Firefly luciferase	5
Renilla luciferase	3
PCS2+ (empty vector)	42 (up to 50 ng/well)
GFP-USP42	5
USP39	5
ZNRF3-HA	0.5
RNF43-FLAG-HA	1
hLRP6	3
Wnt1	5
mFzd8	1
Dvl1	20
Xβ-catenin	1

24 hours later, the cells were treated with either control conditioned medium (1:5),

Wnt3a conditioned medium (1:5) or a combination of Wnt3a and R-spondin conditioned medium (1:5 and 1:50) overnight. For harvesting the cells, the medium was removed and the cells were lysed in 60 µl of TF lysis buffer. They were incubated for 15-20 minutes on the shaker at 4 °C. Afterwards, the plate could be stored at -20 °C or analysed with the Tecan plate reader. Therefore, 30 µl of the cell lysates were transferred to a white flat bottom 96-well plate, without creating bubbles. Then, 50 µl of the P/RlucA (pH 8) solution was added to the wells and the chemoluminescence was measured using these settings:

Step	**Settings**
Shaking (Linear)	Duration: 2 s Amplitude: 2 mm
Waiting time	2 min
Shaking (Linear)	Duration: 3 s Amplitude: 2 mm
Firefly luminescence	Integration time: 100 ms
Add Renilla substrate (P/RlucB, pH 5)	
Shaking (Linear)	Duration: 2 s Amplitude: 2 mm
Renilla luminescence	Integration time: 200 ms

p53 reporter assay

For p53 reporter assays, HEK293T cells were seeded on a 96-well plate with the indicated siRNA. On the next day, the medium was changed and the cells were transfected with the following plasmids:

Plasmid	Amount per well [ng]
PG13-luc	10
Renilla	5
PCS2+	35

p53 signalling was induced by treating the cells with 10 nM Actinomycin D overnight, before being harvested.

FGF reporter assay

For the FGF reporter assay, HEK293T cells were seeded on a 96-well plate and transfected with these plasmids:

Plasmid	Amount per well [ng]
Gal-luc	10
Gal-ELK	2
Renilla	5
PCS2+	33

The next day, they were treated with 10 ng/ml bFGF overnight.

TGFβ reporter assay

For the TGFβ reporter assay, HEK293T cells were seeded on a 96-well plate and transfected with the indicated plasmids. 24 hours later, they were treated with 2 ng/ml TGFβ overnight.

Plasmid	Amount per well [ng]
ARE-luc	10
Fast 1	1
Renilla	8
PCS2+	31

NuPAGE Bis-Tris gel electrophoresis and Western Blot

Western blot samples were harvested in PBS on ice using a cell scraper. Per sample, the cells of 3 wells were collected in an Eppendorf tube and centrifuged at 2000 rpm for 3 minutes. The supernatant was carefully discarded and the cell pellet was resuspended in 100 µl 2% NP-40 lysis buffer. The cells were lysed on ice for 10 minutes and centrifuged again at 2000 rpm for 3 minutes. 75 µl of the supernatant was transferred into a new Eppendorf tube and mixed with 25 µl of 4x NuPAGE sample buffer supplemented with 20 mM DTT. Then, the samples were incubated in the heat block at 65-70°C for 5-10 minutes, depending on the protein size. The larger the protein, the longer the sample was the incubated at a higher temperature (e.g. LRP6 at 180 kDa). After boiling the samples, they were cooled to RT before loading the gels.

For the NuPAGE gel electrophoresis, the following gels were cast (4 gels). For large proteins, such as LRP6, a 12% separating gel was cast, instead of an 8% gel.

Component	Separating gel (8%)	Stacking gel (4%)
40% Bis-acrylamide	4 ml	1 ml
1.25 M Bis-Tris pH 6.8	5.714 ml	2.858 ml

ddH_2O	10.286 ml	6.142 ml
TEMED	20 µl	10 µl
10% APS	200 µl	100 µl
Final volume	20 ml	10 ml

After loading the samples into the pockets, the electrophoresis was run at 120 V for 1 hour. Then, the proteins were transferred onto a nitrocellulose membrane by a semi-dry blot, at a current of 100 mA per gel for 30 minutes and a limited voltage of 25 V. The membranes were blocked with 5% milk powder in TBS-T for 30 minutes and incubated with the primary antibodies diluted in blocking solution overnight at 4 °C on a shaker.

On the next day, the primary antibody solution was removed and the membranes were washed three times with TBS-T for 10 minutes. The HRP-conjugated secondary antibody solution was added to the membranes and they were incubated for at least 1 hour at RT on the horizontal oscillator. Finally, the membranes were washed again three times with TBS-T, before the luminescence was measured with the INTAS ECL Chemocam Imager. Therefore, the solutions 1 and 2 of the Clarity Max ECL substrate kit were mixed in the same volumes in an Eppendorf tube. One membrane at the time was incubated in the ECL solution. For the measurement, the membrane was transferred onto a transparent plastic sheet.

Co-immunoprecitation

For co-immunoprecipitations, 500,000 HEK293T cells per well were seeded on a 6-well plate, using 3 wells per sample. Once the cells have adhered to the bottom of the wells, 300 ng of the indicated plasmids were transfected per well. After 24-48 hours, the cells were harvested on ice in cold PBS by using a cell scraper. The cells were transferred into Eppendorf tubes and centrifuged at 2000 x g for 3 minutes at 4 °C. The supernatant was discarded and the cells were lysed in 500 µl of lysis buffer

for 10 minutes on ice. In parallel, the protein A agarose beads (for rabbit antibodies) or protein G agarose beads (for mouse antibodies) were prepared. For each sample, 20 µl of a 50% slurry was needed for the clearing and 30 µl was used for the immunoprecipitation. First, the beads were washed three times with the lysis buffer and centrifuged at 500 rpm for 2 minutes, at 4 °C. To avoid clogging of the tips and bead loss, the pipette tips were cut and the bead pellet was disturbed by adding the lysis buffer directly on top, without resuspending with the pipette.

After the cells were lysed, 20 µl of the bead slurry was added to the lysates and incubated for 5-10 minutes on ice to clear the lysates from unspecific binding proteins. Then, the lysates were centrifuged at 13,000 rpm for 5 minutes at 4 °C and the supernatants were transferred into new Eppendorf tubes (2 for each sample: input and IP). 30 µl of each supernatant were used for the inputs which were not incubated with antibodies. The inputs were mixed with the same volume of 4x Laemmli Buffer. The rest of the supernatants were incubated with 0.5 µg of antibody per sample. The samples were incubated for 1 hour at 4 °C in rotation. Then, 30 µl of the bead slurry was added to each sample and incubated for another 2 hours. Afterwards, the samples were centrifuged at 500 rpm for 2 minutes and washed three times with the lysis buffer. Finally, the proteins are eluted in 60 µl of a 1:2 mix of Laemmli buffer with lysis buffer and boiled at 95 °C for 5-10 minutes. The samples should be analysed by SDS-PAGE on the same day. Therefore, gels were casted as followed:

Component	**Separating gel (8%)**	**Stacking gel (4%)**
Water dest.	11 ml	6.5 ml
40% Bis-acrylamide	4 ml	1 ml
Solution B	5 ml	-
Solution C	-	2.5 ml
TEMED	10 µl	6 µl

10% APS	200 µl	120 µl
Final volume	20 ml	10 ml

The gel electrophoresis was run in Laemmli running buffer at 120 V for 90 minutes and transferred by a semi-dry western blot with methanol transfer buffer for 90 minutes at 100 mA per gel (voltage limited to 25 V).

Ubiquitination assay

For the ubiquitination assays, HEK293T cells were seeded on a 6-well plate as for the co-immunoprecipitations. Here, also 3 wells were used per sample. If control siRNA and siUSP42 were transfected, the double amount of cells were seeded. Next day, the media were changed and the cells were transfected with 2 µg of ZNRF3-FLAG together with 1 µg of HA-Ubiquitin and if needed 2 µg GFP-USP42. 24 hours after transfection, the cells were treated for 6 hours with 20 µM MG132 and 20 nM Bafilomycin A to avoid degradation of ZNRF3. Then, the cells were harvested with PBS and lysed in 60 µl of Ub lysis buffer for 10 minutes on ice. The cells were centrifuged at maximum speed for 10 minutes at 4 °C. 50 µl of the supernatants were then transferred to a new Eppendorf tube. Extra 15 µl of the lysates were saved for the inputs and were mixed with 15 µl 4x NuPAGE + DTT. 5 µl of 10% SDS were added to the 50 µl lysates and incubated at 95 °C for 5 minutes for denaturation. After the lysates cooled down to room temperature, they were mixed with 450 µl lysis buffer and incubated for 15 minutes on ice for quenching. A master mix of antibody and beads was prepared in lysis buffer. In total, 2.5 µl of Rb-anti-FLAG antibody, as well as 25 µl of washed protein A agarose beads were added to each sample and incubated overnight in rotation. The next morning, the samples were washed three times with lysis buffer. At last, the samples were eluted with 50 µl of a 1:2 Lysis and 4x NuPAGE + DTT mix and incubated at 70 °C for 10 minutes.

Surface biotinylation assay

These experiments were performed by Marlene Tietje and Vanesa Fernández-Sáiz (TUM). HEK293T cells were seeded on Ø 15 cm plates and transfected with ZNRF3-FLAG or RNF43-FLAG, HA-Ubiquitin and pEGFP-USP42 plasmids with $CaCl_2$ transfection as described above. Before the biotinylation, the cells were washed with ice-cold PBS to remove any contaminants. The proteins at the cell surface were marked with biotinylation with approximately 80 µl of a 10 mM EZ-Link Sulfo-NHS-SS-Biotin solution (per ml) at 4 °C 30 minutes according to the product manual (Pierce Cell Surface Protein Isolation Kit, Thermo Cat. No. 89881) followed by a pull-down with NeutrAvidin Agarose beads after cell lysis. The cell surface proteins were eluted in Strep-Tactin Elution Buffer (IBA Lifesciences Cat. No. 2-1206-002). Then, the samples were diluted up to 1 ml of co-immunoprecipitation lysis buffer and a co-IP was performed against the substrates ZNRF3-FLAG or RNF43-FLAG, using the M2 affinity gel (Sigma, Cat. No. A2220). Finally, the proteins were eluted with Laemmli buffer and analysed by SDS-PAGE and western blot.

Immunofluorescent stainings

When preparing HEK293T cells for immunofluorescent stainings, the coverslips were previously coated with poly-L-lysine. Therefore, the coverslips were place into 12-well plates and 100 µl of a 10% poly-L-lysine solution (in water) was added on top of the coverslips. They were incubated for 5-10 minutes at RT and washed three times with water, before seeding the cells. All other cell lines strongly adhered to the coverslips, so no coating was required for them.

In general, for the different experiments the cells were either transfected with siUSP42 on the day of seeding the cells (day 0: 120,000 cells per well), or transfected with the indicated plasmids on the next day (day 1) and harvested the following day after treatment with conditioned media (day 2). In contrast, the USP42 shuttling experiment required an overnight treatment with the indicated reagents and conditioned media.

Treatment	Concentration
Control CM	1:5
Wnt3a CM	1:5
Wnt3a + R-spondin 3 CM	1:5 + 1:50
BIO	1 µM
DKK1	1:5
EGF	100 ng/ml
FGF	50 ng/ml
TGFβ	2 ng/ml
BMP4	50 ng/ml
KT5720 (PKA inhibitor)	1 µM
Akti-1/2 (PKB inhibitor)	10 µM
Sotrastaurin (PKC inhibitor)	10 µM
MEK inhibitor	1 µM
Y-27632 (ROCK inhibitor)	10 µM
Rapamycin	25 nM

The cells were washed with PBS and fixed in 2% PFA in PBS for 10 minutes. Only the centrosome co-localisation experiment required a methanol fixation, by fixing the cells for 2 minutes with 3% PFA followed by a methanol fixation for another 3 minutes on ice.

For the β-catenin accumulation (in H1703 cells) and overexpression of the different

USP42 constructs (in HEK293T cells), 125 ng of the indicated plasmids were transfected per well using the X-tremeGENE 9 transfection reagent. The HEK293T cells tested for the different siRNA, as well as the overexpression of the different GFP-tagged USP42 constructs, were only stained with DAPI before the coverslips were mounted. For the USP42 shuttling experiment, HEK293T cells were seeded

For the β-catenin accumulation, USP42 shuttling, centrosome co-localisation and E-cadherin stainings the cells were permeabilised with 0.2% Triton X-100 in PBS for 10 minutes on the horizontal oscillator at RT. Then, the cells were incubated in blocking solution for 20 minutes at RT (also on the horizontal oscillator) to decrease unspecific binding of the antibodies. In parallel, a sheet of parafilm was laid into the humidified staining chamber and the primary antibody solutions were prepared in blocking buffer. 30 µl drops were placed onto the parafilm and a coverslip was put onto each drop with the cells facing downward. To not dilute the antibody solution, the remaining drop of blocking buffer was tapped off the coverslip onto a tissue paper, before placing the coverslips. The cells were incubated for 3 hours at RT or overnight at 4 °C in the primary antibody solution. The next day, the cells were washed three times for 5 minutes with 0.1% Triton X-100 in PBS on the horizontal oscillator at RT. After washing, the coverslips were incubated for at least 1 hour in the fluorescent-tagged secondary antibody solution supplemented with 5 µg/ml DAPI. The cells are washed twice for 5 minutes with 0.1% Triton X-100 in PBS and once with PBS. Finally, the coverslips are rinsed with water before being mounted with Fluoromount and dried overnight at RT.

All fluorescent stained samples were imaged at the epifluorescence microscope Nikon Eclipse T_i, most of the time with the 60x oil immersion objective. Images were taken using the NIS Elements program.

Proximity ligation assay

HEK293T cells were seeded on coverslips and transfected with ZNRF3-HA together with either GFP, GFP-USP42, GFP-USP42 ΔC or Dishevelled-GFP. If indicated, cells were treated with 1:50 R-spondin3 CM overnight. After the cells were fixed with 2%

PFA in PBS, they were permeabilised with 0.2% Triton X-100 for 10 minutes and the staining was performed following the Duolink PLA Fluorescence Protocol from Merck. In short, the permeabilised samples were blocked with the Duolink Blocking Solution for 60 minutes at 37 °C followed by the incubation of the primary antibodies (diluted in the Duolink Antibody Diluent) as for the immunofluorescent stainings in a humidified chamber. Then, the PLUS (rabbit) and MINUS (mouse) PLA Probes were diluted 1:5 and added to the samples after washing them twice with wash buffer A. The samples were incubated for 1 hour at 37 °C and washed twice with wash buffer A, before incubating them in 1x Duolink Ligation buffer containing the Ligase. The ligation step was performed at 37 °C for 30 minutes and washed two times with wash buffer A. Next, the samples were treated with 1x Amplification buffer supplemented with the Polymerase for 100 minutes at 37 °C. Finally, the samples were washed twice with wash buffer B and once with 0.01x wash buffer B prior to mounting them with the Duolink In Situ Mounting Medium with DAPI. Afterwards, the samples were stored at -20 °C and analysed at the epifluorescence microscope Nikon Eclipse T_i.

SNAP-assay

HEK293T cells were seeded on coverslips coated with poly-L-lysine. The following day, they were transfected with 100 ng SNAP-Frizzled plasmid together with either 200 ng PCS2+ (empty vector), 100 ng pEGFP-USP42 or 100 ng ZNRF3-HA. After 24 hours, the samples were incubated with 30 µl of 1 µM SNAP-Surface substrate 549 for 15 minutes at RT in a dark humidity chamber (Koo *et al.* 2012). Then, the cells were carefully washed twice with DMEM and chased for 10 minutes and fixed with 4% PFA in PBS.

Immunohistochemistry

First, a mouse was sacrificed and dissected. The small intestine and colon were separately transferred to PBS and carefully freed from fatty tissue without injuring the intestines. Next, the small intestine and colon were flushed several times with PBS to remove all remaining feces inside. Then, they were placed into Flacon tubes

and fixed overnight in 4% PFA in rotation at 4 °C. On the next day, the PFA was discarded and exchanged with 30% sucrose solution. Here, the intestine and the colon were flushed a few times with sucrose solution to replace all PFA solution. The intestines were incubated in sucrose solution in rotation for 48-72 hours at 4 °C. Before embedding the organs in Tissue-Tek, the were briefly rinsed in Tissue-Tek in a separate cryosection mold to get rid of the sucrose solution. Otherwise the tissue would have detached from the frozen Tissue-tek and the cryosectioning would have been difficult.

For embedding, half a cryosection mold was filled with Tissue-Tek and the small intestine was cut in three pieces, because it did not completely fit into a small mold. Then, the colon or an intestinal piece was placed into the mold. With a small forceps, the tissue was pushed to the bottom, so that it laid flat on the ground without squishing the tissue. With a pipette tip, bubbles were removed to enable a homogenous freezing. Finally, the molds were placed on a metal cooling block on dry ice until the Tissue-Tek was completely frozen. Afterwards, the blocks were stored at -20 °C, before the cryosectioning.

Cryosections were produced with 8 µm thickness and three sections were mounted onto Thermo Superfrost Plus microscope slides (they would fall of the Thermo Superfrost slides), using the Thermo cryostat. The tissue sections were allowed to dry at RT, before storing them at -20 °C.

Prior to performing the stainings, the slides were warmed to room temperature for 5 minutes. The slides were then placed in a holder into a large glass beaker filled with PBS to wash them for 5 minutes. Meanwhile, 1 litre the 1x cryo antigen retrieval buffer was prepared from the 10x stock and 500 µl Tween 20 was added fresh.

The holder with the slides is transferred into plastic containers filled with the cryo antigen retrieval buffer and microwaved for 5 minutes. Here, it was important that the slides were fully submerged. If some antigen retrieval buffer got lost during microwaving, it was immediately refilled with fresh buffer. After boiling, the slides in the microwaving container were cooled on ice for 30 minutes. Then, the slides were

placed into a glass jar with PBS to wash away the residual detergent. With a liquid blocker pen, borders were drawn around the tissue sections and they were incubated with IF blocking buffer at RT for 30 minutes in a humidity chamber. Afterwards, the blocking buffer is removed and the primary antibodies dissolved in blocking buffer were added on to the slides and incubated overnight at 4 °C in the humidified chamber. The following day, the slides were washed three times with PBS for 5 minutes per wash. The fluorescent-labelled secondary antibodies (1:500) supplemented with 5 µg/ml DAPI were added to the cryosections and incubated for at least 1 hour at RT in a dark humidity chamber. After washing three times with PBS, the slides were briefly rinsed with water and mounted with Fluoromount by adding the rectangular coverslips on top.

The slides were dried overnight at 37 °C, before imaging them at the Nikon Eclipse T_i.

Immunofluorescent staining of organoids

For staining organoids, they were grown to day 5 where they developed a lot of crypts. The medium was removed and the Matrigel domes were disrupted with 250 µl PBS per well, using a P1000 pipette without destroying the organoids. The organoids were transferred to a Falcon tube and centrifuged at 300 x g for 3 minutes. The supernatant was discarded and the organoids were fixed in 4% PFA for 15-20 minutes at RT. Then, they were washed three times with PBS, transferred to Eppendorf tubes and permeabilised with 500 µl 10% horse serum blocking buffer in PBS supplemented with 0.5% Triton X-100 and incubated for 1 hour. The primary antibodies are diluted in blocking buffer and 100 µl antibody solution was added to the samples (600 µl total volume). Under rotation, the organoids were incubated at 4 °C with the primary antibodies overnight. On the following day, the samples were washed three times with PBS supplemented with 0.2% Triton X-100. Shortly after, they were incubated in the fluorescent-labelled secondary antibodies (1:500) and DAPI (5 µg/ml) diluted in blocking buffer for 1 hour at RT in rotation. Finally, they were washed three times with PBS.

For imaging, the organoids were mounted in a drop of PBS and imaged at the Nikon

Imaging Center Heidelberg with the help of Nicolas Dross and Ulrike Engel. The microscope used was the Nikon A1 laser scanning confocal microscope.

Growth factor withdrawal experiment

For the growth factor withdrawal experiment non-edited and Usp42 KO organoids were split as described above (at least 3 wells were used per condition) and cultured in the indicated media for at least 2 passages:

1) Full organoid growth medium: EN medium supplemented with 20 nM Wnt surrogates and 10% R-Spondin 1 CM

2) EN medium without external Wnt supplemented with 10% R-spondin 1 CM

3) EN medium supplemented with 5% R-spondin 1 CM

4) EN medium supplemented with 2% R-spondin 1 CM

5) EN medium supplemented with 2% R-spondin 1 CM and 5 µM Wnt secretion inhibitor IWP2

5 days into passage number 2, the organoids were imaged at the Nikon binocular microscope SMZ25.

Spheroid growth assay

For the spheroid growth assay, 2,000 HCT116 parental and USP42 KO cells were seeded in 30 µl hanging drops of RPMI medium supplemented with 10% FBS and if indicated, also with 20 µM of the PORCN inhibitor LGK-974. The spheroids were grown for 6 days and images were taken at the Nikon SMZ25 binocular microscope.

Afterwards, the images were analysed in Fiji by creating a binary image (Process → Binary → Make Binary; **Figure 2.1**). If two spheroids were joined in one image and were in close proximity, the option 'Watershed' (Process → Binary → Watershed) was used to separate them. Then, the spheroid area was selected with the Wand

tool and measured (Analyze → Measure). Displayed were the pixel counts which were then multiplied by the pixel size (1.47 µm).

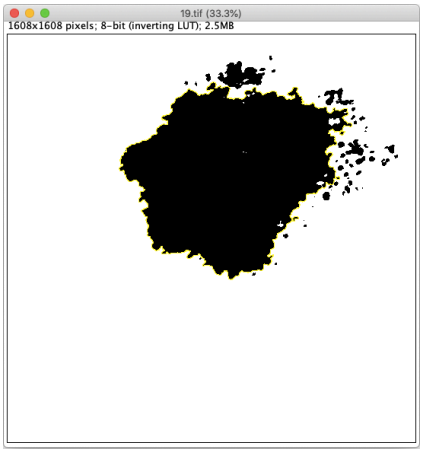

Figure 2.1: Example binary picture of a spheroid analysed in Fiji.

The spheroid growth assays were performed by Anchel de Jaime-Soguero. He seeded the cells and imaged the spheroids at the Nikon SMZ25 binocular microscope. For my PhD thesis, I re-analysed the images.

Bulk RNA sequencing sample preparation and analysis

The bulk RNA sequencing experiment was performed by Anchel de Jaime-Soguero and the members of the Genomics Core Facility (EMBL) Jonathan Landry, Laura Villacorta and Vladimir Benes. For my PhD thesis, I plotted the genes for epithelial-to-mesenchymal transition and intestinal stem cell signature genes in volcano plots (Merlos-Suarez *et al.* 2011, Rokavec *et al.* 2017).

For the bulk RNA sequencing samples, HCT116 cells were seeded in 6-well plates. On the next day, they were transfected with control siRNA or siUSP42. 48 hours later, they were harvested and the RNA of 3 independent experiments was extracted with the RNeasy Mini Kit (Qiagen). The assessment of total RNA integrity (RIN value) was

done with the Agilent 2100 Bioanalyzer machine using an Agilent RNA 6000 Nano chip, followed by the library preparation using the NEBNext Ultra II RNA Library Prep Kit for Illumina. After ensuring the quality of the cDNA libraries, they were pooled and sequenced. Using the STAR version 2.6.0a (Dobin *et al.* 2013) with GRCh38.84 human genome as reference, tables of the aligned sequences and counts per gene were generated. This dataset is accessible at European Nucleotide Archive (ENA) under the number PRJEB37946.

For the data analysis, the differential expression of genes was analysed according to Anders and Huber 2010 in R. Significantly up- or downregulated genes were categorized in signalling pathways and functions in the cells using the model-based gene set analysis (MGSA) according to Bauer *et al.* 2010. The analysed datasets were published in Giebel *et al.* 2021.

Volcano plots were generated by plotting the negative $\log_{10}$ of the p-values against the $\log_2$ fold change values of signature genes for Intestinal Stem Cells (ISC) (Merlos-Suarez *et al.* 2011) or epithelial-to-mesenchymal transition in cancer cells (Rokavec *et al.* 2017).

***In silico* analysis: Expression of USP42 and mutations in colorectal cancer**

In silico analysis of USP42 was performed on the TCGA PanCancer Atlas colorectal adenocarcinoma dataset with samples collected from 524 patients on cBioPortal for cancer genomics (Cerami *et al.* 2012 and Gao *et al.* 2013).

***In silico* analysis: Multiple sequence alignment**

The aminoacid sequences of USP42 for *H. sapiens*, *D. Rerio, M. musculus, X. laevis* and *X. tropicalis* were obtained from Uniprot. Using the Clustal Omega website a Multiple Sequence Alignment was performed.

Statistical analysis

Results of statistical analyses are shown as mean ± standard deviation. Statistical significance was assessed in GraphPad Prism 8 by performing either a Student's t-

test for two groups or a one-way ANOVA analysis with Tukey correction for three or more groups. *P-values < 0.05 were considered significant (**P < 0.01, ***P < 0.001) and not significant was indicated with ‘n.s.’.

3. Results

3.1 USP42 negatively regulates Wnt signalling on the Wnt receptor level

The E3 ubiquitin-protein ligases ZNRF3 and RNF43 have been shown to be the main negative Wnt regulators in adult stem cells, and are also often mutated in Wnt-associated cancer cells, such as colorectal cancer. They ubiquitinate and destabilise the Wnt receptors Frizzled and LRP, thereby inhibiting Wnt signalling. Upon binding to R-spondin and LGR4/5/6 ZNRF3 and RNF43 autoubiquitinate themselves and are then internalised, rendering active Wnt signalling. To identify a potential candidate deubiquitinase which can counteract this autoubiquitination, I performed a biased Wnt reporter assay screening (Figure 3.1.1A). Various deubiquitinases, which have been shown to be mutated over 5% in colorectal cancer (cBioPortal, Genentech, Nature 2012), were knocked down by siRNA and compared to the effect of ZNRF3 in HEK293T cells upon Wnt activation. I hypothesised that a deubiquitinase that stabilises ZNRF3 should have a similar negative effect on Wnt signalling. In fact, when ZNRF3, USP42 (3.5-fold induction) or USP31 were silenced, Wnt signalling increased in those cells upon Wnt activation in comparison to the control siRNA treated cells. Interestingly, when USP42 was knocked down in HEK293T ZNRF3/RNF43 double knockout cells, Wnt signalling increased in the parental cells, but not in the double knockout cells (Figure 3.1.1B). This indicates that USP42 controls Wnt signalling through ZNRF3 and RNF43.

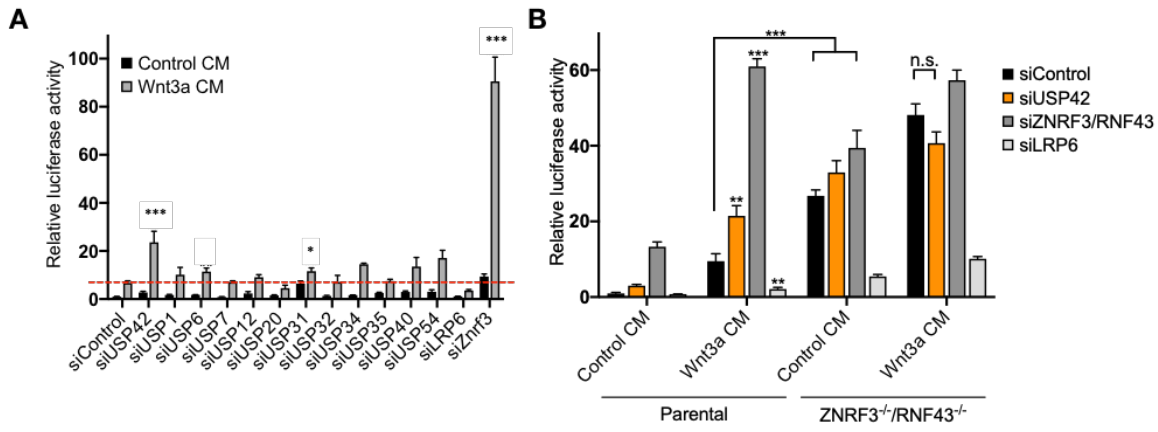

Figure 3.1.1: Screen in a Wnt reporter assay of deubiquitinating enzymes (DUB) which could potentially stabilise ZNRF3/RNF43

A) HEK293T cells were transfected with the indicated siDUBs or the controls siLRP6 and siZNRF3 and treated with either control or Wnt3a conditioned media (CM).

B) Parental or ZNRF3$^{-/-}$/RNF43$^{-/-}$ cells were transfected with siRNA against USP42, ZNRF3/RNF43 or LRP6, scrambled siRNA served as the control. The cells were treated with either control or Wnt3a conditioned media.

Displayed are representative images of three independent experiments with three biological replicates. Statistical significant differences between the means with standard deviations were calculated with a one-way ANOVA analysis with Tukey correction (*$p < 0.05$, **$p < 0.01$, ***$p < 0.001$, n.s. is not significant).

In the last years, cell signalling crosstalk and interactions have gained a lot of interest. Since USP42 is known to interact with and deubiquitinate p53 in DNA damage stress response, I wanted to exclude that the observed effects of USP42 on Wnt signalling are mediated by p53, instead of ZNRF3/RNF43 (Hock *et al.* 2011). Therefore, I performed a Wnt reporter assay, as well as a p53 reporter assay, upon knockdown of USP42 and p53 (TP53) in HEK293T cells (Figure 3.1.2). Knockdown of USP42 was able to activate Wnt signalling (by 2.7-fold) in HEK293T cells in comparison to the control even without exogenous Wnt stimulation. Upon Wnt activation, Wnt signalling strongly increased in siUSP42 treated cells, but not upon siTP53. On the other hand, siUSP42 as well as siTP53 were able to decrease p53 signalling in a p53 reporter assay, showing that both siRNA are functional. Thus, these data indicate that the increase of Wnt reporter activity upon USP42 knockdown are independent from p53 signalling, but instead mediated by ZNRF3/RNF43.

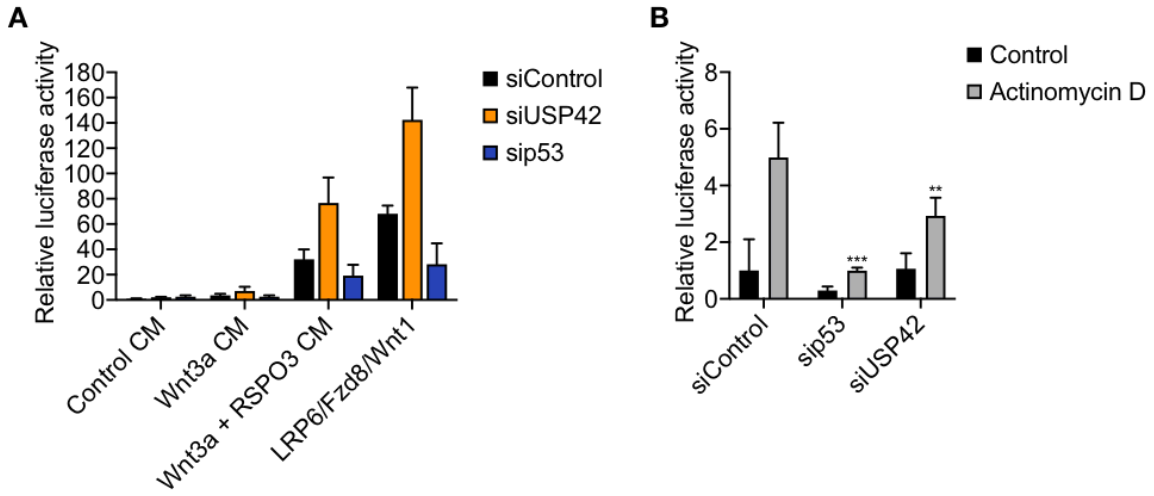

Figure 3.1.2: The effect of siUSP42 in Wnt signalling is independent of USP42 function in p53 signalling

A) HEK293T cells were transfected with siRNA against USP42 or p53. To activate Wnt signalling, the cells were either treated with the indicated media or transfected with LRP6/Fzd8/Wnt1.

B) siRNA against p53 or USP42 were transfected into HEK293T cells in a p53 reporter assay. To activate p53 signalling, cells were treated with Actinomycin D.

Displayed are representative images of three independent experiments with three biological replicates. Statistical significant differences between the means with standard deviations were calculated with a one-way ANOVA analysis with Tukey correction (*$p < 0.05$, **$p < 0.01$, ***$p < 0.001$).

In addition, I wanted to validate the signal specific response of USP42 by checking its activity through other known signal pathways. I tested the effect of USP42 in a FGF and TGFβ reporter assays by knocking down of USP42 in HEK293T cells (Figure 3.1.3A). Knockdown of USP42 did not have any effect on FGF signalling, but increased TGFβ signalling in comparison to the control by 1.3-fold. To validate this effect, the TGFβ reporter assay was additionally performed in a USP42 knockout cell line, as well as in an APC knockout cell line (Figure 3.1.3B). Knockout of USP42 and APC both increased TGFβ signalling in comparison to the control, which means that the effect of USP42 in TGFβ signalling is unspecific to USP42, but rather to increased Wnt signalling.

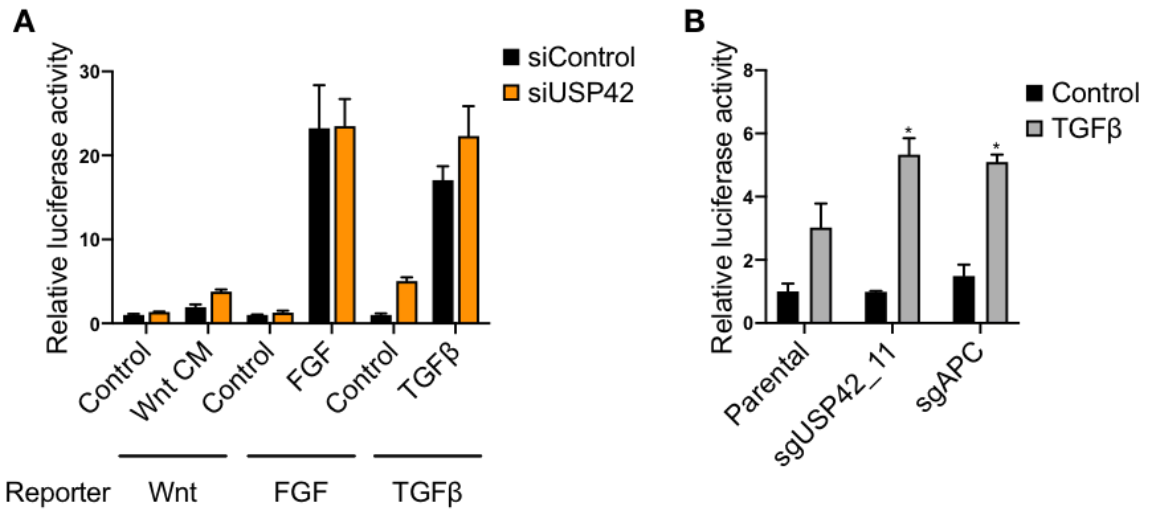

Figure 3.1.3: Loss of USP42 and APC function increases TGFβ signalling
A) HEK293T cells were transfected with either siControl or siUSP42 and treated with either Wnt3a conditioned medium (1:5), 50 ng/ml FGF or 2 ng/ml of TGFβ in the respected reporter.
B) Parental HEK293T cells, sgUSP42 or sgAPC knockout cell lines were treated with TGFβ in a TGFβ reporter assay.
Displayed are representative images of three (A) and two (B) independent experiments with three biological replicates. Statistical significant differences between the means with standard deviations were calculated with a one-way ANOVA analysis with Tukey correction with a two-tailed distribution (*$p < 0.05$, **$p < 0.01$, ***$p < 0.001$).

siRNA validation is an important control when silencing gene expression. Therefore, I tested several siRNA against USP42 (single siRNA and in pools) in Wnt reporter assays in HEK293T cells to ensure a proper knockdown of USP42 (Figure 3.1.4A). This assay shows that siRNA #D3, #D7 and #D12 were able to increase Wnt signalling in HEK293T cells without (2.5-fold increase) and upon external Wnt activation in comparison to the control siRNA (1.8- to 2.5-fold). Next, I validated that siRNA against USP42 decreases its protein levels in HEK293T cells by immunofluorescent stainings (Figure 3.1.4B). In control conditions, USP42 mainly localises in the nucleus and in a smaller proportion in the cytoplasm. Transfection with siUSP42 decreases the protein amounts in both cellular compartments.

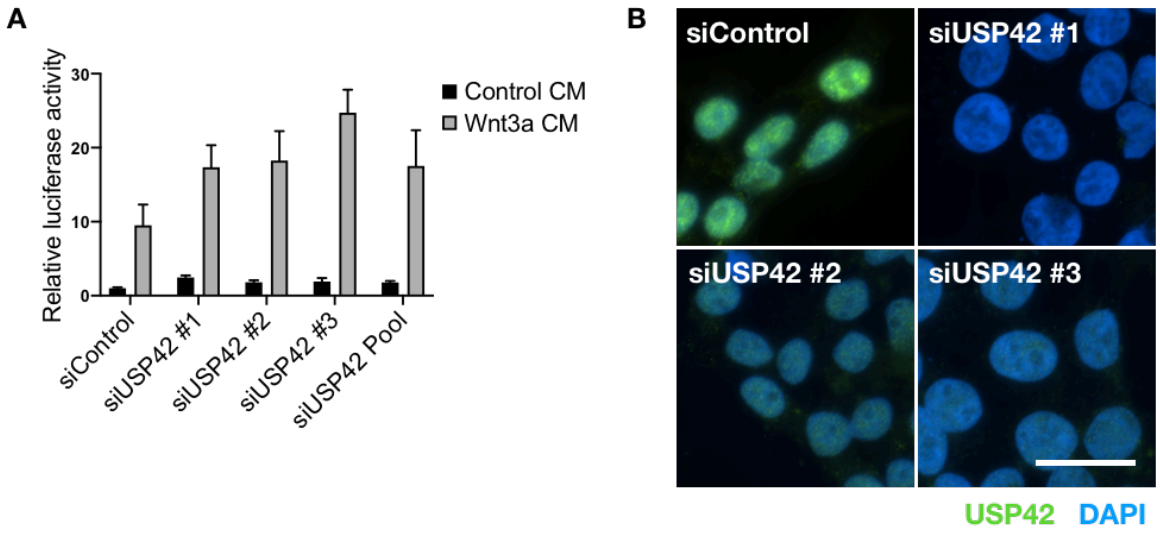

Figure 3.1.4: Different siUSP42 increase Wnt signalling and reduce USP42 protein levels in HEK293T cells.

A) Representative (out of 3 independent experiments) TOPflash dual-luciferase reporter assay, in which HEK293T cells were transfected with different siUSP42 and treated with either control or Wnt3a conditioned media to test their efficiency to increase Wnt signalling.

B) Test of different siUSP42 of their efficiency to reduce USP42 protein levels in HEK293T cells (green = USP42, blue = DAPI, scale bar = 10 µm).

To further validate USP42 as a negative Wnt regulator, I analysed the effect of USP42 on β-catenin accumulation (Figure 3.1.5). Since H1703 cells show clear β-catenin accumulation in immunofluorescent stainings, H1703 cells were transfected with either GFP or GFP-USP42 and treated with control or Wnt3a conditioned media. Overexpression of USP42 decreased the amount of nuclear β-catenin, which indicates that overexpression of USP42 decreases Wnt signalling in H1703 cells.

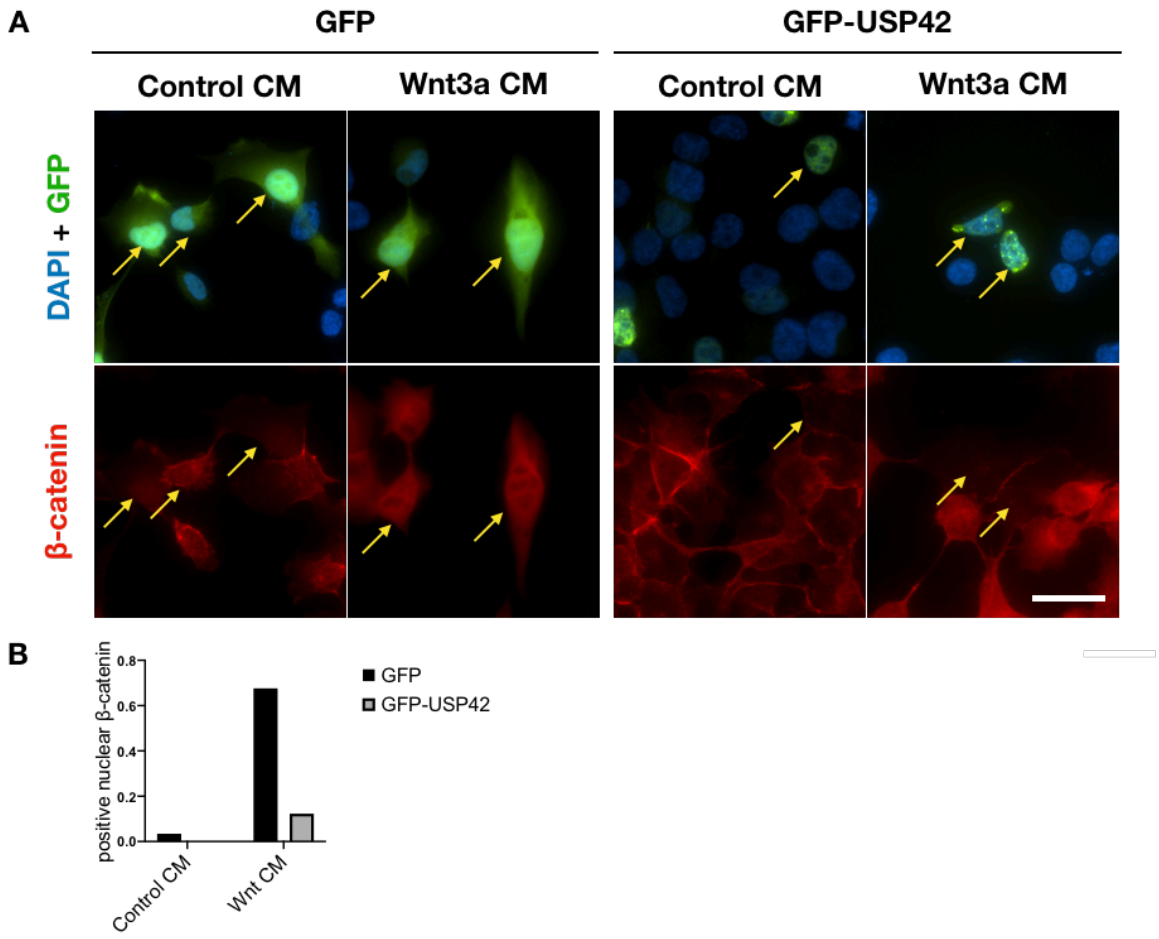

Figure 3.1.5: USP42 inhibits Wnt signalling in H1703 cells.
A) Immunofluorescent staining of endogenous β-catenin upon USP42 overexpression (green = GFP or GFP-USP42, red = β-catenin, blue = DAPI, yellow arrows indicate transfected cells, scale bar = 10 µm).
B) Quantification of nuclear β-catenin positive cells upon USP42 overexpression with or without Wnt activation (n = 50 cells per condition).

ZNRF3 and RNF43 can be antagonised by R-spondin and LGR4/5/6. To further determine USP42 as a potential candidate to regulate Wnt signalling via ZNRF3/RNF43, I analysed the effect of USP42 on the Wnt receptor level in Wnt reporter assays upon treatment with the four R-spondin proteins (Figure 3.1.6). HEK293T cells were treated with either control or a combination of Wnt and the indicated R-spondin conditioned media and Wnt signalling was monitored by Wnt reporter assays. Knockdown of USP42 increased Wnt signalling upon R-spondin treatments in comparison to the control (RSPO1 and 4: 3-fold, RSPO2: 2.43-fold and RSPO3: 1.57-fold), while R-spondin 3ΔC (lacking the C-

terminal) increased Wnt signalling the strongest in treated cells. On the other hand, overexpression of USP42 or ZNRF3 successfully decreased Wnt signalling upon treatment with the different R-spondins (RSPO1, 2 and 4: reduction of 2/3, RSPO3: ½). Moreover, the catalytically inactive mutant USP42 C120A was not able to decrease Wnt signalling upon R-spondin treatment, indicating that the catalytically active centre of USP42 is required for the inhibition of Wnt signalling at the Wnt receptor level.

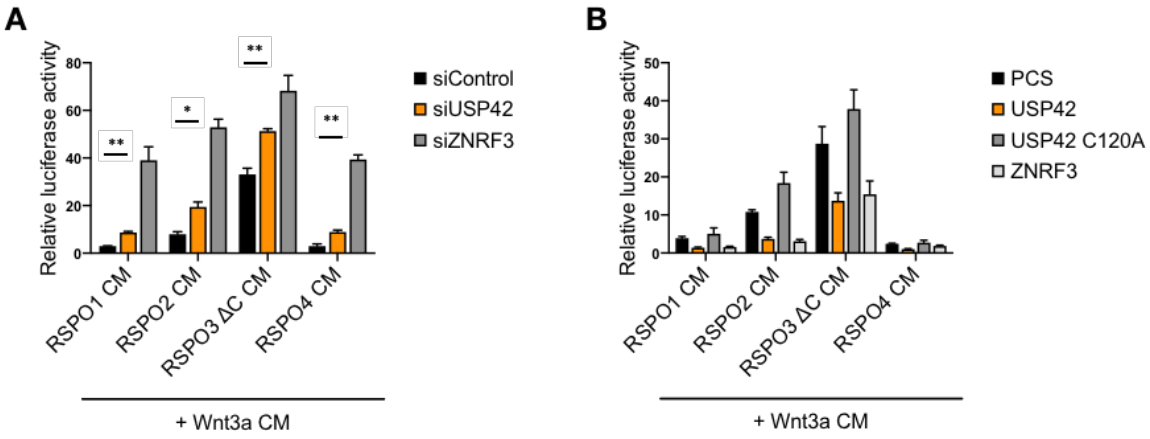

Figure 3.1.6: USP42 negatively regulates Wnt signalling on the R-spondin/LGR level
A) TOPflash reporter assay in HEK293T cells upon siUSP42 treated with different R-spondin conditioned media together with Wnt3a CM.
B) Wnt reporter assay in HEK293T cells upon overexpression of USP42, the catalytically inactive mutant USP42 C120A or ZNRF3, treated with the different R-spondin conditioned media together with Wnt3a.
These are representative experiments out of three independent experiment, with three biological replicates. Signals were normalised to the siControl or empty vector (PCS) sample treated with control conditioned medium. Statistical significant differences between the means with standard deviations were calculated with a one-way ANOVA analysis with Tukey correction with a two-tailed distribution (*$p < 0.05$, **$p < 0.01$, ***$p < 0.001$).

Additionally, I performed an epistasis experiment with either knockdown or overexpression of USP42 in Wnt reporter assays (Figure 3.1.7 and 3.1.8). HEK293T cells were transfected with the indicated siRNA and plasmids, or were treated with either control, Wnt3a or a combination of Wnt3a and R-spondin 3ΔC conditioned media, to activate Wnt signalling on different levels of the signalling cascade. Knockdown of USP42 or APC increased Wnt signalling by about 2-fold (siUSP42) in comparison to the controls.

The strongest effect of USP42 could be observed on the Wnt receptor level, narrowing down the interaction partners for USP42 in Wnt signalling. Also, knockdown of USP42 did not have any effect on the β-catenin level, indicating that USP42 works upstream of β-catenin.

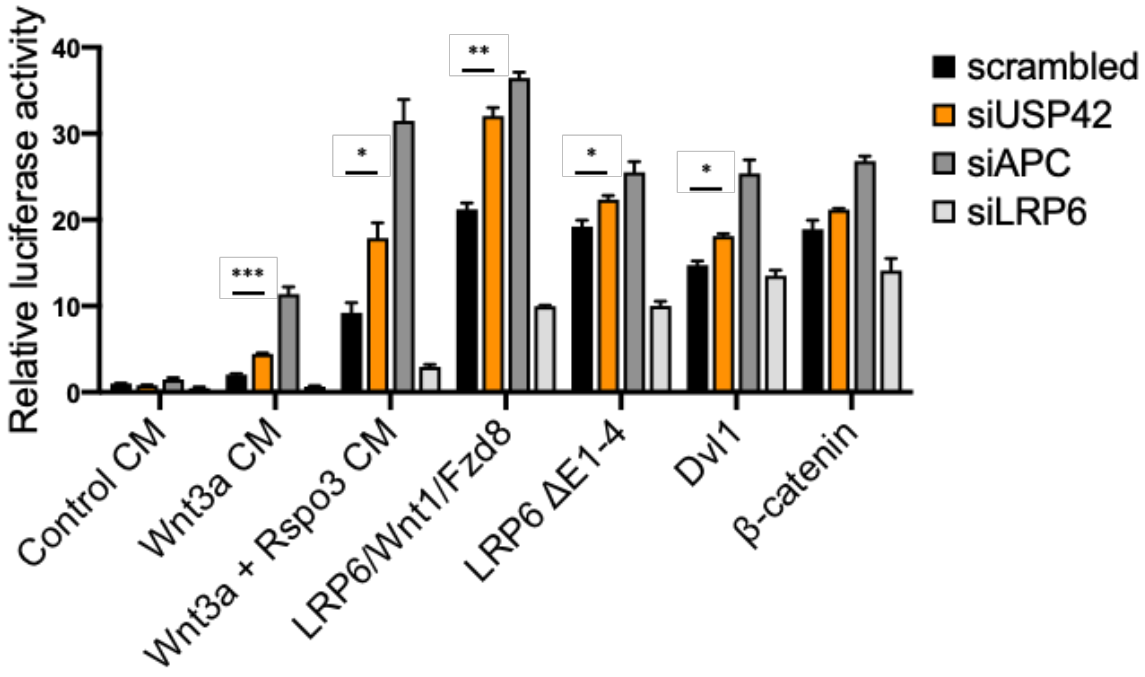

Figure 3.1.7: Knockdown of USP42 increases Wnt signalling on the Wnt receptor level
HEK293T cells were transfected with the indicated siRNA. Wnt signalling was activated on different levels of the Wnt signalling pathway by overexpression of the indicated plasmids or treatment with Wnt3a or Wnt3a + R-Spondin3 conditioned media. Representative epistasis experiment in a TOPflash reporter assay (out of three independent experiments, each condition in triplicates).
Displayed are representative images of three independent experiments with three biological replicates. Statistical significant differences between the means with standard deviations were calculated with a one-way ANOVA analysis with Tukey correction with a two-tailed distribution (*$p < 0.05$, **$p < 0.01$, ***$p < 0.001$).

Then, overexpression of USP42 decreased Wnt signalling upstream of β-catenin by half of the control signal (PCS), whereas the catalytically inactive mutant USP42 C120A, as well as the control deubiquitinating enzyme USP39 did not have any effect on Wnt signalling.

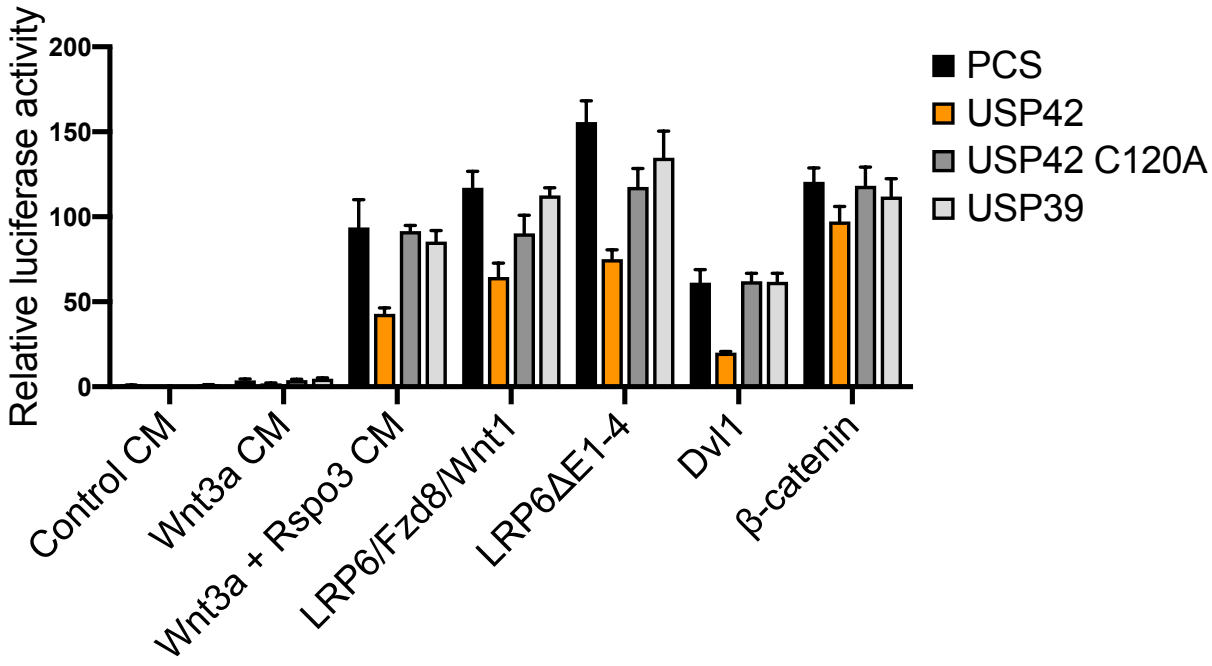

Figure 3.1.8: USP42 inhibits Wnt signalling upstream of β-catenin
HEK293T cells were transfected with either USP42, catalytically inactive USP42, the control deubiquitinating enzyme USP39 or the control empty vector (PCS2+). To activate Wnt signalling, the indicated plasmids were overexpressed or the cells were treated with Wnt3a or Wnt3a + R-Spondin 3 conditioned media. Representative experiment out of three independent experiments.

Finally, I demonstrated that the loss of USP42 in Wnt signalling can be rescued by overexpression of USP42 or ZNRF3/RNF43 (Figure 3.1.9). Therefore, I transfected USP42 knockout cells and the parental cells with either USP42, the catalytically inactive mutant C120A or ZNRF3/RNF43 and treated them with either control or Wnt3a conditioned media. Wnt signalling is increased in USP42 knockout cells even under control conditions. When transfected with USP42 or ZNRF3, Wnt signalling is clearly decreased in comparison to a transfection with the C120A mutant or the empty plasmid.

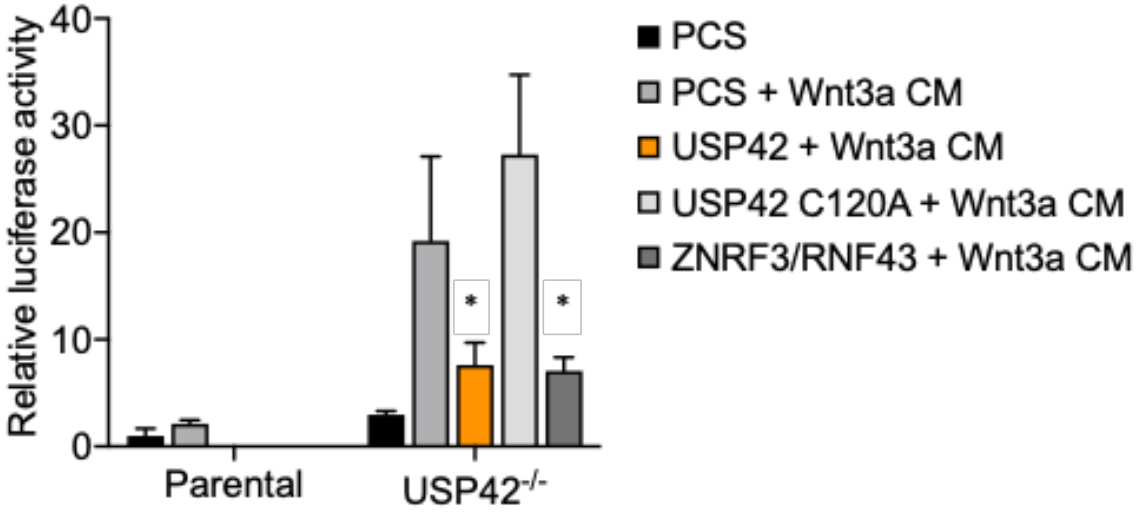

Figure 3.1.9: Functional USP42 overexpression rescues inhibition of Wnt signalling in USP42$^{-/-}$ HEK293T cells.
Comparison of parental and USP42$^{-/-}$ HEK293T cells in a TOPflash reporter assay, upon overexpression of USP42, catalytically inactive mutant USP42 C120A or ZNRF3/RNF43. Wnt signalling was activated by adding Wnt3a to the cells. Firefly luciferase signals were normalised to the control conditioned medium. This is a representative experiment out of two independent experiments with three biological replicates. Statistical significant differences between the means with standard deviations were calculated with a one-way ANOVA analysis with Tukey correction with a two-tailed distribution (*$p < 0.05$, **$p < 0.01$, ***$p < 0.001$).

Taking these results together, I concluded that USP42 functions as a negative Wnt regulator which acts at the Wnt receptor level via ZNRF3/RNF43 and not p53.

3.2 USP42 deubiquitinates and stabilises ZNRF3/RNF43 at the plasma membrane

To test whether USP42 and ZNRF3 are direct interaction partners, I performed a proximity ligation assay (PLA, Figure 3.2.1). Therefore, HEK293T cells were transfected with plasmids encoding either pEGFP-USP42, pEGFP-USP42 ΔC, EGFP-N1 (as negative control) or xDVL-GFP (as positive control) together with ZNRF3-HA. The primary antibodies used in the PLA bind to the HA-tag, or the GFP-tag respectively. These are detected by secondary antibodies tagged with oligonucleotides, which can be ligated to

a circular DNA, if the interacting proteins are in close proximity. After amplification, fluorescent-labelled oligonucleotides hybridise to the complementary sequence and the localisation of the interaction is revealed as tiny dots. In this proximity ligation assay, I was able to detect signals of the interaction, especially in the cytoplasm of cells overexpressing ZNRF3 together with USP42 ΔC and Dishevelled. Interestingly, PLA signals could also be detected in the nucleus in cells overexpressing USP42 together with ZNRF3. I hypothesised that treatment with R-spondin 3 could increase the interactions, since R-spondin 3 and Lgr4/5/6 antagonise ZNRF3/RNF43. Cells transfected with ZNRF3 and USP42 with additional R-spondin 3 treatment showed similar interaction levels as without the treatment. I concluded, that there probably was not enough endogenous Lgr4/5/6 present in the cells to increase the amount of interactions. Indeed, overexpression is necessary for an increase in interactions between ZNRF3 and USP42 (Figure 3.2.9).

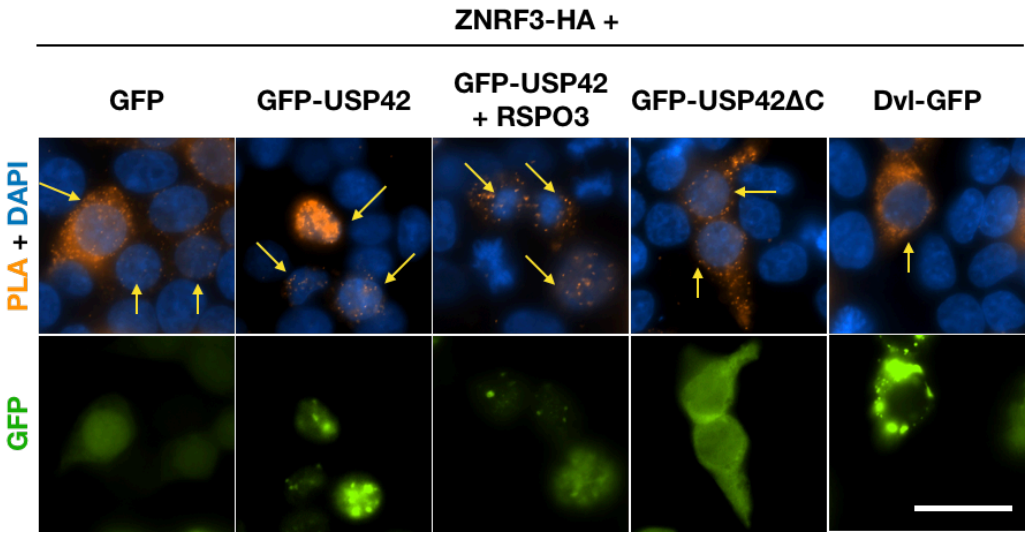

Figure 3.2.1: USP42 interacts with ZNRF3 in the cytoplasm
Representative proximity ligation assay upon overexpression of ZNRF3 together with GFP-USP42, cytoplasmic GFP-USP42 ΔC or the controls GFP (negative control) or Dishevelled (positive control). PLA signal indicates the amount of interaction between ZNRF3 and the overexpressed constructs (green = GFP construct, orange = PLA signal, blue = DAPI, scale bar =10 µm).

Quantifying the PLA interaction signal, I noticed that the amount of interactions with the negative control GFP correlates with the amount of overexpressed GFP in the cells and results in unspecific interactions. Due to high amounts of expressed GFP, close proximity with overexpressed ZNRF3 was inevitable, which resulted in positive PLA signal. For this reason I quantified the interactions only in the GFP cells with similar green intensity as USP42 overexpressing cells (Figure 3.2.2). PLA signal dots were counted and divided into five groups, with grade 5 having the highest counted interactions and grade 1 having none.

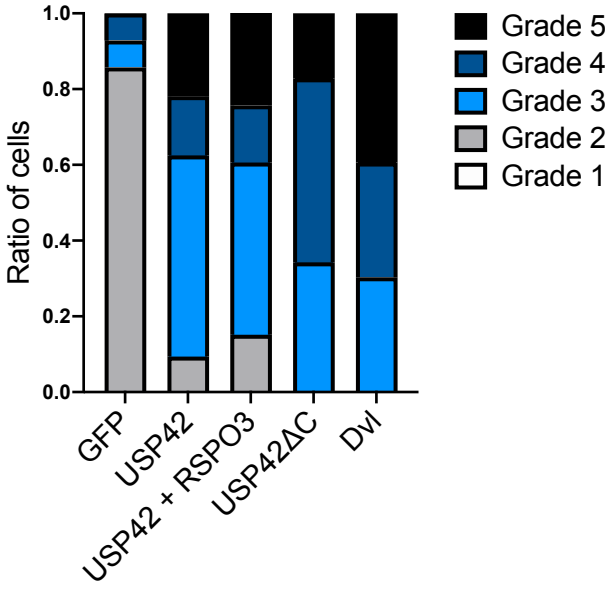

Figure 3.2.2: Cytoplasmic USP42 strongly interacts with ZNRF3.
Quantification of the proximity ligation assay shown in Figure 3.2.1. Counted were the PLA signal dots and the quantity was assigned to a group. For each condition except GFP (n = 14), at least 30 cells were analysed. Grade 5 = highest interactions, grade 1 = no interaction.

Next, I verified this interaction between USP42 and ZNRF3 by a co-immunoprecipitation (Figure 3.2.3). HEK293T cells were transfected with either pEGFP-FLAG-USP42, xDvl-GFP or EGFP-N1 plasmids, together with the negative Wnt regulators ZNRF3-HA or Axin1. The immunoprecipitation was performed against GFP. GFP was able to co-precipitate neither Axin1 nor ZNRF3 (lane 7 and 8), whereas Dishevelled co-precipitated both (lane 11 and 12). USP42 co-precipitated ZNRF3 (lane 10), but not Axin1 (lane 9), which confirms the

direct interaction between USP42 and ZNRF3. Also, I analysed by co-immunoprecipitation if USP42 could bind other negative Wnt regulators, such as GSK3 or CK1α (Figure 3.2.4). However, USP42 did not co-precipitate GSK3 or CK1α. This shows that the interaction between USP42 and ZNRF3 is specific.

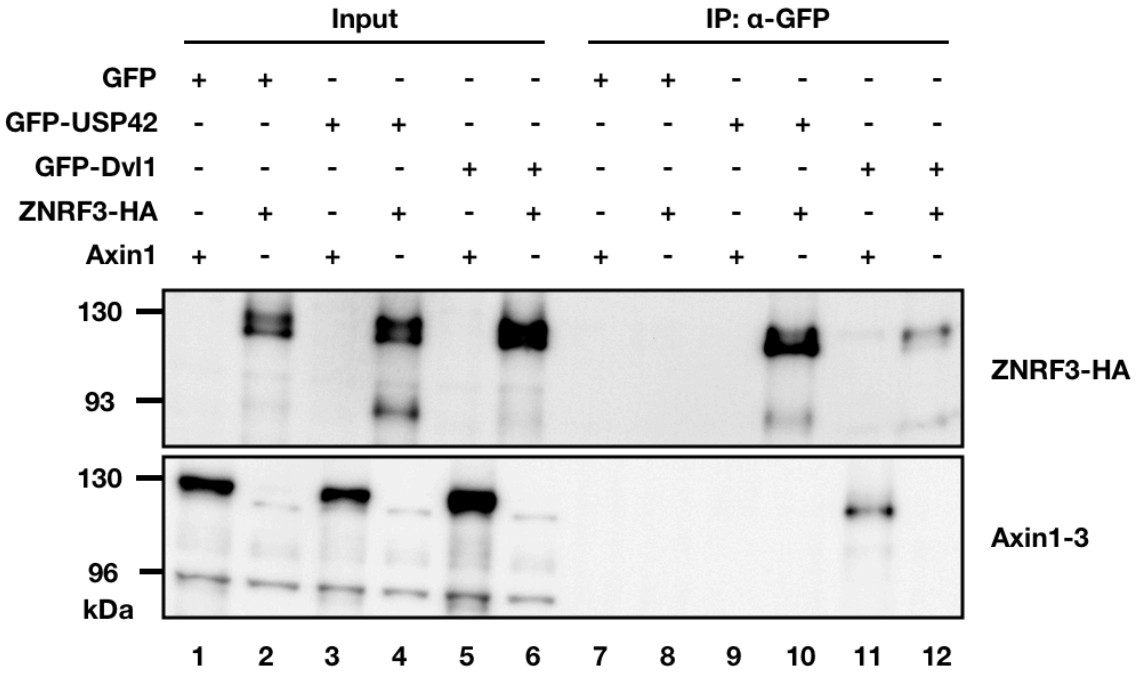

Figure 3.2.3: USP42 co-precipitates ZNRF3, but not Axin.
Representative (out of 3 independent experiments) α-GFP co-immunoprecipitation upon overexpression of ZNRF3 or Axin1 together with either GFP (negative control), Dishevelled (positive control) or USP42.

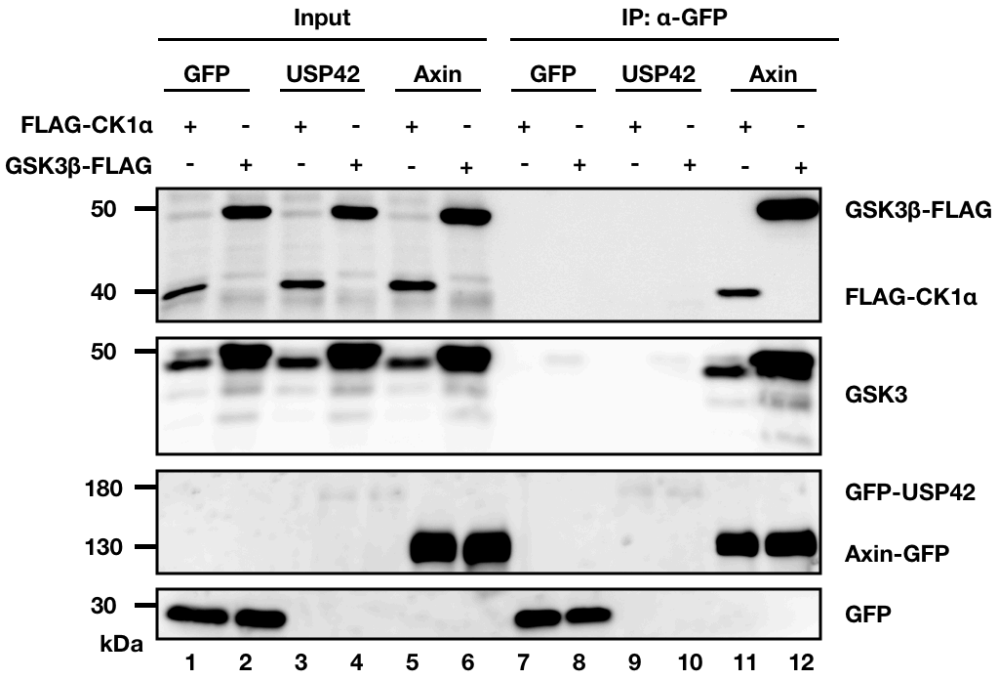

Figure 3.2.4: USP42 does not co-precipitate GSK3β or CK1α.
Co-immunoprecipitation against GFP upon overexpression of either GSK3 or CK1 together with GFP (negative control), Axin (positive control) or USP42. Representative IP out of 2 independent experiments.

Then, the question arose whether the interaction between USP42 and ZNRF3 has a functional impact. Since USP42 is a deubiquitinase and I wanted to investigate a mechanism which counteracts the auto-ubiquitination of ZNRF3 and RNF43, I performed an ubiquitination assay upon overexpression and knockdown of USP42 (Figure 3.2.5, 3.2.6 and 3.2.7). HEK293T cells were transfected with either ZNRF3-FLAG or RNF43-FLAG, together with the ubiquitin-HA WT plasmid and the pEGFP-USP42 plasmid. In addition, the cells were treated with the proteasome inhibitor MG132 and the vacuolar-type H^+-ATPase (V-ATPase) inhibitor, which blocks lysosomal acidification. The ubiquitination assay shows that overexpression of USP42 not only decreased the amount of ubiquitinated ZNRF3 and RNF43, but also increased the amount of ZNRF3 in comparison to the control siRNA (Figure 3.2.5 and 3.2.6, lane 4). Contrary, the amount of ubiquitinated ZNRF3 increases upon knockdown of USP42 compared to the control siRNA (Figure 3.2.7, lane 4-6). Here, ZNRF3 was overexpressed together with siRNA against USP42 and ubiquitin WT, K48 ubiquitin or K63 ubiquitin.

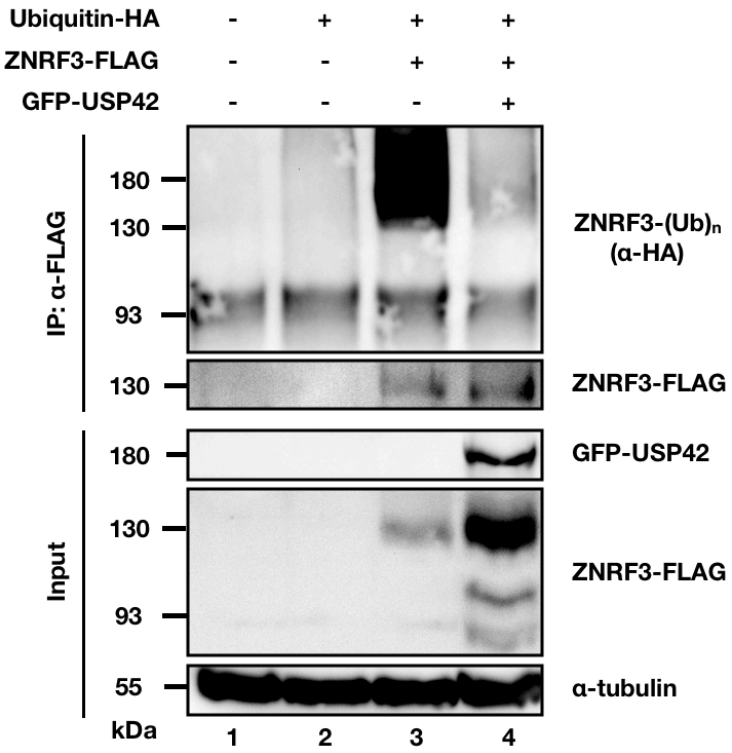

Figure 3.2.5: USP42 stabilises ZNRF3 and decreases the amount of ubiquitinated ZNRF3.

HEK293T cells were transfected with Ubiquitin-HA and ZNRF3-FLAG with or without USP42. The pulldown was performed against the substrate ZNRF3-FLAG. Representative image (out of 3 independent experiments) of an ubiquitination assay upon overexpression of USP42.

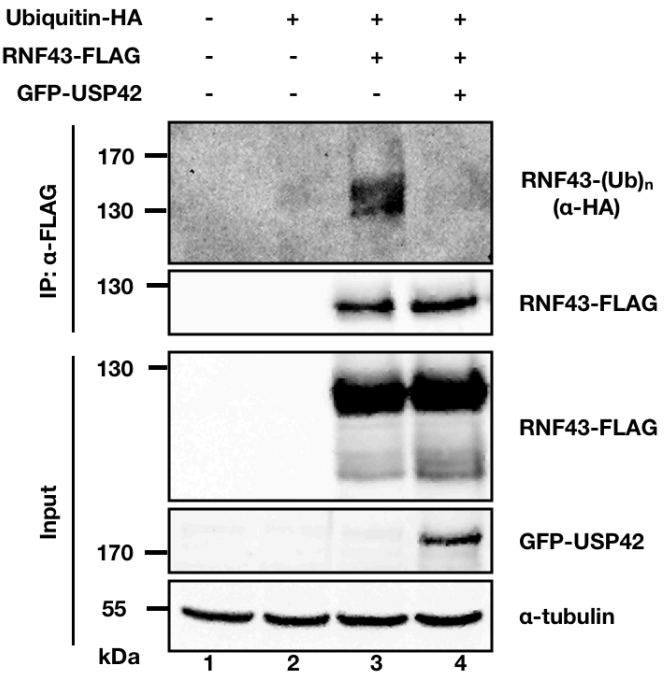

Figure 3.2.6: USP42 stabilises RNF43 by deubiquitination.
HEK293T cells were transfected with Ubiquitin-HA and RNF43-FLAG together with or without USP42. The pulldown was performed against the substrate RNF43-FLAG Representative ubiquitination assay of RNF43 upon USP42 overexpression (out of 3 independent experiments).

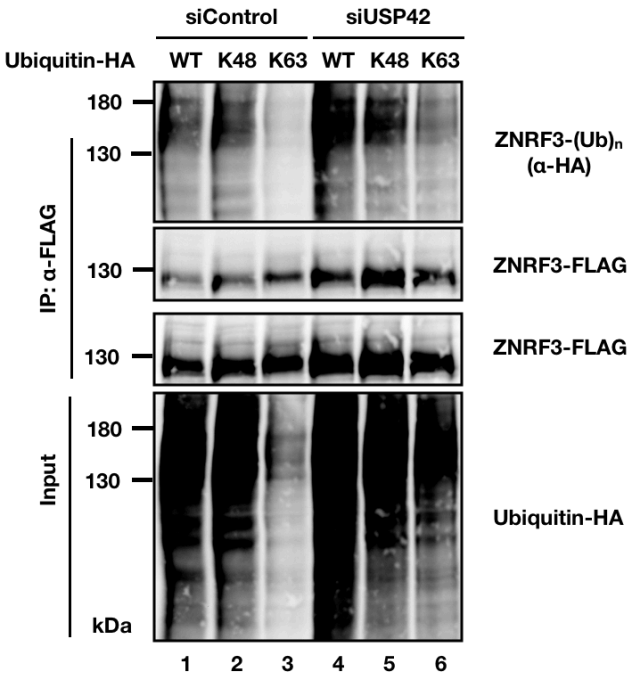

Figure 3.2.7: Loss of USP42 increases the amount of ubiquitinated ZNRF3.
HEK293T cells transfected with control siRNA or siUSP42 overexpressed ZNRF3- FLAG and Ubiquitin-HA WT, K48 or K63. The IP was performed against ZNRF3-FLAG. Representative experiment of three independent ubiquitination assays upon knockdown of USP42.

Furthermore, our collaborator Vanesa Fernández-Saíz (TranslaTUM, TUM, Munich, Germany) performed a surface biotinylation assay (Figure 3.2.8). First, the proteins at the cell membrane are marked by Biotin-Avidin binding and immunoprecipitated against Biotin/Avidin. The second immunoprecipitation targets the substrate, in this case ZNRF3 and RNF43. CUL1 served as the loading control. Similar to my results from the co-immunoprecipitation, overexpression of USP42 was able to stabilise ZNRF3 (lane 4) and RNF43 (lane 8) at the cell membrane and decreased the amount of ubiquitinated ZNRF3 and RNF43.

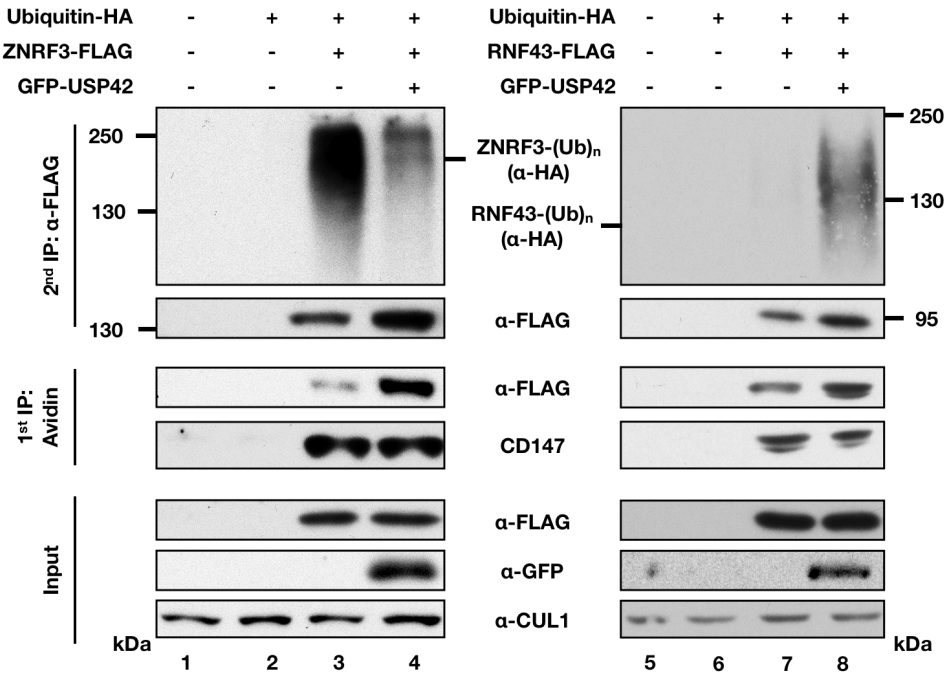

Figure 3.2.8: USP42 deubiquitinates ZNRF3/RNF43 at the membrane.
Cell surface biotinylation assay upon USP42 overexpression. The first IP was performed against Biotin/Avidin, the second IP was against the substrate ZNRF3 (left) or RNF43 (right, α-FLAG). CUL1 served as the loading control.

Finally, Sergio performed a co-immunoprecipitation to analyse the effect of R-spondin and LGR binding on the interaction between USP42 and ZNRF3 (Figure 3.2.9). USP42 ΔNLS co-precipitated more ZNRF3 when R-spondin and LGR4 were actively binding (lane 4), in comparison to the control without R-spondin (lane 2).

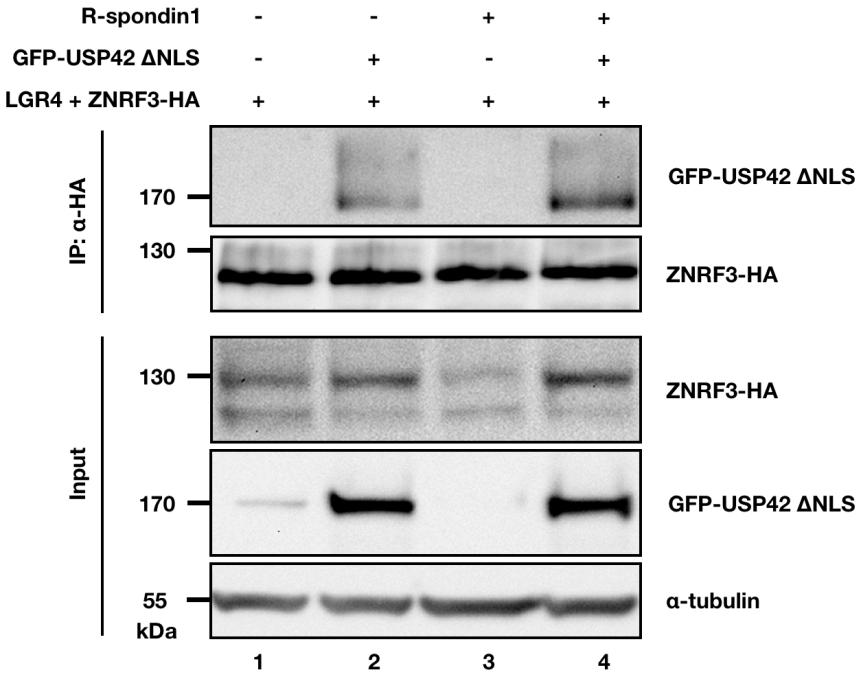

Figure 3.2.9: USP42 binds better to ZNRF3 upon binding to R-spondin and LGR4.
HEK293T cells were transfected with LGR4 and ZNRF3-HA, together with or without USP42 ΔNLS and upon R-Spondin 1 treatment. The co-IP was performed against ZNRF3-HA. Representative co-IP of overexpressed USP42 ΔNLS forming a complex with ZNRF3, R-spondin and LGR4.

3.3 USP42 and ZNRF3 interact through the Dishevelled interacting region (DIR) of ZNRF3

Now that the functional interaction between USP42 and ZNRF3/RNF43 was confirmed, I wanted to determine the protein domains required for this interaction. Therefore, I generated truncation mutants for ZNRF3 and USP42 by PCR with the help of Ana García del Arco and Anchel de Jaime-Soguero (Figure 3.3.1). The USP42 truncations were lacking either the predicted nuclear localisation signal, the C- or N-terminal, whereas the

ZNRF3 truncations lacked the RING domain, the Dishevelled interaction region or the linker between those two domains.

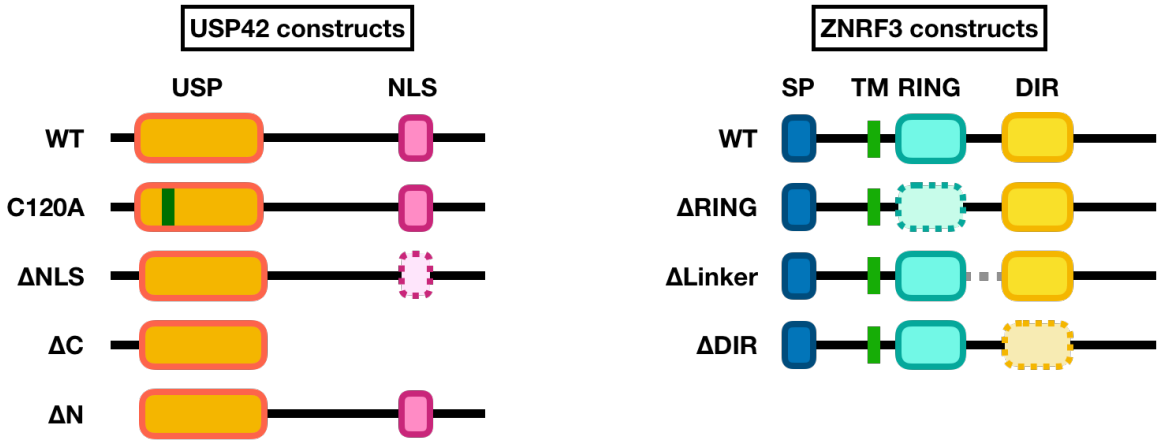

Figure 3.3.1: USP42 and ZNRF3 truncation mutants
Left: USP42 truncation mutants, USP = ubiquitin specific protease domain, NLS = nuclear localisation signal, C120A = catalytically inactive USP42 mutant
Right: ZNRF3 truncation mutants, SP =signal peptide, TM = transmembrane domain, RING = RING finger domain, DIR = Dishevelled interacting region.
Dotted lines indicate the excluded region.

I overexpressed the GFP-tagged USP42 truncation mutants and the catalytically inactive mutant C120A in HEK293T cells and analysed them by fluorescent microscopy to see if the truncation mutations change the subcellular localisation of USP42 (Figure 3.3.2). Indeed, USP42 wild type (WT) and the C120A mutant were mainly localised in the nucleus, while the ΔN mutant was ubiquitously expressed. Interestingly, the ΔNLS and ΔC mutants were only present in the cytoplasm.

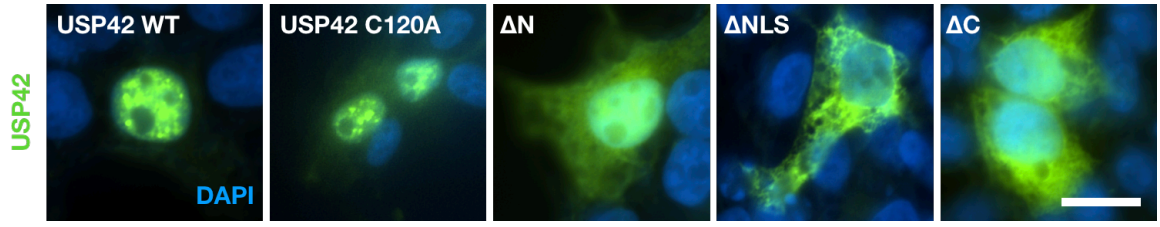

Figure 3.3.2: Deletion of the C-terminal and NLS of USP42 leads to a change of localisation into the cytoplasm.
HEK293T cells overexpressing the different constructs of GFP-tagged USP42 (green, blue = DAPI, scale bar = 5 µm).

To investigate the impact of the USP42 deletion constructs I performed a Wnt reporter assay. If overexpressed in HEK293T cells and analysed for their functionality in a Wnt reporter assay, USP42 WT, ΔNLS and ΔC were able to inhibit Wnt signalling significantly in comparison to the control, whereas USP42 C120A and USP42 ΔN did not have any effect on Wnt signalling (Figure 3.3.3). USP42 ΔC also seems to have the highest negative effect on Wnt signalling. In addition, I tested the different ZNRF3 truncation mutants in a Wnt reporter assay upon Wnt activation with Wnt3a and R-spondin3 conditioned media (Figure 3.3.4). Besides the ZNRF3 ΔRING mutant, the ZNRF3 constructs inhibited Wnt signalling upon Wnt activation.

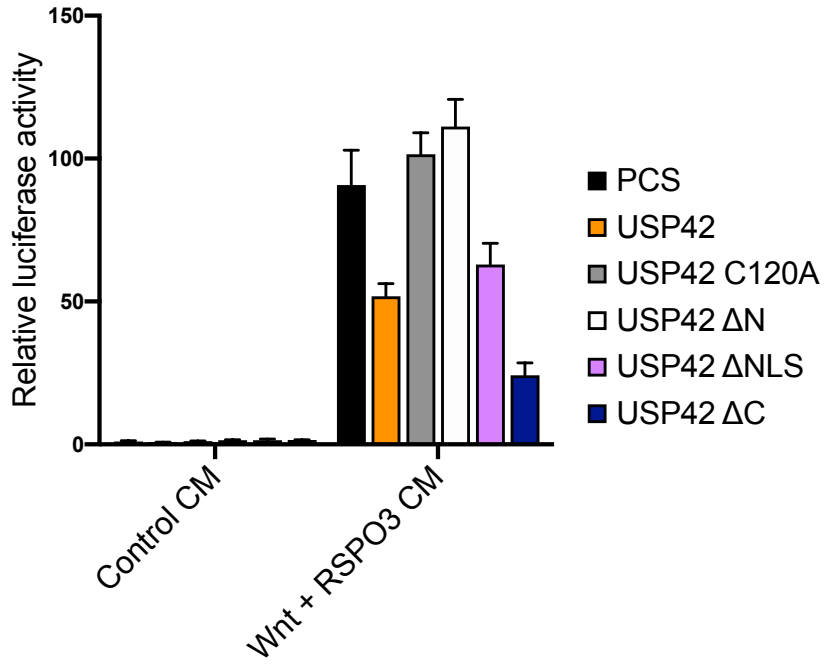

Figure 3.3.3: Cytoplasmic USP42 ΔC and ΔNLS efficiently inhibit Wnt signalling.
TOPflash reporter assay in HEK293T cells overexpressing the different USP42 constructs and treated with either control or Wnt3a with R-spondin3 conditioned media. This is a representative image out of at least three independent experiments with biological replicates (in triplicates).

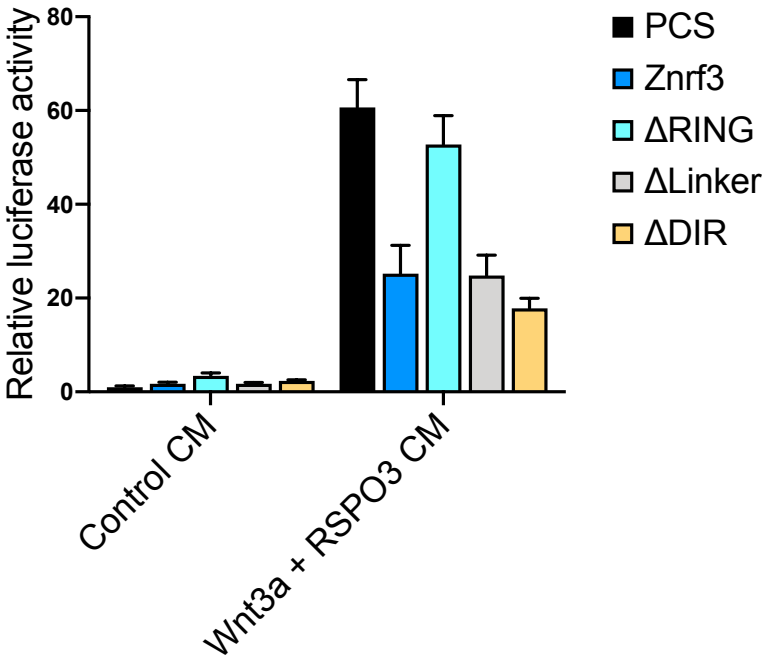

Figure 3.3.4: The activity of the RING domain is important for ZNRF3 to inhibit in Wnt signalling.
Wnt reporter assay in HEK293T cells overexpressing the different ZNRF3 constructs and treated with either control or Wnt3a with R-spondin3 conditioned media. Representative of two independent experiments with three biological replicates.

Afterwards, I performed a co-immunoprecipitation of the USP42 constructs together with ZNRF3 WT to examine which domains are required for the interaction between USP42 and ZNRF3 (Figure 3.3.5).

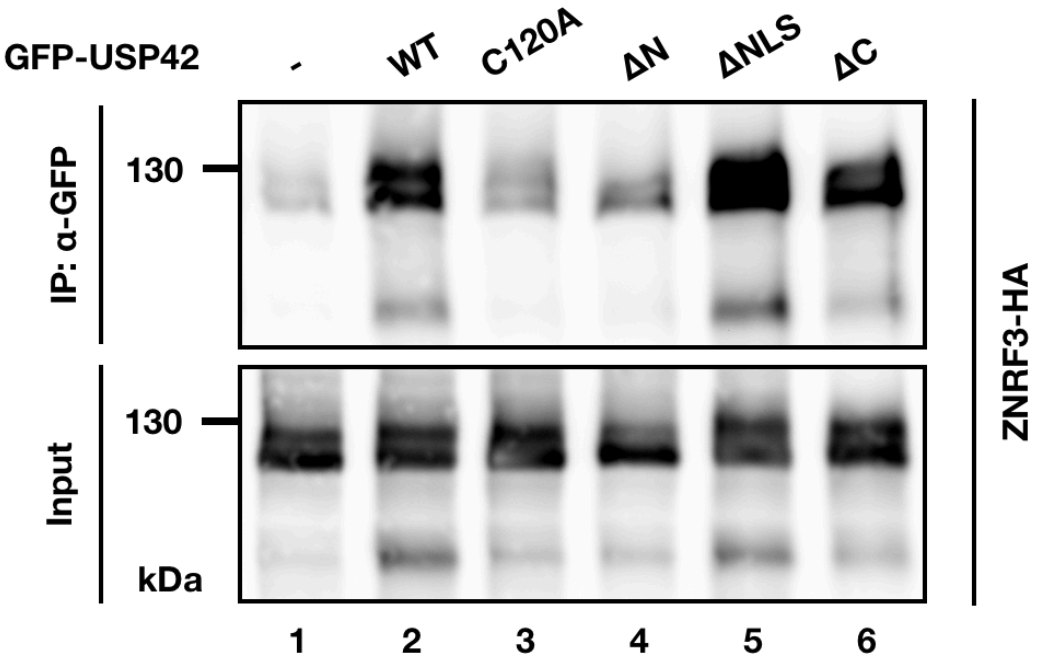

Figure 3.3.5: The N-terminal and the catalytical activity of USP42 are required for the interaction between USP42 and ZNRF3.
Co-immunoprecipitation in HEK293T cells overexpressing the USP42 constructs together with ZNRF3 WT. Representative co-IP out of three independent experiments.

In parallel, Sergio Acebrón co-immunoprecipitated the ZNRF3 constructs together with USP42 WT (Figure 3.3.6). USP42 WT, as well as the ΔNLS and ΔC mutants, co-precipitated ZNRF3 WT. In contrast, USP42 C120A and USP42 ΔN did not co-precipitate ZNRF3. ZNRF3 ΔRING and ΔLinker mutants co-precipitated USP42 WT similar to ZNRF3 WT, whereas ZNRF3 ΔDIR did not.

This suggests that the N-terminal of USP42 and the Dishevelled interacting region of ZNRF3 are required for the interaction between these two proteins. In summary, I could show that USP42 ΔNLS and ΔC localised in the cytoplasm in contrast to the USP42 WT, which was mainly nuclear. In the Wnt reporter assay, USP42 ΔC was the strongest inhibitor among the USP42 constructs and co-precipitated similar levels of ZNRF3 as the WT USP42. USP42 ΔNLS had a similar Wnt inhibitory effect as WT USP42, but co-precipitated more ZNRF3 than USP42 WT or ΔC.

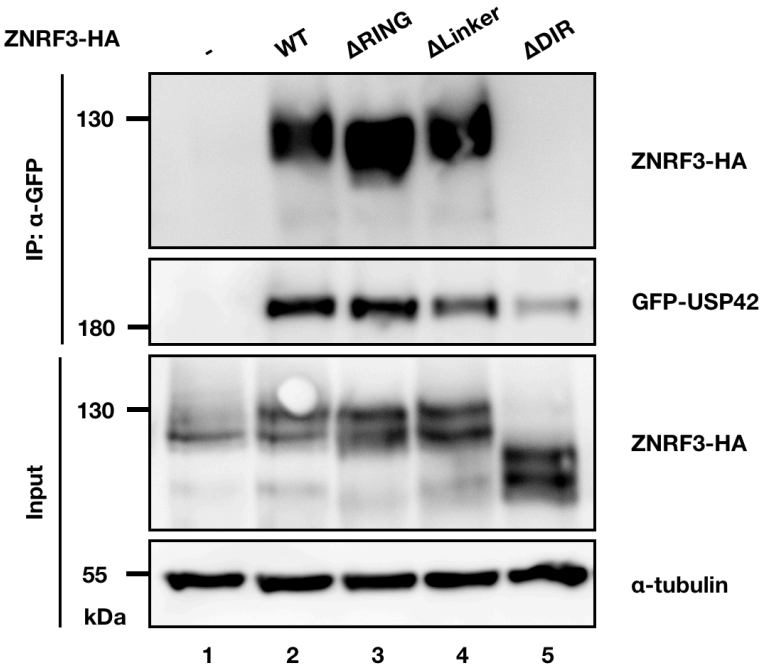

Figure 3.3.6: The Dishevelled interacting region of ZNRF3 is important for the interaction between USP42 and ZNRF3.
Representative co-immunoprecipitation in HEK293T cells overexpressing the ZNRF3 constructs together with USP42 WT.

3.4 USP42 regulates Wnt receptor turnover via ZNRF3/RNF43

ZNRF3 and RNF43 are E3 protein-ubiquitin ligases which ubiquitinate and destabilise the Wnt receptors Frizzled and LRP. As I showed that USP42 stabilises ZNRF3 and RNF43 (Figure 3.2.5-8), I next looked into the effect of USP42 on Wnt receptor internalisation. For this purpose, I transfected HEK293T cells with a SNAP-Frizzled5 construct together with pEGFP-USP42 and ZNRF3-HA (Figure 3.4.1). After incubating the cells in the SNAP substrate, the cells were chased for 10 minutes to allow internalisation of the Frizzled receptors. The Frizzled proteins which got internalised appeared as small punctae at the cell membrane in ZNRF3 overexpressing cells. Similarly, USP42 overexpression also increased Frizzled internalisation in comparison to the control. Moreover, the cells overexpressing both USP42 and ZNRF3, showed more internalised Frizzled proteins, indicating a synergistic effect.

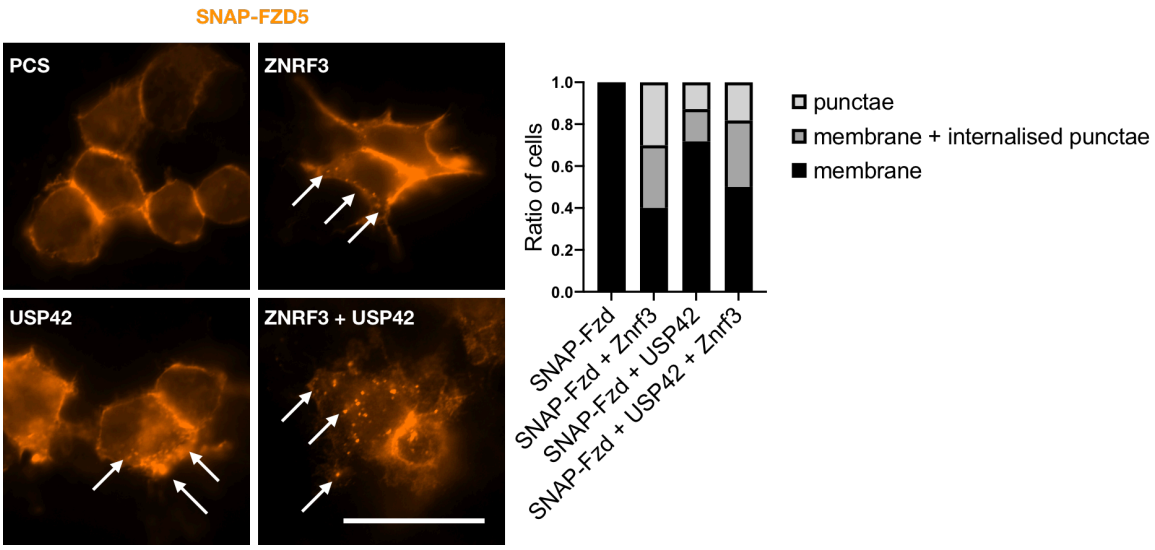

Figure 3.4.1: USP42 promotes internalisation of the Wnt receptor Frizzled, similar to ZNRF3.
The SNAP-Frizzled5 construct was transfected together with either the empty vector PCS, USP42, ZNRF3 or USP42 and ZNRF3 combined into HEK293T cells. After incubating the cells with the SNAP-substrate, the cells were chased for 10 minutes prior to fixation. SNAP-Frizzled is labelled in orange, internalised SNAP-Frizzled is indicated by the white arrows. Scale bar = 10 µm.

I further validated this data by analysing Frizzled5-V5 protein levels upon USP42 overexpression using western blot analysis (Figure 3.4.2). USP42 overexpression clearly reduced Frizzled protein levels in HEK293T cells (lane 3), while ZNRF3 overexpression completely abrogated Frizzled protein levels (lane 2). Interestingly, when LGR4 and R-spondin were overexpressed, there seemed to be even less Frizzled5-V5 in USP42 overexpressing cells (lane 7).

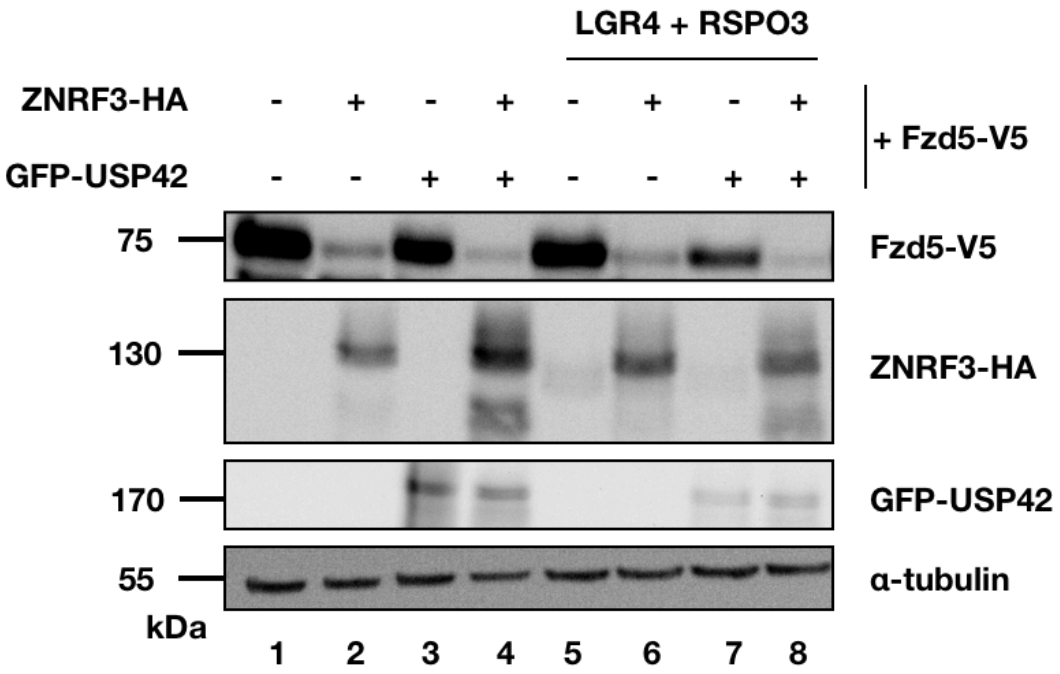

Figure 3.4.2: USP42 and ZNRF3 overexpression reduce Frizzled5-V5 levels in HEK293T cells.

Western blot analysis of Frizzled5-V5 protein levels upon USP42 and ZNRF3 overexpression. In addition, the cells were co-transfected with LGR4 and treated with R-spondin3 conditioned medium. Representative of at least 2 independent experiments.

Likewise, I analysed LRP6 protein levels in HEK293T cells upon USP42 knockdown (Figure 3.4.3). Ablation of USP42 increased endogenous LRP6 protein levels already without Wnt induction in comparison to the control (lane 3 and 4).

Taken together, USP42 regulates Wnt receptor turnover via ZNRF3 preventing Wnt stimulation at the plasma membrane.

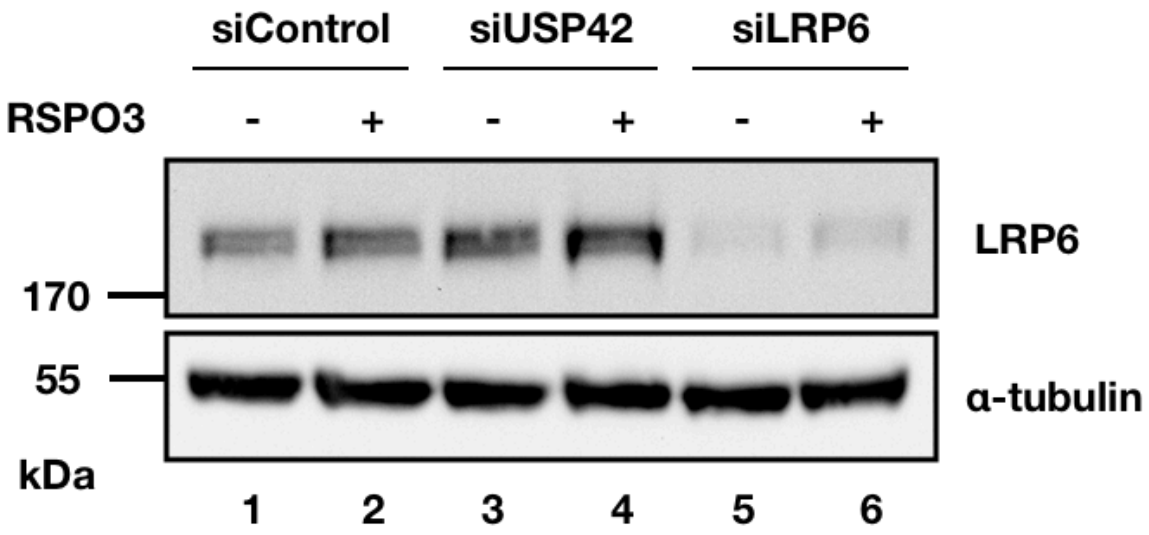

Figure 3.4.3: Knockdown of USP42 increases LRP6 protein levels in HEK293T cells.
Western blot analysis of endogenous LRP6 protein levels upon knockdown of USP42 or LRP6 in HEK293T cells. The cells were also treated with R-spondin3 conditioned medium.

3.5 The role of USP42 in adult stem cells

Since ZNRF3 and RNF43 are the two main Wnt regulators in adult stem cells (i.e. intestinal stem cells, hepatocyte zonation, limb regeneration) and they are often mutated in Wnt-associated cancers, I wanted to analyse if USP42 also participates in the regulation of Wnt signalling in adult stem cells. First, I performed immunohistochemical stainings of the Paneth cell marker lysozyme, the proliferation marker Ki67 and endogenous Usp42 in tissue sections of the small intestine and the colon derived from a wild type mouse (Figure 3.5.1 - 3.5.3). In 2D cell culture (HEK293T cells), USP42 was mainly localised in the nucleus (Figure 3.3.2), with only a small amount being in the cytoplasm. The immunohistochemical staining revealed that endogenous Usp42 is differently expressed throughout the tissue. Ki67 is expressed in the intestinal and colon crypts and mark proliferating cells. The Paneth cells in the intestinal crypts were lysozyme positive. Surprisingly, in the villi nuclear Usp42 is prominent, whereas more cytoplasmic Usp42 is found in the crypts. Similar results were obtained from the colon tissue sections (Figure 3.5.3). Since the colon does not have strongly pronounced villi as the small intestine, it was difficult to distinguish the different zones. In general, nuclear

Usp42 was absent from the crypts, where it was expressed more in the cytoplasm. Also, it seems there is a larger gap between Ki67 positive cells and cells harbouring nuclear Usp42. To confirm this, additional stainings of Usp42 together with markers against different types of intestinal and colon cells are required.

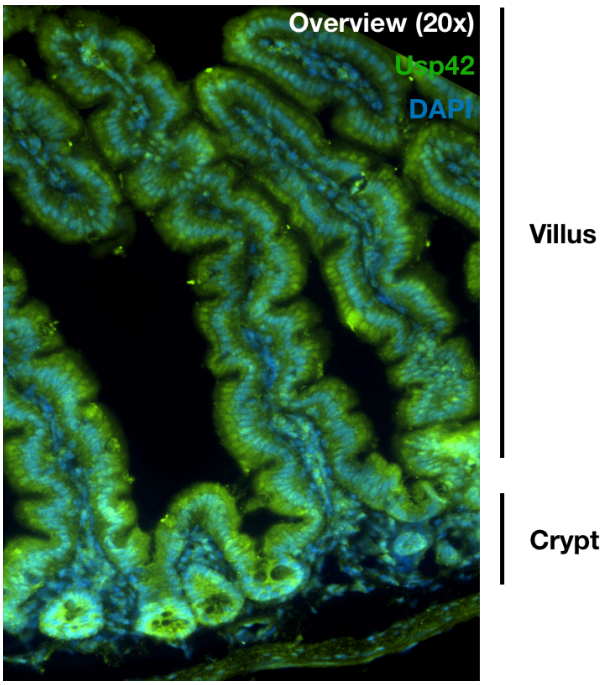

Figure 3.5.1: Nuclear Usp42 is present in the villus, but not in the mouse intestinal crypts.
Overview of the mouse small intestinal tissue with staining against endogenous Usp42 (green) and DAPI (blue), 20 x magnification.

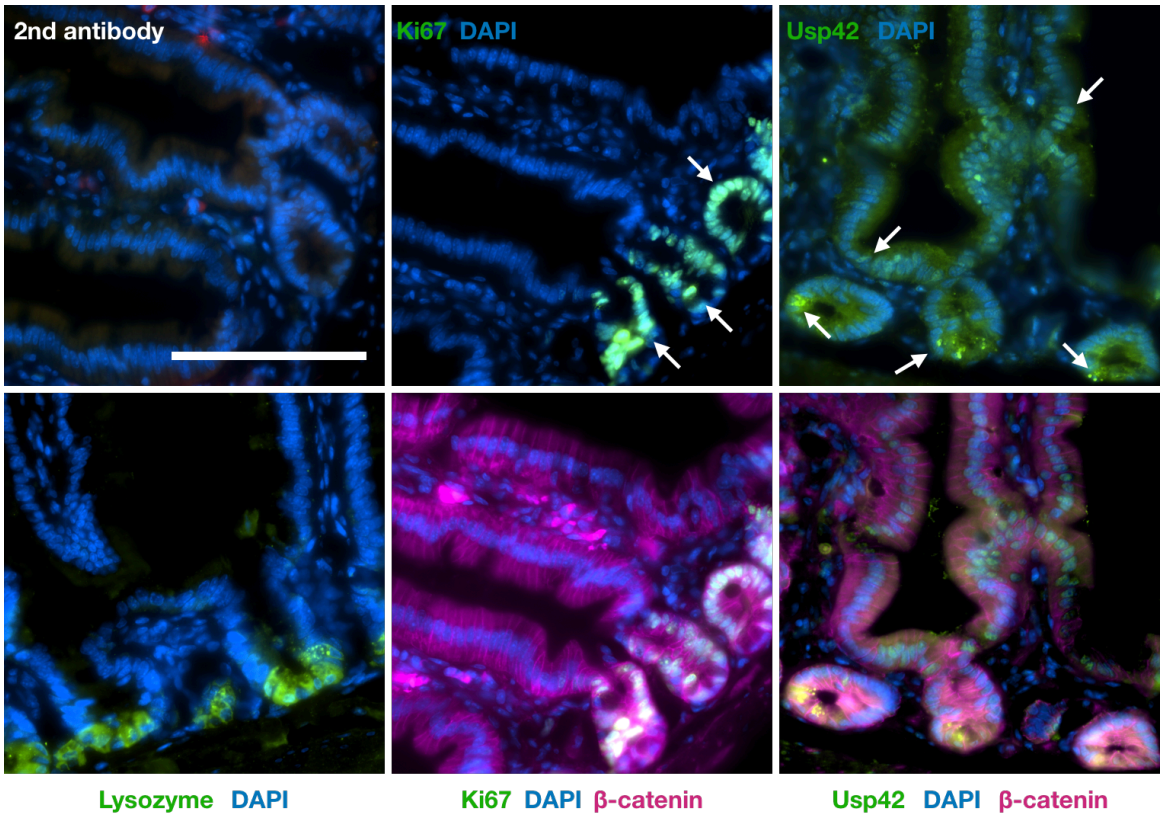

Figure 3.5.2: Usp42 has nuclear localisation in the villus and is cytoplasmic in the mouse intestinal crypts.
Close-up of the mouse intestinal tissue stained with antibodies against either the Paneth cell marker lysozyme, the proliferation marker Ki67 or Usp42 (green), β-catenin (magenta) and DAPI (blue), scale bar = 100 µm.

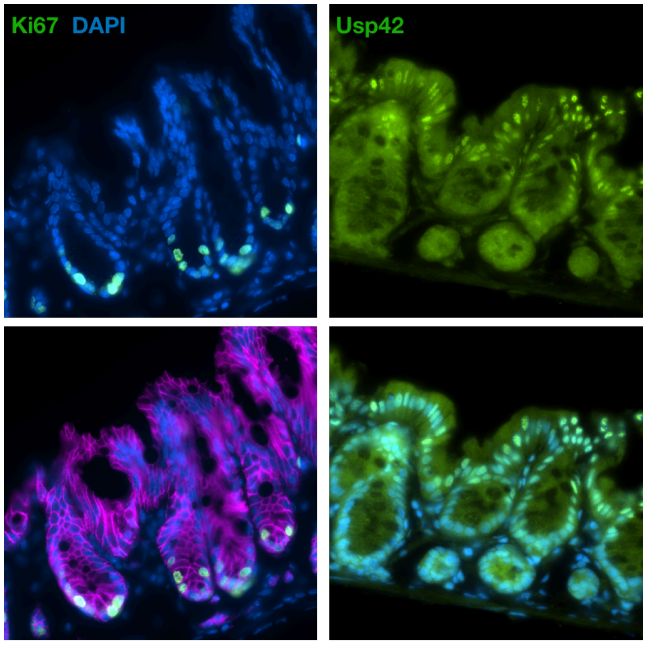

Figure 3.5.3: In the colon, nuclear Usp42 is mainly present in the villus rather than in the crypts.
Immunohistochemical stainings of endogenous Ki67 and Usp42 (green), β-catenin (magenta) and DAPI (blue).

Previously, it has been published that double knockout of Znrf3 and Rnf43 render mouse intestinal organoids hypersensitive to Wnt ligands (Merenda *et al.* 2017, Spit *et al.* 2020). If USP42 regulates Wnt signalling in adult stem cells via ZNRF3/RNF43, I hypothesised that knockout of USP42 had a similar effect in intestinal organoids. Thus, I generated Usp42 knockout mouse intestinal organoids by CRISPR/Cas9 genome editing with the 2 gRNA concatemer (Merenda *et al.* 2017). To check the efficiency of the knockout, I compared endogenous Usp42 staining in control versus the Usp42 knockout organoids (Figure 3.5.4). Endogenous Usp42 was completely absent from the knockout organoids. In control organoids, nuclear Usp42 staining was again absent from the crypts (yellow arrows), but present in the villi (white arrows). A close-up of an intestinal crypt reveals that there are two distinct signals of Usp42 stainings (Figure 3.5.5). On the one hand, there are single cells containing high amounts of Usp42, emitting a bright signal overall. On the other hand, there are cells in which Usp42 appears to be concentrated in small foci. This indicates that localisation of Usp42 changes with the differentiation status of the cell and probably also its function in those cells.

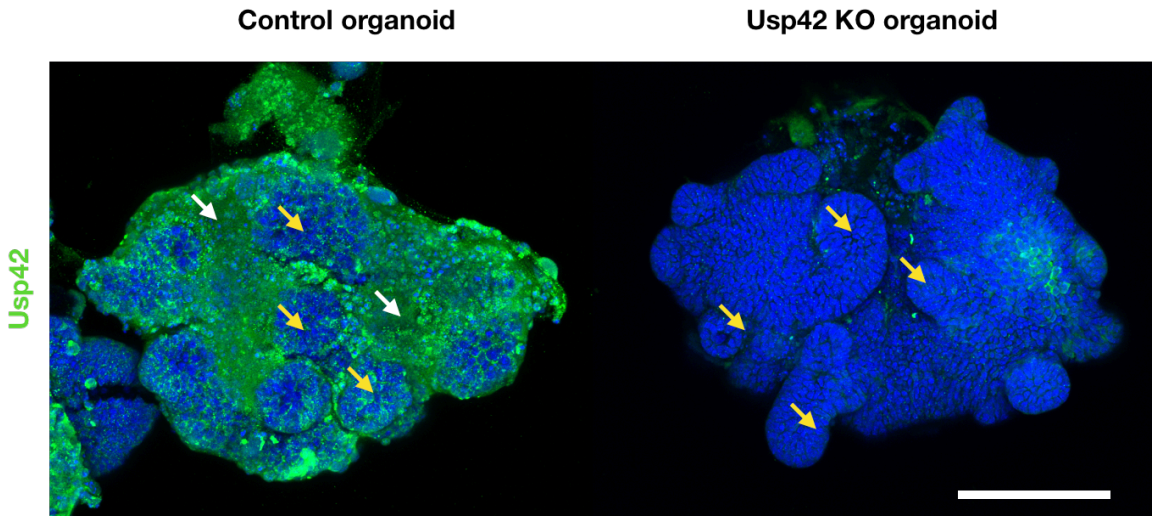

Figure 3.5.4: Nuclear Usp42 staining is absent from the crypts of mouse intestinal organoids.
Usp42 (green) and DAPI (blue) staining in mouse WT intestinal organoids (left) and Usp42 knockout organoids (right). Yellow arrows indicate the crypts, white arrows the more differentiated cells outside the crypts. Scale bar = 200 µm.

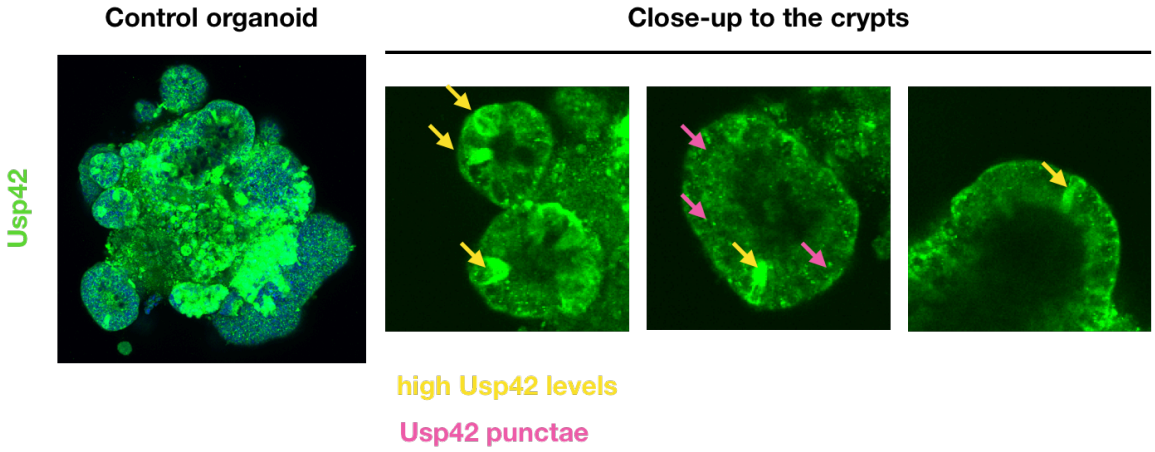

Figure 3.5.5: Usp42 subcellular localisation in the intestinal crypts comes in two distinct patterns.
Endogenous Usp42 (green) staining in control organoids with a close-up to the crypts. Yellow arrows mark cells with high Usp42 levels throughout the cell, pink arrows mark cells with cytoplasmic Usp42 punctae.

Next, I performed a growth factor withdrawal experiment to see whether Usp42 knockout organoids can survive the absence of exogenously added Wnt3a and R-spondin1 in the organoid medium, similar to ZNRF3/RNF43 double knockout organoids (Figure 3.5.6). In the full organoid medium containing Wnt3a and R-spondin1, control and Usp42 knockout organoids grew in undifferentiated spheres (Figure 3.5.6, from left to right). When Wnt3a conditioned medium was removed from the organoid medium, the control organoids formed crypts, giving them the characteristic shape of intestinal organoids. However, the Usp42 knockout organoids remained as undifferentiated spheres. Further reduction of exogenous Wnt activity by depleting the medium from R-spondin1 lead to apoptosis of control organoids, whereas Usp42 knockout organoids differentiated and survived under these conditions. Only when Wnt secretion was blocked by adding the Wnt secretion inhibitor IWP2, both organoid cultures died. To sum up, Usp42 knockout help mouse intestinal organoids to survive growth factor withdrawal, similar to ZNRF3/RNF43 double knockout organoids.

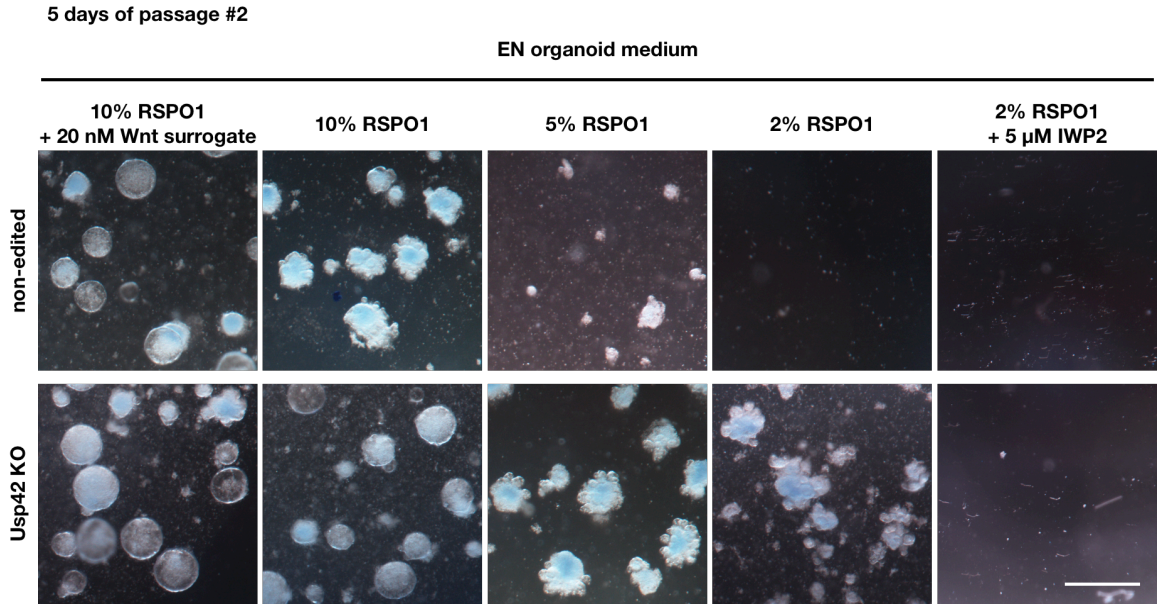

Figure 3.5.6: Usp42 knockout renders mouse intestinal organoids hypersensitive to Wnt ligands.

Representative growth factor withdrawal experiment with non-edited (empty CRISPR-concatemer vector + hSpCas9) or Usp42 knockout organoids. The organoids were grown for 2 passages in the indicated media. The pictures represent the organoids after 5 days into passage 2. Displayed on the left are the organoids growing in full organoid growth

medium, including Wnt and R-spondin1. Wnt is then depleted from the medium and R-spondin concentrations are reduced. On the right are the organoids treated with the Wnt secretion inhibitor IWP2. Scale bar = 1 mm.

Based on my observation that Usp42 is differentially expressed in the mouse intestine and that cytoplasmic USP42 efficiently inhibits Wnt signalling (Figure 3.3.3), I wanted to know which signals lead to shuttling of USP42 between the nucleus and cytoplasm. Proteins containing a nuclear localisation signal are often shuttled between the nucleus and cytoplasm by importins (Nakielny and Dreyfuss 1999, Fontes *et al.* 2003, Harremann *et al.* 2004). Their affinity to importins can be modified by phosphorylation adjacent or within the nuclear localisation signal (Kaffman *et al.* 1999, Jans *et al.* 2000). Hence, I performed a screening in HCT116 cells by activating different signalling pathways or inhibiting specific kinases (Figure 3.5.7). I then analysed the cells by fluorescent microscopy and determined the ratio of cytoplasmic to nuclear USP42 signal upon the different treatments. Besides R-spondin3, treatment with the mTOR inhibitor Rapamycin (which leads to the inhibition of the serine/threonine kinase S6K) increased the amount of cytoplasmic USP42.

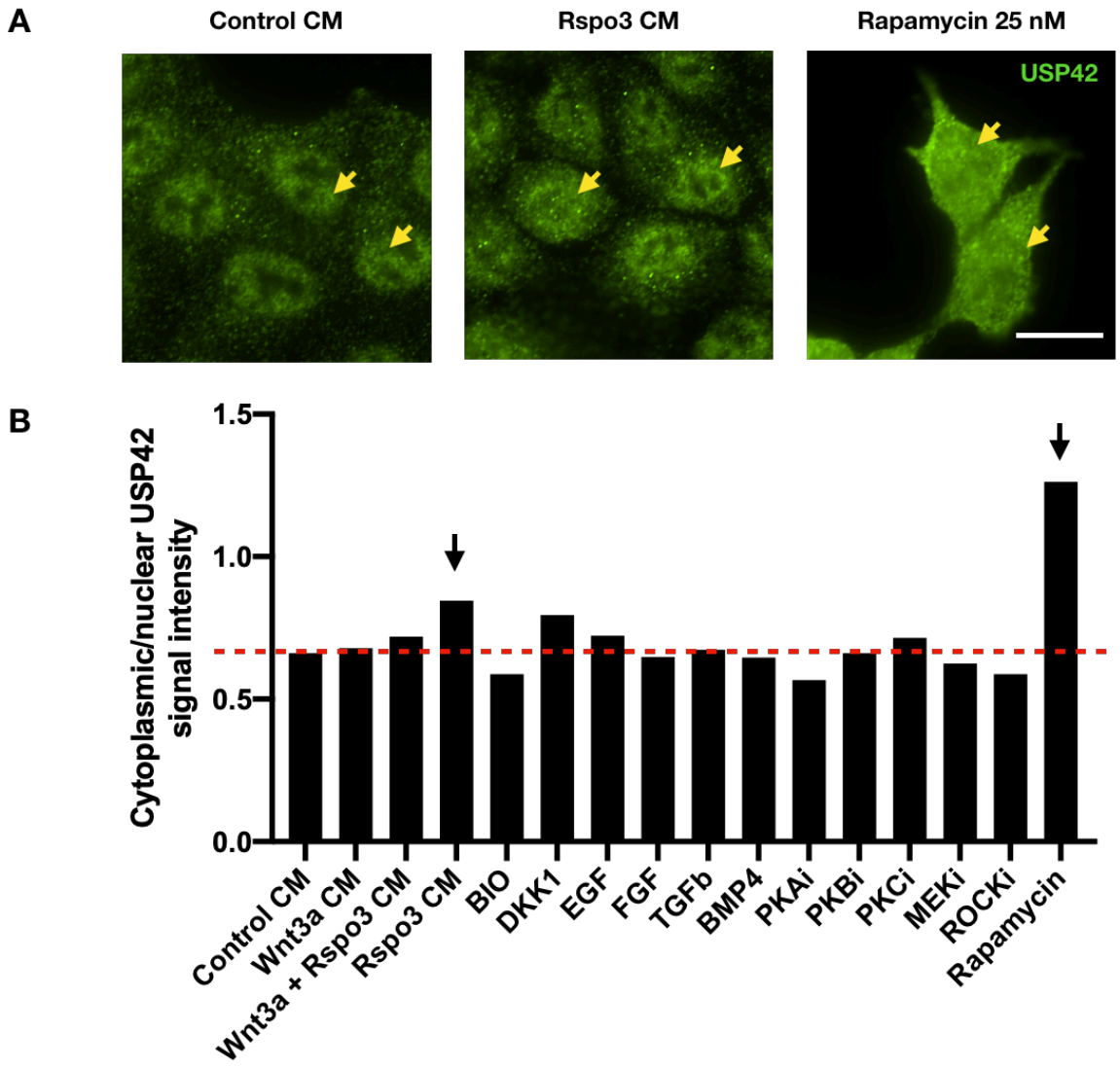

Figure 3.5.7: Rapamycin treatment leads to USP42 export from the nucleus.
A) Representative images of a screening for nuclear export inducers in HCT116 cells Yellow arrows indicate where the nucleus is located, green = endogenous USP42, scale bar = 5 µm.
B) Quantification of the screening based on the ratio of cytoplasmic/nuclear USP42 signal intensity (n = 120 cells/condition).

While staining the HCT116 cells, I noticed that USP42 signal also concentrates at a small structure near the nucleus. After consulting with my colleagues, we hypothesised that USP42 might localise to the centrosome. To test this hypothesis, I stained endogenous USP42 and the centrosomal marker ɣ-tubulin in HCT116 cells and analysed co-localising signals throughout the cell cycle (Figure 3.5.8). USP42 does not necessarily co-localise with ɣ-tubulin, especially when there are two foci for ɣ-tubulin at the transition from

interphase to metaphase, but it localises adjacent to ɣ-tubulin in the interphase and to at least one of the duplicated centrosomes in early mitosis. In meta- and anaphase USP42 is homogeneously distributed in the cell undergoing mitosis.

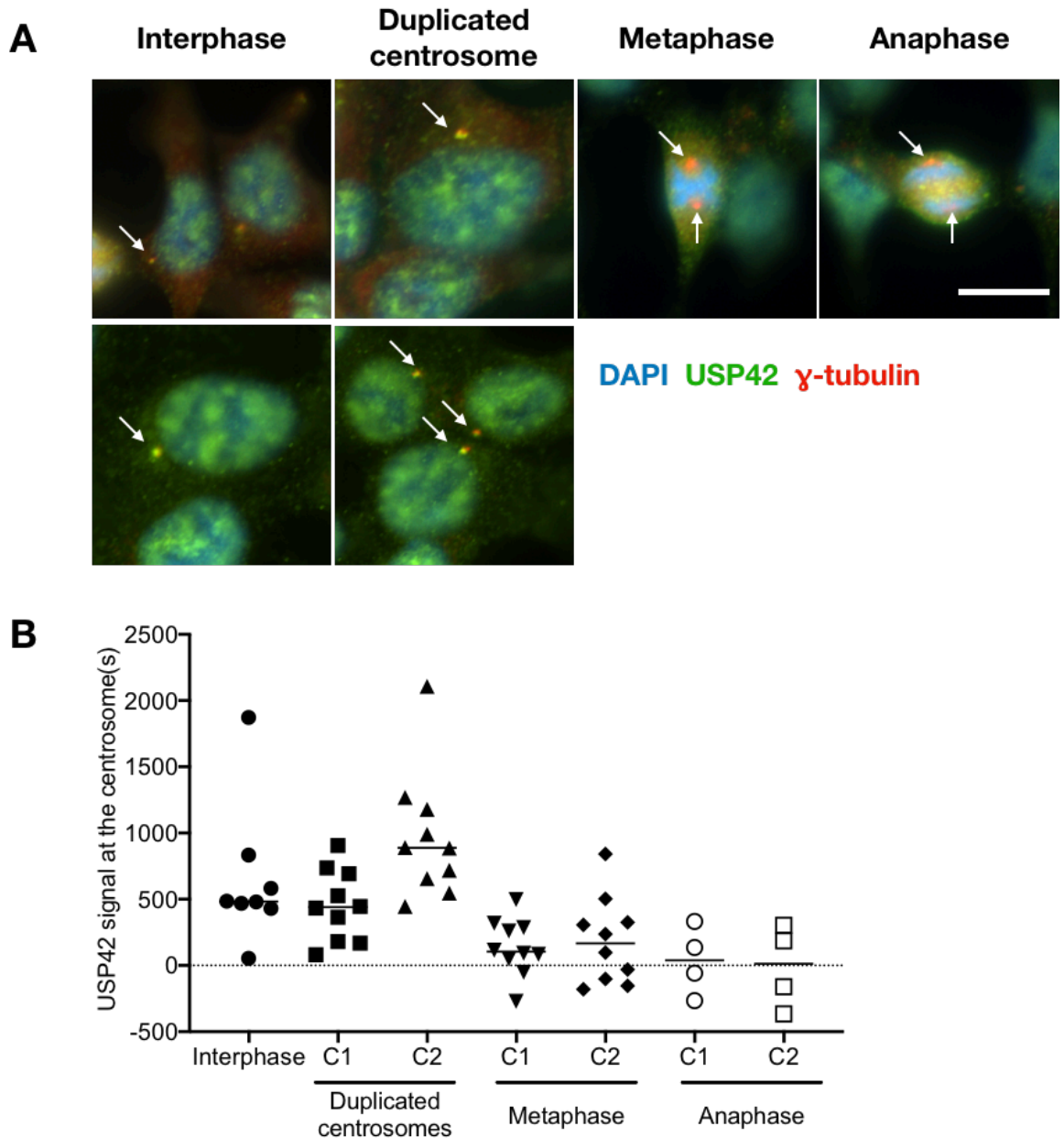

Figure 3.5.8: USP42 localises adjacent to the centrosomes in early mitosis.
A) Representative images of USP42 (green) and ɣ-tubulin (red) staining in HCT116 cells. The centrosomes are indicated by the white arrows. Scale bar = 5 µm. Preliminary data.
B) Quantification of USP42 signal in close proximity to the centrosomes. The signal of cytoplasmic USP42 was subtracted from the USP42 signal near the centrosomes. If there were duplicated centrosome visible: C1 = Centrosome 1, C2 = Centrosome 2.

Taken together, Usp42 shows a differential expression pattern throughout the small intestine and colon tissue, where nuclear Usp42 is present in the villi, but has a cytoplasmic localisation in the crypts. This could be confirmed by stainings in mouse intestinal organoids. Loss of Usp42 help mouse intestinal organoid survive growth factor withdrawal (without external Wnt activation) and keep the organoids less differentiated. Treatment with the mTOR inhibitor Rapamycin and to a milder degree R-spondin 3 change the subcellular localisation of USP42 in HEK293T cells, which indicated that USP42 localisation could be regulated by the serine/threonine kinase S6K activity (a downstream target of mTOR). Finally, USP42 might have a function in early mitosis, as it localises near the centrosomes.

3.6 Loss of USP42 promotes proliferation and epithelial-to-mesenchymal transition in HCT116 cells

ZNRF3 and RNF43 are often mutated in Wnt-associated cancer cells, such as colorectal cancer (Bond *et al.* 2016, Hao *et al.* 2016). Loss of ZNRF3/RNF43 leads to increased proliferation and EMT of cancer cells. *In silico* analysis (TCGA, PanCancer Atlas) revealed that USP42 is also mutated in colorectal cancer, specifically in mucinous adenocarcinoma, and USP42 mRNA is upregulated in rectal and colon adenocarcinoma Further *in silico* analysis show an overlap of high mRNA expression with missense mutations of TP53, APC and KRAS, as well as a few cases of truncation mutants of RNF43 (Figure 3.6.1).

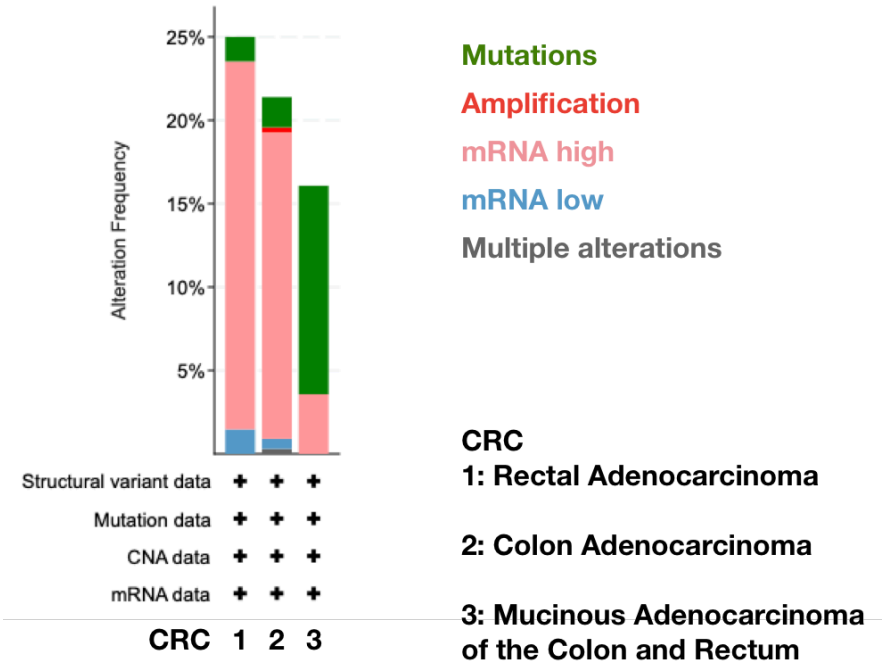

Figure 3.6.1: USP42 is often mutated in mucinous adenocarcinoma of the colon and rectum.
cBioPortal analysis of USP42 alterations in colorectal adenocarcinoma (TCGA, PanCancer Atlas).

Although these mutations remain uncharacterised, I wanted to investigate how loss of USP42 activity contributes to cancer development. Therefore, I first tested the effect of USP42 overexpression on Wnt signalling in HCT116 and H1703 with a Wnt reporter assay to assess whether USP42 has an effect on Wnt signalling in these two cancer cell lines (Figure 3.6.2 and Figure 3.6.3). USP42 successfully inhibited Wnt signalling back to control levels in the colorectal cancer cell line HCT116 and the lung squamous cell carcinoma cell line H1703 in comparison to the control. One observation I made was that Wnt activation in HCT116 cells did not change much in fold induction compared to the Wnt reporter assay in HEK293T cells which might indicate that HCT116 cells have higher Wnt signalling in basal levels as they lack RNF43 (e.g. in Figure 3.1.8).

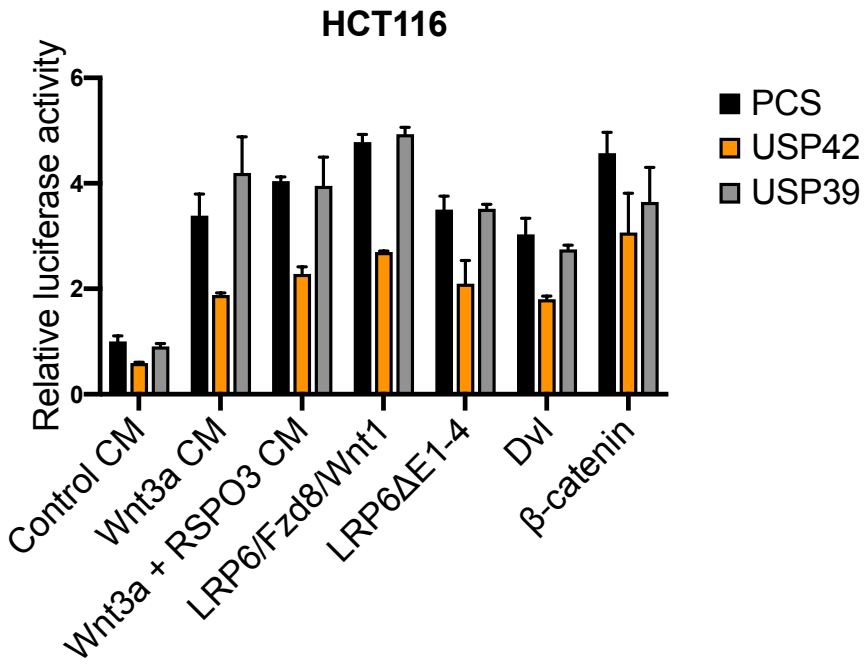

Figure 3.6.2: USP42 inhibits Wnt signalling upstream of Dishevelled in HCT116 cells. HCT116 cells were transfected with either empty vector (PCS), USP42 or the control deubiquitinating enzyme USP39. Activation of the Wnt signalling pathway was induced by overexpression of the indicated plasmids or treatment with Wnt3a and Wnt3a + R-Spondin 3 conditioned media. Representative epistasis experiment (out of 4 independent experiments) of a TOPflash reporter assay in HCT116 cells upon USP42.

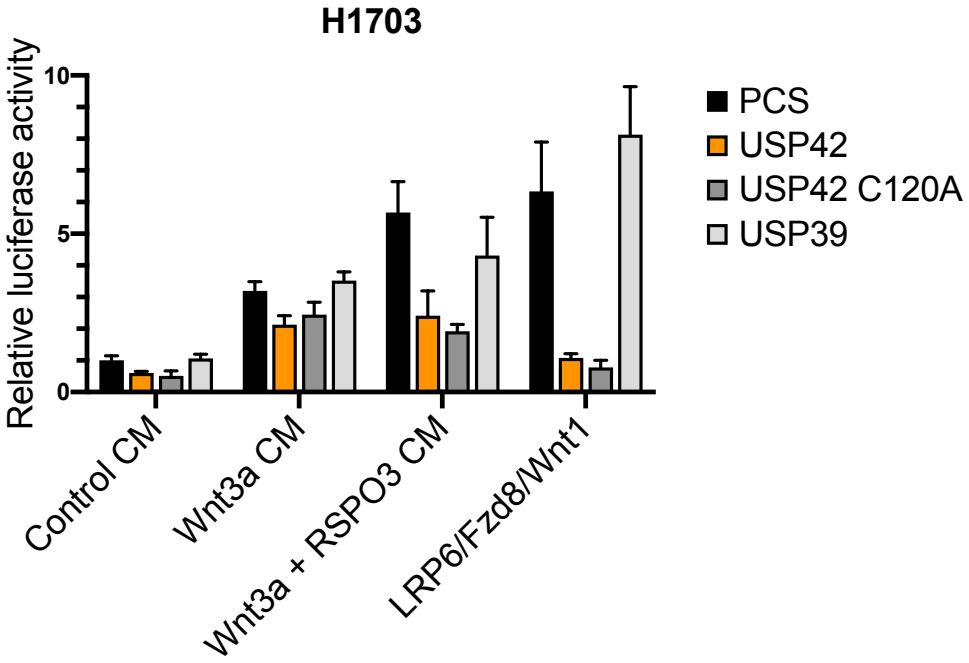

Figure 3.6.3: USP42 inhibits Wnt signalling on the Wnt receptor level in H1703 cells. H1703 cells overexpressing PCS, USP42, the catalytically inactive mutant USP42 C120A or USP39 were treated with control, Wnt3a or Wnt3a + R-Spondin 3 conditioned media, or transfected with LRP6/Fzd8/Wnt1 to activate Wnt signalling. Representative TOPflash reporter assay (out of four independent experiments)

Accordingly, I also tested the effect of USP42 knockdown in HCT116, HCT116 Evi knockout, H1703 and an additional colorectal cancer cell line, namely RKO cells (Figure 3.6.4 and 3.6.5). I wanted to compare the effect of USP42 knockdown in two different colorectal cancer cell lines (HCT116 and RKO) to increase the significance. Since the organoid data showed that the effect of loss of Usp42 is dependent on paracrine Wnt signalling, I used HCT116 Evi KO cells to investigate, if Evi KO could rescue loss of USP42. Knockdown of USP42 increased Wnt signalling in HCT116 and RKO cells, but not in H1703 cells, in comparison to the controls. Evi knockout reversed this effect in HCT116 cells. Regarding the H1703 cells, this is in contrast to the overexpression of USP42 in H1703 cells, where USP42 efficiently inhibited Wnt signalling. At first I hypothesised that the siRNA was not transfected efficiently into the cells, but knockdown of APC was able to strongly increase Wnt signalling in H1703 cells. This could mean, that H1703 cells (as a lung squamous cell carcinoma) does not have high levels of ZNRF3/RNF43, so that a destabilisation of these would not affect Wnt signalling similar to the HEK293T ZNRF3/RNF43 DKO cells.

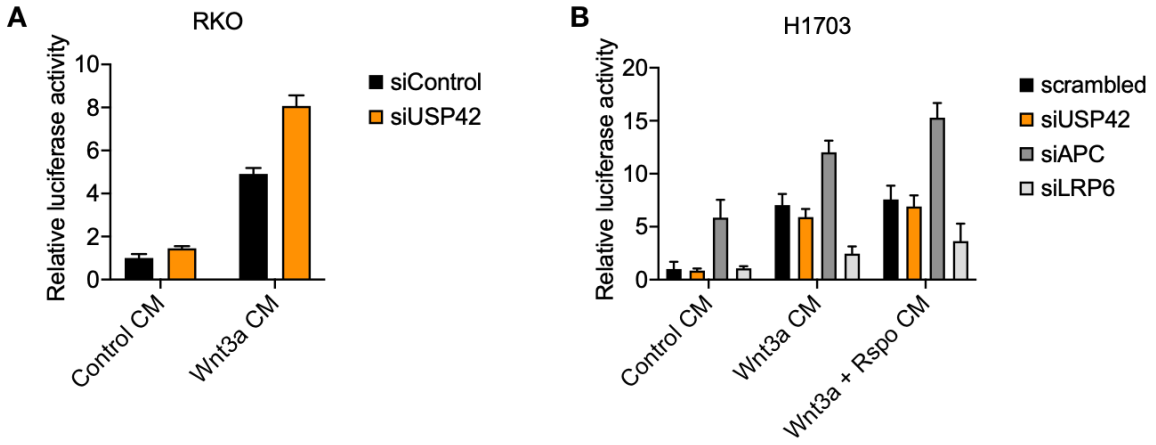

Figure 3.6.4: Loss of USP42 increases Wnt signalling in HCT116 cells and is rescued by Evi knockout.
HCT116 WT or Evi KO cells were treated with control siRNA, siUSP42 or siAPC, as well as control, Wnt3a or Wnt3a + R-Spondin conditioned media. Representative TOPflash reporter assays in HCT116 and Evi knockout cells (four independent experiments each).

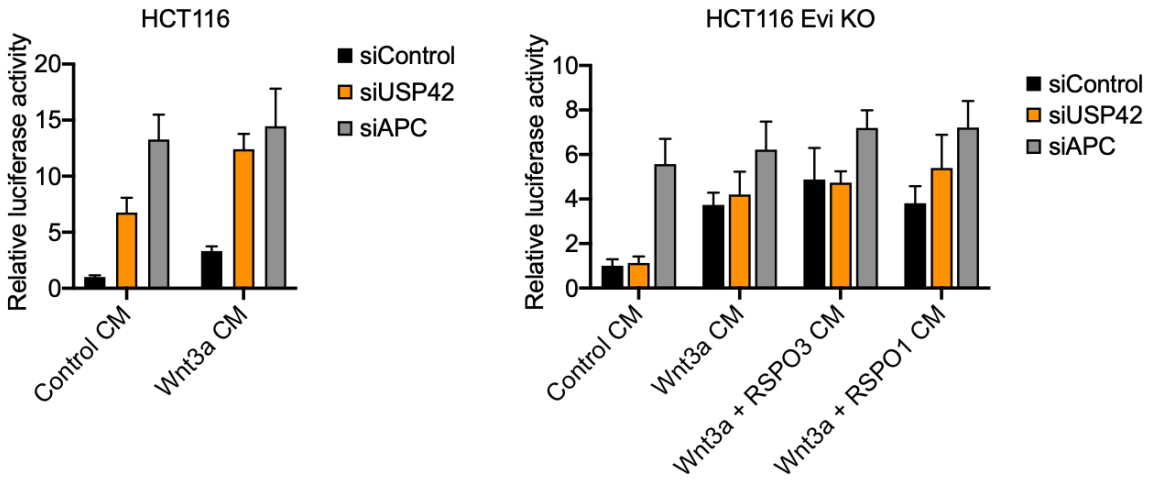

Figure 3.6.5: Loss of USP42 increases Wnt signalling in RKO, but not H1703 cells.
The colorectal cancer cells (RKO) and lung cancer cells (H1703) were transfected with the control siRNA or siUSP42, as well as siAPC (knockdown of a negative Wnt regulator) and siLRP6 (knockdown of a positive Wnt regulator) in H1703. Then, the cells were treated with either control, Wnt3a or Wnt3a + R-Spondin 3 conditioned media to activate Wnt signalling. Representative Wnt reporter assays upon knockdown of USP42 in RKO (A) or H1703 (B) cells (four independent experiments each).

Transcriptomic analysis of USP42 depleted colorectal cancer cells could give us a hint on the biological functions of this Wnt regulator in the disease. Therefore, we performed a bulk RNAseq analysis in HCT116 cells upon loss of USP42, in collaboration with the Vladimir Benes group (Genomics Core Facility, EMBL, Heidelberg, Germany, data shown in Giebel *et al.* 2021). Based on my observations in the immunohistochemical stainings of the mouse small intestinal tissue, I hypothesised a role for USP42 in the proliferation of intestinal stem cells. Therefore, I analysed the expression of ISC proliferation markers upon loss of USP42 (Figure 3.6.6, Merlos-Suarez *et al.* 2011). Loss of USP42 increased the expression of the ISC proliferation signature genes. The genes upregulated the most were MCM3, EXO1, FANCB, CLSPN and CENPI. This suggests a function of the cytoplasmic USP42 as a proliferation inhibitor in the intestinal crypts. It has been shown

that loss of RNF43 has a increasing effect on epithelial-to-mesenchymal transition (EMT) (Wang *et al*. 2016), which is a hallmark for invasive cancer types. Thus, I wanted to elucidate whether USP42 is associated with EMT, too. Interestingly, loss of USP42 increased expression of mesenchymal markers (upregulated the most: TTL, CFL2, STX2, SGCB, AP1S2, TTC7B and GNG11) and decreased the expression of epithelial markers (downregulated the most: PROM2, TMC4, ELMO3,, PRR15L), such as E-cadherin (Figure 3.6.6, Rokavec *et al.* 2017). This indicates that loss of USP42 could lead to increased mesenchymal transition in colorectal cancer and contribute to its aggressiveness.

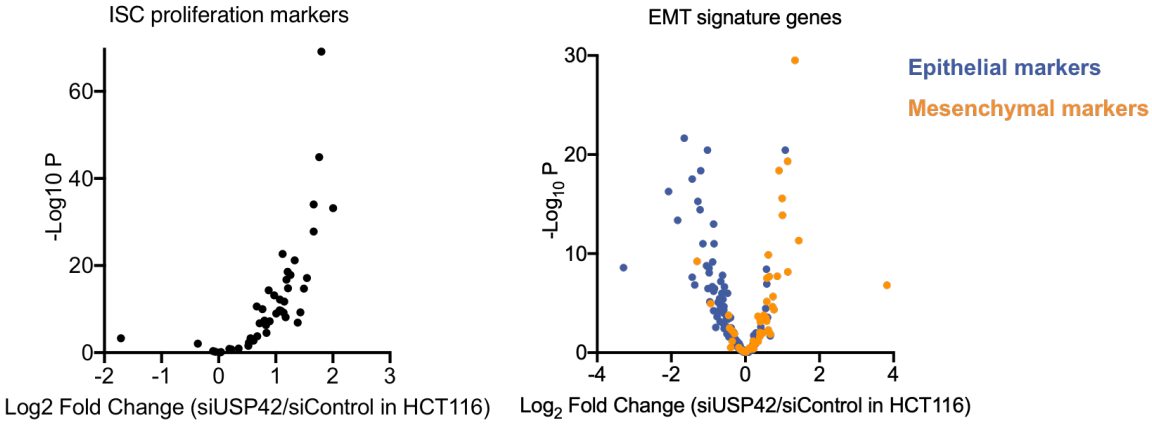

Figure 3.6.6: Loss of USP42 promotes ISC proliferation (left) and epithelial-to-mesenchymal transition (right).
A RNAseq analysis was performed on USP42 was knocked down in HCT116 cells compared to the control siRNA transfected cells. Volcano plots of Intestinal Stem Cell proliferation markers and EMT signature genes in cancer according to Merlos-Suarez *et al.* 2011 and Rokavec *et al.* 2017.

To further confirm our findings, I generated a bulk HCT116 USP42 knockout cell line and analysed the E-cadherin levels, which is the best known epithelial marker (Figure 3.6.7). The HCT116 cells were electroporated with the gRNA plasmids and selected for positive cells with ouabain. But instead of picking single colonies, all the cells in the plate were combined, because of their genetic variance within the HCT116 cell line. Together with Anchel de Jaime-Soguero, I performed stainings against E-cadherin in HCT116 parental and bulk USP42 KO cells. Knockout of USP42 in HCT116 strongly decreased E-cadherin protein levels in comparison to the parental cells.

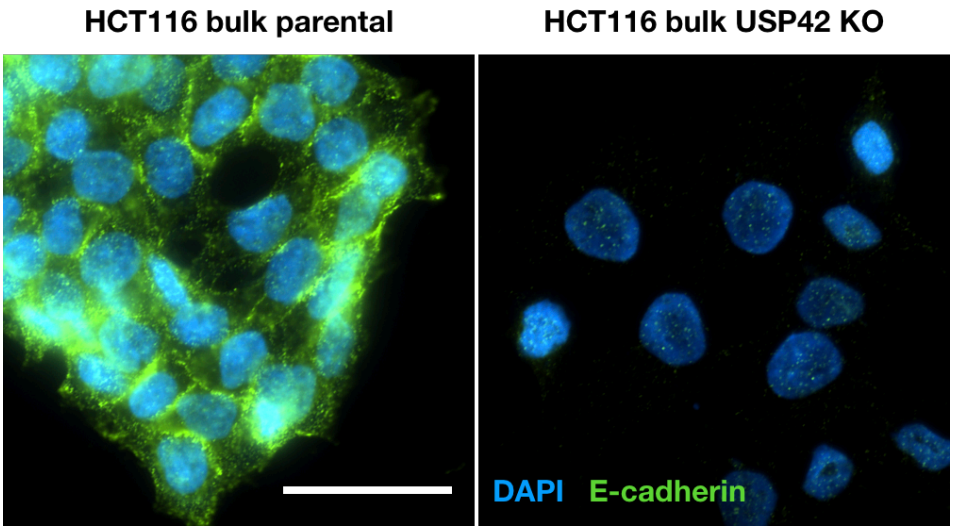

Figure 3.6.7: Genetic ablation of USP42 abolishes E-cadherin protein levels.
Representative immunofluorescent stainings against E-cadherin in HCT116 bulk parental (left) and USP42 knockout cells (right). Green = E-cadherin, blue = DAPI, scale bar = 10 µm.

A hallmark of cancer is increased proliferation. Thus, we wanted to evaluate if loss of USP42 is also associated with increased cell proliferation. Besides, we noticed that loss of USP42 increased proliferation in HCT116 cells as well as highlighted the proliferative signature in the RNAseq. To quantify these observations, Anchel de Jaime-Soguero performed a spheroid formation assay with the USP42 knockout and parental cells (Figure 3.6.8). Additionally, the cells were treated with the Wnt secretion inhibitor LGK-974. Genetic ablation of USP42 increased the spheroid size in comparison to the control. This effect was reversed to control spheroid size by the addition of LGK-974. These results show that the effect of loss of USP42 on proliferation in colorectal cancer cells is Wnt-dependent.

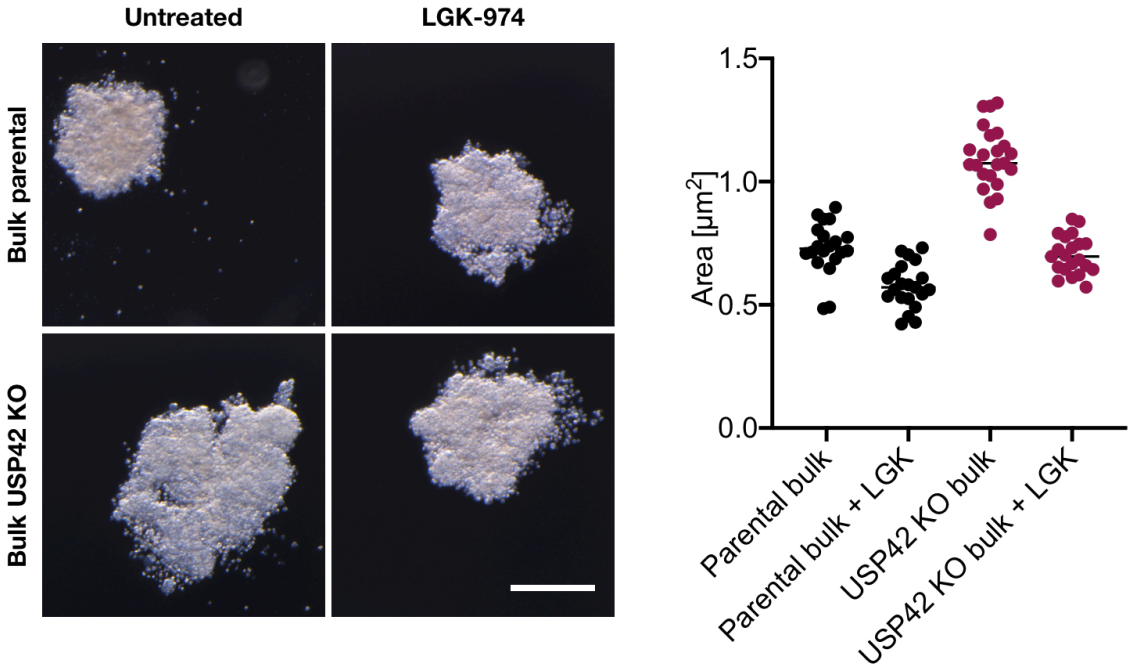

Figure 3.6.8: Loss of USP42 promotes proliferation in HCT116 cells.
HCT116 bulk parental or USP42 knockout cells were grown into spheroids for 6 days upon LGK-974 or control conditions. Images were taken at the Nikon binocular microscope to analyse the size of the spheroids. Representative images of the spheroids grown in each condition (left, scale bar = 500 µm). Spheroid area of bulk parental and USP42 knockout spheroids, treated with or without LGK-974, were calculated by generating a binary image of each spheroid and multiplying the pixel counts with the pixel size (right).

Lastly, we contacted the National Center for Tumor Diseases Heidelberg (NCT Heidelberg) and asked them to perform a tissue microarray of colorectal carcinoma tissue grade 1, 2 and 3, as well as adenoma and healthy tissue derived from anonymised patients (Figure 3.6.9 and Figure 3.6.10). They performed the stainings against USP42, the proliferation marker Ki67 and the Wnt signalling marker β-catenin. Then, I analysed if there were any correlations between the protein levels of the three proteins. Overall, it seems that Ki67 protein levels do not change much between the tissues. Comparing the healthy tissue with the grade 3 colorectal carcinoma tissue, it is obvious that the nuclear Ki-67 mainly localises in the nuclei of proliferating cells which can be found in the crypts. In grade 3 carcinoma tissue, the proliferation zone seems to be expanded. Also, the colon epithelium seems to be thicker in comparison to healthy tissue.

Concerning β-catenin protein levels, it seems that cytoplasmic β-catenin is increased in grade 1 and 3 colorectal carcinoma tissue compared to healthy tissue, while the β-catenin levels in grade 2 carcinoma tissue seem to be on the same level as the healthy tissue (Figure 3.6.9). Regarding the USP42 protein levels, I quantified the cytoplasmic and nuclear signal of USP42 (Figure 3.6.10). The biggest difference in cytoplasmic/nuclear ratio of USP42 is found between healthy tissue and grade 3 carcinoma tissue. Grade 3 carcinoma tissue show a higher ratio of cytoplasmic/nuclear USP42. This might indicate a biological relevance in disease, even though it is not clear if the increased ratio concerns healthy or mutated USP42.

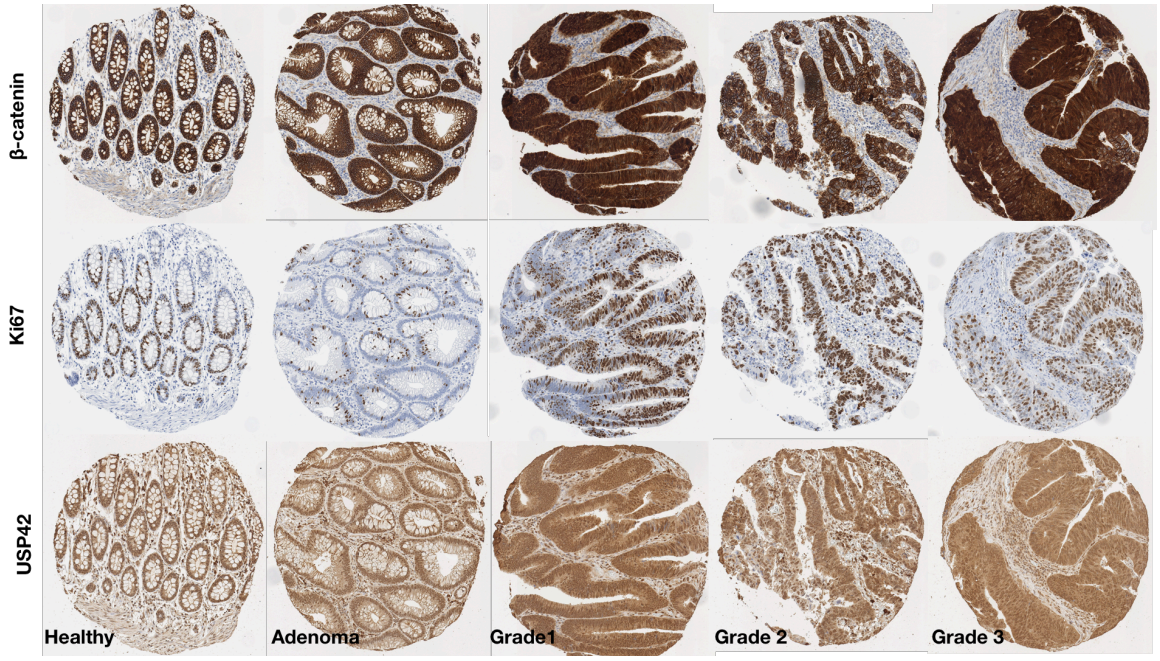

Figure 3.6.9: The ratio of cytoplasmic/nuclear USP42 is increased in grade 1 and 3 colorectal carcinoma in comparison to healthy tissue.
Overview of the tissue microarray of healthy, adenoma or colorectal carcinoma grade 1, 2 and 3 tissue samples stained for endogenous β-catenin, Ki67 or USP42. The tissue sections displayed here were chosen according to representative Ki67 protein levels.

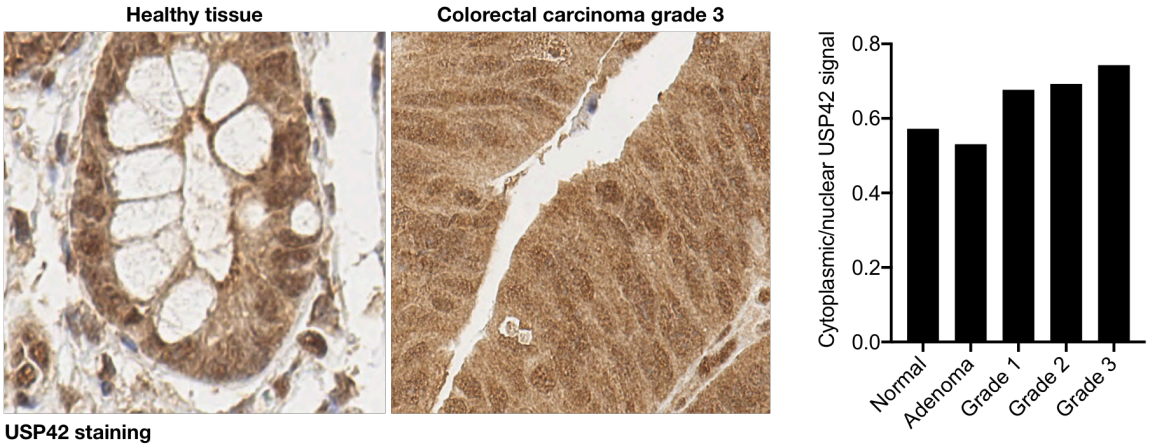

Figure 3.6.10: Cytoplasmic USP42 is enriched in colorectal carcinoma in comparison to the healthy and adenoma tissue.
Close-up of the tissue section of healthy (left) and colorectal carcinoma grade 3 (middle). The cytoplasmic and nuclear USP42 signal was measured of at least 160 cells per condition and the cytoplasmic/nuclear ratio was calculated.

To sum up, I could show that USP42 is a negative Wnt regulator which stabilises ZNRF3/RNF43 at the cell membrane by deubiquitinating them. This interaction is mediated through the N-terminal domain of USP42 and the DIR of ZNRF3. By stabilising ZNRF3/RNF43, USP42 promotes Wnt receptor turnover. Here, I could also show that Usp42 is differentially expressed throughout the mouse intestine and depletion of Usp42 help mouse intestinal organoids to survive growth factor withdrawal. Finally, grade 3 colorectal carcinoma seem to have an increased amount of cytoplasmic USP42, and loss of USP42 leads to epithelial-to-mesenchymal transition and Wnt-dependent proliferation in the colorectal cancer cell line HCT116.

4. Discussion

In recent years, research on ZNRF3 and RNF43 has received increased attention, due to their importance in regulating canonical Wnt signalling in adult stem cells. In stem cells, they promote the turnover of the Wnt receptors Frizzled and LRP5/6, thereby inhibiting Wnt signalling (Hao *et al.* 2012, Koo *et al.* 2012). ZNRF3/RNF43 are often mutated in Wnt-associated cancers (Bond *et al.* 2016), which makes it a crucial task to elucidate the mechanisms of ZNRF3/RNF43 regulation. For instance, it has been shown that binding to R-spondin and LGR4/5/6 antagonises ZNRF3/RNF43 activity, inducing their auto-ubiquitination and clearance from the cell membrane (de Lau *et al* 2011, Hao *et al.* 2012). On the other hand, Dishevelled - a scaffold protein of the β-catenin destruction complex – recruits ZNRF3/RNF43 to the Wnt receptors, leading to the destabilisation of Frizzled and LRP5/6 (Jiang *et al.* 2012). Regarding post-translational modifications of ZNRF3/RNF43, studies have shown that phosphorylation plays an important role in regulating their activity. ZNRF3/RNF43 is phosphorylated by casein kinase 1 (CK1), while their dephosphorylation is promoted by PTPRK (Chang *et al.* 2020, Spit *et al.* 2020, Tsukiyama *et al.* 2020).

In this work, I could show that USP42 is a novel interaction partner and regulator of ZNRF3 and RNF43. I demonstrated that USP42 deubiquitinates and stabilises ZNRF3/RNF43 at the cell membrane, thereby promoting Frizzled and LRP6 receptor turnover, leading to the inhibition of canonical Wnt signalling (Figure 4.1). By generating the truncation mutants, I could show that the Dishevelled interacting region of ZNRF3/RNF43 and the C-terminal of USP42 are important for this interaction. In mouse intestine and colon tissue, USP42 proteins are heterogenously expressed in the villus and in the crypts. Also, USP42 changes its subcellular localisation upon treatment with Rapamycin. Loss of USP42 leads to increased Wnt-dependent proliferation and EMT in colorectal cancer cells and also increases survival of mouse intestinal organoids in Wnt depleted medium.

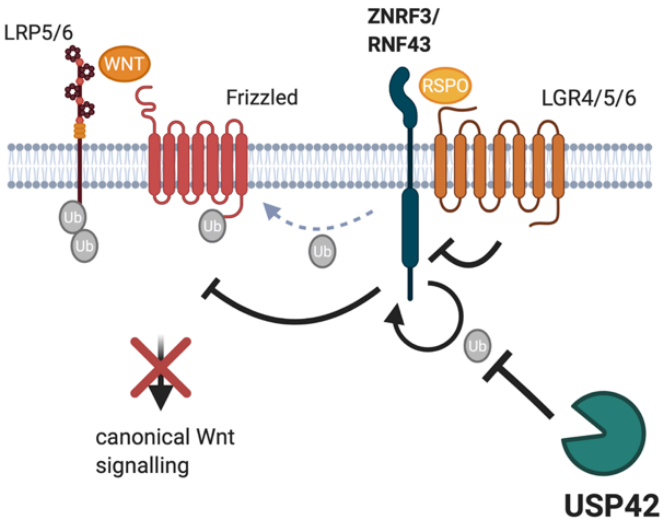

Figure 4.1: USP42 stabilises ZNRF3/RNF43 at the plasmamembrane and inhibits Wnt signalling.
The current working model describes how USP42 inhibits Wnt signalling. R-Spondin and LGR4/5/6 antagonise ZNRF3/RNF43 which leads to their auto-ubiquitination and internalisation. This is where USP42 interferes by deubiquitinating ZNRF3/RNF3 at the plasma membrane. ZNRF3/RNF43 are stabilised and ubiquitinate the Wnt receptors Frizzles and LRP6, which results in Wnt inhibition. (Made with BioRender.)

USP42 in colorectal cancer

Colorectal cancer cells harbour different mutations in Wnt-proteins (such as APC, ZNRF3/RNF43, β-catenin), which makes colorectal cancer a Wnt-associated cancer (cBioPortal analysis). USP42 is also mutated in 6% of colorectal cancer, peaking at a mutation rate of 11% in mucinous adenocarcinoma of the colon and rectum, but the mutations remain uncharacterised (TCGA, PanCancer Atlas and Genentech, Nature 2012). Also, USP42 mRNA is upregulated in rectal and colon adenocarcinoma. *In silico* analysis showed that there is an overlap of high mRNA expression with missense mutations of mainly TP53, APC and KRAS (which are often mutated in left-sided colorectal cancer), but also with truncated RNF43. These data suggest a different role of USP42 in right and left sided colorectal cancer, meaning it might act

as a rescue mechanism to activate p53 signalling in left-sided colorectal cancer, but stabilises truncated RNF43 in right-sided colorectal cancer.

In this project, I generated Usp42 knockout mouse intestinal organoids to test, how Usp42 contributes to cancer development. It has been previously shown, that ZNRF3/RNF43 double knockout increases the proliferation zone of intestinal stem cells and renders DKO mouse intestinal organoids hypersensitive to Wnt ligands (Koo *et al.* 2012 and 2015, Spit *et al.* 2020). Usp42 knockout organoids were able to phenocopy loss of ZNRF3/RNF43 in mouse intestinal organoids.

Analysing the tissue microarray obtained from the NCT Heidelberg, there seems to be an increase in the cytoplasmic-to-nuclear ratio of USP42 protein levels in grade 3 colorectal carcinoma compared to healthy tissue. This might indicate a higher deubiquitinating activity in the cytoplasm, if USP42 is not mutated in these tissue samples itself. Nevertheless, other occurring mutations or tumour characteristics in these tissue samples are unknown. For example, studies have shown that specific sets of mutations occur in right-sided versus left-sided colorectal cancer (Matsumoto *et al.* 2020, Salem *et al.* 2020). Right-sided colorectal carcinoma include mutations in BRAF, KRAS, RNF43, ARIDIA, KMT2D, PIK3CA, PTEN, MLH1, MSH2, BRAF whereas left-sided colorectal carcinoma tissue harbours mutations in TP53, APC and KRAS. In healthy cells, USP42 stabilises p53 and inhibits Wnt signalling, but loss of function would lead to the inactivation of p53 signalling and an increase in Wnt signalling. Even though USP42 might not affect basal levels of p53 and is only required for the rapid activation of early stress response, small changes of Usp42/p53 interaction may lead to more drastic consequences (Hock *et al.* 2011). Given the role of USP42 as a regulator of p53 and Wnt signalling, this suggests that USP42 acts as a molecular switch between p53 and Wnt signalling. However, depending on the types of mutations in colorectal cancer, I can only speculate how USP42 contributes to colorectal cancer development and progression, for example by stabilising oncogenic RNF43 or p53, contributing to cancer development and progression without necessarily being mutated itself.

How are USP42 localisation and function regulated?

Previous research has shown that USP42 localises mainly to the nucleus, where it

deubiquitinates H2B to regulate transcription, deubiquitinates p53 in early stress response and also localises to nuclear speckles to promote homologous recombinant repair and drive phase separation (Hock *et al.* 2011, Hock *et al.* 2014, Matsui *et al.* 2020, Liu *et al.* 2021). Here, I revealed a function of cytoplasmic USP42 (Giebel *et al.* 2021). Then again, I observed that USP42 is differentially expressed in the small intestine, where the differentiated cells in the villus have mainly nuclear USP42 and the cells of the crypts cytoplasmic USP42. Taking a closer look to the intestinal crypts, there are also two different localisation patterns visible. Single cells have high levels of cytoplasmic USP42, whereas the others concentrate USP42 in small foci in the cytoplasm. Now the question arises, how USP42 distribution within the cell is determined.

In my work I could show that the NLS sequence of USP42 determines its subcellular localisation. When USP42 lacks the NLS, it localises to the cytoplasm and is excluded from the nucleus. Proteins which have an NLS are commonly imported to the nucleus via importins (reviewed in Lu *et al. 2021)*. Phosphorylation within or adjacent to the NLS change the binding affinity to the importins, thereby altering nuclear import. *In silico* analysis has predicted several phosphorylation sites in this region (phosphosite.org). This raises the question, which signals induce nuclear USP42 export and recruitment to the cytoplasm, or more specific to the cell membrane. During my experiments, I noticed that USP42 is not immediately shuttled between the cytoplasm and the nucleus, when treated with different reagents. Preliminary experiments included testing the different reagents (e.g. Importazole, Rapamycin, R-spondin3) for 1 – 4 hours of treatment to observe changes in protein distribution and to avoid effects on the transcriptional level. Because no changes could be detected, I increased the duration of the treatments to 6, 9 and 16-20 (overnight) hours. Only in the overnight treatments I could observe the changes, which implies that USP42 is quite stable and is not actively transported out of the nucleus. Hence, I hypothesise that USP42 distribution changes after cell division. My data also shows that the mTOR inhibitor Rapamycin clearly increases the cytoplasmic USP42 protein level. One potential candidate for the phosphorylation could be the S6K, but the mechanism remains to be elucidated. There was also a milder increase in cytoplasmic USP42 upon R-spondin3 treatment. This could be explained as a

feedback loop due to the fact that the Wnt agonist R-spondin3, together with LGR, bind ZNRF3/RNF43 and induce their auto-ubiquitination. In this case, the factor recruiting USP42 to the cell membrane would be the availability of ubiquitinated ZNRF3/RNF43.

Taken together, USP42 seems to not only have different functions depending on its subcellular localisation, but also in different cell types.

USP42 in mammalian physiology

ZNRF3/RNF43 play important roles in animal physiology and development, for example in adrenal gland homeostasis (Basham *et al.* 2019), liver zonation (Planaz-Paz *et al.* 2016), limb development (Szenker-Ravi *et al.* 2018), lense development (Hao *et al.* 2016), embryogenesis (Harris *et al.* 2018, Chang 2020, Lee 2020) and intestinal stem cell homeostasis (Koo *et al.* 2012).

The bulk RNAseq data and the stainings in mouse intestine and colon tissue provide first insights of a physiological role of USP42. Loss of USP42 upregulates target genes related to cell cycle progression, ubiquitination, DNA replication and Wnt, NFκB and TNF-mediated signalling, as well as intestinal stem cell proliferation genes (Merlos-Suarez *et al.* 2011, Giebel *et al.* 2020). In addition, I observed that USP42 might recruit to the centrosomes during Interphase and centrosome duplication. Of course, this gives an interesting opportunity to study the role of USP42 in cell cycle regulation, especially mitosis. There is already evidence, that p53 localises to the centrosomes (Chen *et al.* 2017, Contadini *et al.* 2019), which could be a potential interaction partner during mitosis.

In mouse intestinal villi, Usp42 is mainly found in the nucleus, whereas the crypts show more cytoplasmic USP42 either as single punctae or in a great amount. It is of great interest to identify the cells and their USP42 expression pattern. From the preliminary data I obtained, I hypothesise according to the large cell size that the highly expressing cells could be secreting cells, such as paneth cells, and the slimmer bell shaped cells could be tuft cells that are responsible for the immune response in the intestine, or even intestinal stem cells. To correctly identify the cells, I suggest to perform co-stainings with different markers of intestinal cells, such as stem cells (LGR5, LRIG1, OLFM4), paneth cells (lysozyme), goblet cells (MUC2), enteroendocrine

(CHGA, synaptophysin) and tuft cells (DCAMKL1) (Qin *et al.* 2020). In contrast to the mouse tissue sections, the NCT scans of healthy, adenoma and colorectal carcinoma tissue sections show that nuclear USP42 is also found in the cells of the crypts. To clarify this, I first suggest to further optimise the staining in mouse tissue, by trying different fixation methods. Nevertheless, the subcellular localisation of human and mouse USP42 could vary between the two species due to its function as a negative regulator of Wnt signalling. As previously described, ZNRF3/RNF43 are important negative Wnt regulators in the small intestinal crypt (Koo *et al.* 2012). A double knockout resulted in an elongated proliferation zone, as well as longer villi (Koo *et al.* 2012). The regulation of homeostasis in the intestinal crypt is dependent on the interplay between different signalling pathways, creating inhibitory and overlapping gradients along the villus and crypt. Considering the fact that mice are smaller than humans, the intestinal villi are shorter and might require a tighter spatial and temporal regulation of proliferating cells in the small intestine. This is where Usp42 may be required for the fast inhibition of Wnt signalling by stabilising the two strong negative regulators ZNRF3 and RNF43. Thus, further proliferation is prevented. The elevated levels of cytosolic Usp42 may provide a higher availability for interaction at the cell membrane or for being secreted and might explain the difference in mouse crypts compared to human cells.

Furthermore, we are currently generating a Usp42 knockout mouse model to study the role of Usp42 in development and disease. In addition to the Usp42 knockout intestinal organoids, staining cryosections (e.g. with the proliferation marker Ki-67, or p53) of the knockout mouse tissues can provide better understanding of how loss of Usp42 can alter tissue composition in the intestine, liver and adrenal gland, compared to ZNRF3/RNF43 double knockout tissue. Also, it would be interesting to observe differences and similarities of an inducible Usp42 knockout mouse compared to its wild type, since the impact of Usp42 might be limited to a specific time frame, as suggested in p53 signalling (Hock *et al.* 2011). Even though Usp42 KO in mouse intestinal organoids could mimic ZNRF3/RFN43 DKO, the tissue of the mouse model might give milder phenotypes, because USP42 is a regulator of ZNRF3/RNF43 (similar to the Wnt reporter assays). It is also possible, that there are other deubiquitinating enzymes stabilising ZNRF3/RNF43 which have not been

discovered yet. They could possibly compensate the loss of Usp42 in the mouse model. In addition, loss of Usp42 in the mouse could have Wnt-independent effects, because USP42 has other functions, such as regulating transcription, p53 and the spliceosome.

There has been one study attempting to characterise Usp42 in mouse embryogenesis and spermatogenesis, which shows that Usp42 is expressed in all tissues, but especially strong in the testis, brain, lungs and thymus. Regarding spermatogenesis, they report that Usp42 expression increases from the round-spermatid stage 2 weeks after birth and decreases from the round-spermatid stage (Kim *et al.* 2006). Also, they performed *in situ* hybridisation on mouse embryos (E9.5 – 12.5), by which they detected Usp42 expression in the mid- and forebrain, optic vesicles and eyes at day E10.5, which increases to day E12.5. Interestingly, Usp42 expression was not detected in the limbs, gut and liver. In regards to the intestine, it has been shown that Wnt5a and PCP signalling are responsible for early gut development in the E9.5-14.5 stage (Spence 2011, Shyer 2015). Thus, I suggest to also compare Usp42 mRNA and protein levels in later stages, when the villi form. As a study has shown, p53 mRNA is strongly expressed in the intestine from day 14.5 *p.c.* on, also describing the formation of the intestinal villi (Schmid *et al.* 1991). They state that cells in the intestinal crypts had a stronger p53 expression compared to the cells of the villus. Together with our data, it could be of interest to investigate the differential roles of Usp42 in Wnt signalling and in p53 signalling.

In conclusion, taking all the data together, USP42 acts as an inhibitor for Wnt signalling, cell cycle and EMT, as opposed to its role in stabilising p53. Comparing the phenotypes of Usp42 depleted tissues with ZNRF3$^{-/-}$/RNF43$^{-/-}$, as well as p53 depleted tissue and organoids, will provide a better insight of the physiological role of USP42 in animal physiology and cancer development.

5. References

- Abrami, L., Kunz, B., Iacovache, I., & van der Goot, F. G. (2008). Palmitoylation and ubiquitination regulate exit of the Wnt signaling protein LRP6 from the endoplasmic reticulum. *Proceedings of the National Academy of Sciences of the United States of America*, *105*(14), 5384–5389. https://doi.org/10.1073/pnas.0710389105
- Angers, S., Thorpe, C. J., Biechele, T. L., Goldenberg, S. J., Zheng, N., MacCoss, M. J., & Moon, R. T. (2006). The KLHL12-Cullin-3 ubiquitin ligase negatively regulates the Wnt-beta-catenin pathway by targeting Dishevelled for degradation. *Nature cell biology*, *8*(4), 348–357. https://doi.org/10.1038/ncb1381
- Annunziato, S., Sun, T., Tchorz, J.S. (2022). The RSPO-LGR4/5-ZNRF3/RNF43 module in liver homeostasis, regeneration, and disease. *Hepatology*, 76: 888–899. https://doi.org/10.1002/hep.32328
- Assié, G., Letouzé, E., Fassnacht, M., Jouinot, A., Luscap, W., Barreau, O., Omeiri, H., Rodriguez, S., Perlemoine, K., René-Corail, F., Elarouci, N., Sbiera, S., Kroiss, M., Allolio, B., Waldmann, J., Quinkler, M., Mannelli, M., Mantero, F., Papathomas, T., De Krijger, R., … Bertherat, J. (2014). Integrated genomic characterization of adrenocortical carcinoma. *Nature genetics*, *46*(6), 607–612. https://doi.org/10.1038/ng.2953
- Bänziger, C., Soldini, D., Schütt, C., Zipperlen, P., Hausmann, G., & Basler, K. (2006). Wntless, a conserved membrane protein dedicated to the secretion of Wnt proteins from signaling cells. *Cell*, *125*(3), 509–522. https://doi.org/10.1016/j.cell.2006.02.049
- Barker, N., van Es, J. H., Kuipers, J., Kujala, P., van den Born, M., Cozijnsen, M., Haegebarth, A., Korving, J., Begthel, H., Peters, P. J., & Clevers, H. (2007). Identification of stem cells in small intestine and colon by marker gene Lgr5. *Nature*, *449*(7165), 1003–1007. https://doi.org/10.1038/nature06196
- Bartscherer, K., Pelte, N., Ingelfinger, D., & Boutros, M. (2006). Secretion of Wnt ligands requires Evi, a conserved transmembrane protein. *Cell*, *125*(3), 523–533. https://doi.org/10.1016/j.cell.2006.04.009
- Basham, K. J., Rodriguez, S., Turcu, A. F., Lerario, A. M., Logan, C. Y., Rysztak, M. R., Gomez-Sanchez, C. E., Breault, D. T., Koo, B. K., Clevers, H., Nusse, R., Val, P., & Hammer, G. D. (2019). A ZNRF3-dependent Wnt/β-catenin signaling gradient is required for adrenal homeostasis. *Genes & development*, *33*(3-4), 209–220. https://doi.org/10.1101/gad.317412.118
- Belenguer, G., Mastrogiovanni, G., Pacini, C., Hall, Z., Dowbaj, A. M., Arnes-Benito, R., Sljukic, A., Prior, N., Kakava, S., Bradshaw, C. R., Davies, S., Vacca, M., Saeb-Parsy, K., Koo, B. K., & Huch, M. (2022). RNF43/ZNRF3 loss predisposes to

hepatocellular-carcinoma by impairing liver regeneration and altering the liver lipid metabolic ground-state. *Nature communications*, *13*(1), 334. https://doi.org/10.1038/s41467-021-27923-z

- Beumer, J., & Clevers, H. (2021). Cell fate specification and differentiation in the adult mammalian intestine. *Nature reviews. Molecular cell biology*, *22*(1), 39–53. https://doi.org/10.1038/s41580-020-0278-0
- Bhanot, P., Brink, M., Samos, C. *et al.* A new member of the *frizzled* family from *Drosophila* functions as a Wingless receptor. *Nature* **382,** 225–230 (1996). https://doi.org/10.1038/382225a0
- Brunx, C. E., McKeone, D. M., Kalimutho, M., Bettington, M. L., Pearson, S. A., Dumenil, T. D., Wockner, L. F., Burge, M., Leggett, B. A., & Whitehall, V. L. (2016). RNF43 and ZNRF3 are commonly altered in serrated pathway colorectal tumorigenesis. *Oncotarget*, *7*(43), 70589–70600. https://doi.org/10.18632/oncotarget.12130
- Callow, M. G., Tran, H., Phu, L., Lau, T., Lee, J., Sandoval, W. N., Liu, P. S., Bheddah, S., Tao, J., Lill, J. R., Hongo, J. A., Davis, D., Kirkpatrick, D. S., Polakis, P., & Costa, M. (2011). Ubiquitin ligase RNF146 regulates tankyrase and Axin to promote Wnt signaling. *PloS one*, *6*(7), e22595. https://doi.org/10.1371/journal.pone.0022595
- Carmon, K. S., Gong, X., Lin, Q., Thomas, A., & Liu, Q. (2011). R-spondins function as ligands of the orphan receptors LGR4 and LGR5 to regulate Wnt/beta-catenin signaling. *Proceedings of the National Academy of Sciences of the United States of America*, *108*(28), 11452–11457. https://doi.org/10.1073/pnas.1106083108
- Cerami, E., Gao, J., Dogrusoz, U., Gross, B. E., Sumer, S. O., Aksoy, B. A., Jacobsen, A., Byrne, C. J., Heuer, M. L., Larsson, E., Antipin, Y., Reva, B., Goldberg, A. P., Sander, C., & Schultz, N. (2012). The cBio cancer genomics portal: an open platform for exploring multidimensional cancer genomics data. *Cancer discovery*, *2*(5), 401–404. https://doi.org/10.1158/2159-8290.CD-12-0095
- Chang, L. S., Kim, M., Glinka, A., Reinhard, C., & Niehrs, C. (2020). The tumor suppressor PTPRK promotes ZNRF3 internalization and is required for Wnt inhibition in the Spemann organizer. *eLife*, *9*, e51248. https://doi.org/10.7554/eLife.51248
- Chaugule, S., Kim, J. M., Yang, Y. S., Knobeloch, K. P., He, X., & Shim, J. H. (2021). Deubiquitinating Enzyme USP8 Is Essential for Skeletogenesis by Regulating Wnt Signaling. *International journal of molecular sciences*, *22*(19), 10289. https://doi.org/10.3390/ijms221910289
- Chen, P. H., Chen, X., Lin, Z., Fang, D., & He, X. (2013). The structural basis of R-spondin recognition by LGR5 and RNF43. *Genes & development*, *27*(12), 1345–1350. https://doi.org/10.1101/gad.219915.113
- Chen, W. J., Wang, W. T., Tsai, T. Y., Li, H. K., & Lee, Y. W. (2017). DDX3 localizes to the centrosome and prevents multipolar mitosis by epigenetically and

translationally modulating p53 expression. *Scientific reports*, *7*(1), 9411. https://doi.org/10.1038/s41598-017-09779-w

- Ci, Y., Li, X., Chen, M., Zhong, J., North, B. J., Inuzuka, H., He, X., Li, Y., Guo, J., & Dai, X. (2018). $SCF^{\beta\text{-}TRCP}$ E3 ubiquitin ligase targets the tumor suppressor ZNRF3 for ubiquitination and degradation. *Protein & cell*, *9*(10), 879–889. https://doi.org/10.1007/s13238-018-0510-2
- Clevers, H., & Nusse, R. (2012). Wnt/β-catenin signaling and disease. *Cell*, *149*(6), 1192–1205. https://doi.org/10.1016/j.cell.2012.05.012
- Contadini, C., Monteonofrio, L., Virdia, I., Prodosmo, A., Valente, D., Chessa, L., Musio, A., Fava, L. L., Rinaldo, C., Di Rocco, G., & Soddu, S. (2019). p53 mitotic centrosome localization preserves centrosome integrity and works as sensor for the mitotic surveillance pathway. *Cell death & disease*, *10*(11), 850. https://doi.org/10.1038/s41419-019-2076-1
- De, A. (2011). Wnt/Ca^{2+} signaling pathway: a brief overview, *Acta Biochimica et Biophysica Sinica*, Volume 43 (10), 745 - 756, https://doi.org/10.1093/abbs/gmr079
- de Lau, W., Barker, N., Low, T. Y., Koo, B. K., Li, V. S., Teunissen, H., Kujala, P., Haegebarth, A., Peters, P. J., van de Wetering, M., Stange, D. E., van Es, J. E., Guardavaccaro, D., Schasfoort, R. B., Mohri, Y., Nishimori, K., Mohammed, S., Heck, A. J., & Clevers, H. (2011). Lgr5 homologues associate with Wnt receptors and mediate R-spondin signalling. *Nature*, *476*(7360), 293–297. https://doi.org/10.1038/nature10337
- de Lau, W., Peng, W. C., Gros, P., & Clevers, H. (2014). The R-spondin/Lgr5/Rnf43 module: regulator of Wnt signal strength. *Genes & development*, *28*(4), 305–316. https://doi.org/10.1101/gad.235473.113
- Ding, Y., Zhang, Y., Xu, C., Tao, Q. H., & Chen, Y. G. (2013). HECT domain-containing E3 ubiquitin ligase NEDD4L negatively regulates Wnt signaling by targeting dishevelled for proteasomal degradation. *The Journal of biological chemistry*, *288*(12), 8289–8298. https://doi.org/10.1074/jbc.M112.433185
- Dimitrova, Y. N., Li, J., Lee, Y. T., Rios-Esteves, J., Friedman, D. B., Choi, H. J., Weis, W. I., Wang, C. Y., & Chazin, W. J. (2010). Direct ubiquitination of beta-catenin by Siah-1 and regulation by the exchange factor TBL1. *The Journal of biological chemistry*, *285*(18), 13507–13516. https://doi.org/10.1074/jbc.M109.049411
- Doumpas, N., Lampart, F., Robinson, M. D., Lentini, A., Nestor, C. E., Cantù, C., & Basler, K. (2019). TCF/LEF dependent and independent transcriptional regulation of Wnt/β-catenin target genes. *The EMBO journal*, *38*(2), e98873. https://doi.org/10.15252/embj.201798873
- Farin, H. F., Van Es, J. H., & Clevers, H. (2012). Redundant sources of Wnt regulate intestinal stem cells and promote formation of Paneth cells. *Gastroenterology*, *143*(6), 1518–1529.e7. https://doi.org/10.1053/j.gastro.2012.08.031

- Fei, C., Li, Z., Li, C., Chen, Y., Chen, Z., He, X., Mao, L., Wang, X., Zeng, R., & Li, L. (2013). Smurf1-mediated Lys29-linked nonproteolytic polyubiquitination of axin negatively regulates Wnt/β-catenin signaling. *Molecular and cellular biology*, *33*(20), 4095–4105. https://doi.org/10.1128/MCB.00418-13

- Finley, D., Sadis, S., Monia, B. P., Boucher, P., Ecker, D. J., Crooke, S. T., & Chau, V. (1994). Inhibition of proteolysis and cell cycle progression in a multiubiquitination-deficient yeast mutant. *Molecular and cellular biology*, *14*(8), 5501–5509. https://doi.org/10.1128/mcb.14.8.5501-5509.1994
- Fontes, M. R., Teh, T., Jans, D., Brinkworth, R. I., & Kobe, B. (2003). Structural basis for the specificity of bipartite nuclear localization sequence binding by importin-alpha. *The Journal of biological chemistry*, *278*(30), 27981–27987. https://doi.org/10.1074/jbc.M303275200
- Gao, B., Song, H., Bishop, K., Elliot, G., Garrett, L., English, M. A., Andre, P., Robinson, J., Sood, R., Minami, Y., Economides, A. N., & Yang, Y. (2011). Wnt signaling gradients establish planar cell polarity by inducing Vangl2 phosphorylation through Ror2. *Developmental cell*, *20*(2), 163–176. https://doi.org/10.1016/j.devcel.2011.01.001
- Gao, J., Aksoy, B. A., Dogrusoz, U., Dresdner, G., Gross, B., Sumer, S. O., Sun, Y., Jacobsen, A., Sinha, R., Larsson, E., Cerami, E., Sander, C., & Schultz, N. (2013). Integrative analysis of complex cancer genomics and clinical profiles using the cBioPortal. *Science signaling*, *6*(269), pl1. https://doi.org/10.1126/scisignal.2004088
- Giannakis, M., Hodis, E., Jasmine Mu, X., Yamauchi, M., Rosenbluh, J., Cibulskis, K., Saksena, G., Lawrence, M. S., Qian, Z. R., Nishihara, R., Van Allen, E. M., Hahn, W. C., Gabriel, S. B., Lander, E. S., Getz, G., Ogino, S., Fuchs, C. S., & Garraway, L. A. (2014). RNF43 is frequently mutated in colorectal and endometrial cancers. *Nature genetics*, *46*(12), 1264–1266. https://doi.org/10.1038/ng.3127
- Giebel, N., de Jaime-Soguero, A., García Del Arco, A., Landry, J., Tietje, M., Villacorta, L., Benes, V., Fernández-Sáiz, V., & Acebrón, S. P. (2021). USP42 protects ZNRF3/RNF43 from R-spondin-dependent clearance and inhibits Wnt signalling. *EMBO reports*, *22*(5), e51415. https://doi.org/10.15252/embr.202051415
- Glinka, A., Dolde, C., Kirsch, N., Huang, Y. L., Kazanskaya, O., Ingelfinger, D., Boutros, M., Cruciat, C. M., & Niehrs, C. (2011). LGR4 and LGR5 are R-spondin receptors mediating Wnt/β-catenin and Wnt/PCP signalling. *EMBO reports*, *12*(10), 1055–1061. https://doi.org/10.1038/embor.2011.175
- Goodrich, L. V., & Strutt, D. (2011). Principles of planar polarity in animal development. *Development (Cambridge, England)*, *138*(10), 1877–1892. https://doi.org/10.1242/dev.054080

- Gross, J. C., Chaudhary, V., Bartscherer, K., & Boutros, M. (2012). Active Wnt proteins are secreted on exosomes. *Nature cell biology*, *14*(10), 1036–1045. https://doi.org/10.1038/ncb2574
- Haglund, K., Di Fiore, P. P., & Dikic, I. (2003). Distinct monoubiquitin signals in receptor endocytosis. *Trends in biochemical sciences*, *28*(11), 598–603. https://doi.org/10.1016/j.tibs.2003.09.005
- Han, T., Schatoff, E. M., Murphy, C., Zafra, M. P., Wilkinson, J. E., Elemento, O., & Dow, L. E. (2017). R-Spondin chromosome rearrangements drive Wnt-dependent tumour initiation and maintenance in the intestine. *Nature communications*, *8*, 15945. https://doi.org/10.1038/ncomms15945
- Hao, H. X., Xie, Y., Zhang, Y., Charlat, O., Oster, E., Avello, M., Lei, H., Mickanin, C., Liu, D., Ruffner, H., Mao, X., Ma, Q., Zamponi, R., Bouwmeester, T., Finan, P. M., Kirschner, M. W., Porter, J. A., Serluca, F. C., & Cong, F. (2012). ZNRF3 promotes Wnt receptor turnover in an R-spondin-sensitive manner. *Nature*, *485*(7397), 195–200. https://doi.org/10.1038/nature11019
- Hao, H.-X., Jiang, X., & Cong, F. (2016). Control of Wnt Receptor Turnover by R-spondin-ZNRF3/RNF43 Signaling Module and Its Dysregulation in Cancer. *Cancers*, *8*(6), 54. doi:10.3390/cancers8060054
- Haramis, A. P., Begthel, H., van den Born, M., van Es, J., Jonkheer, S., Offerhaus, G. J., & Clevers, H. (2004). De novo crypt formation and juvenile polyposis on BMP inhibition in mouse intestine. *Science (New York, N.Y.)*, *303*(5664), 1684–1686. https://doi.org/10.1126/science.1093587
- Harreman, M. T., Kline, T. M., Milford, H. G., Harben, M. B., Hodel, A. E., & Corbett, A. H. (2004). Regulation of nuclear import by phosphorylation adjacent to nuclear localization signals. *The Journal of biological chemistry*, *279*(20), 20613–20621. https://doi.org/10.1074/jbc.M401720200
- Harris, A., Siggers, P., Corrochano, S., Warr, N., Sagar, D., Grimes, D. T., Suzuki, M., Burdine, R. D., Cong, F., Koo, B. K., Clevers, H., Stévant, I., Nef, S., Wells, S., Brauner, R., Ben Rhouma, B., Belguith, N., Eozenou, C., Bignon-Topalovic, J., Bashamboo, A., … Greenfield, A. (2018). ZNRF3 functions in mammalian sex determination by inhibiting canonical WNT signaling. *Proceedings of the National Academy of Sciences of the United States of America*, *115*(21), 5474–5479. https://doi.org/10.1073/pnas.1801223115
- Harrigan, J. A., Jacq, X., Martin, N. M., & Jackson, S. P. (2018). Deubiquitylating enzymes and drug discovery: emerging opportunities. *Nature reviews. Drug discovery*, *17*(1), 57–78. https://doi.org/10.1038/nrd.2017.152
- He, T. C., Sparks, A. B., Rago, C., Hermeking, H., Zawel, L., da Costa, L. T., Morin, P. J., Vogelstein, B., & Kinzler, K. W. (1998). Identification of c-MYC as a target of the APC pathway. *Science (New York, N.Y.)*, *281*(5382), 1509–1512. https://doi.org/10.1126/science.281.5382.1509

- Hermanns, T., Pichlo, C., Woiwode, I. *et al.* A family of unconventional deubiquitinases with modular chain specificity determinants. *Nat Commun* **9,** 799 (2018). https://doi.org/10.1038/s41467-018-03148-5
- Herr P., Basler K. (2012) Porcupine-mediated lipidation is required for Wnt recognition by Wls. *Dev. Biol.* 361, 392–402
- Ho, H. Y., Susman, M. W., Bikoff, J. B., Ryu, Y. K., Jonas, A. M., Hu, L., Kuruvilla, R., & Greenberg, M. E. (2012). Wnt5a-Ror-Dishevelled signaling constitutes a core developmental pathway that controls tissue morphogenesis. *Proceedings of the National Academy of Sciences of the United States of America*, *109*(11), 4044–4051. https://doi.org/10.1073/pnas.1200421109
- Hock, A. K., Vigneron, A. M., Carter, S., Ludwig, R. L., & Vousden, K. H. (2011). Regulation of p53 stability and function by the deubiquitinating enzyme USP42. *The EMBO journal*, *30*(24), 4921–4930. https://doi.org/10.1038/emboj.2011.419
- Hock, A. K., Vigneron, A. M., & Vousden, K. H. (2014). Ubiquitin-specific peptidase 42 (USP42) functions to deubiquitylate histones and regulate transcriptional activity. *The Journal of biological chemistry*, *289*(50), 34862–34870. https://doi.org/10.1074/jbc.M114.589267
- Holstein, T. W. (2012). The evolution of the Wnt pathway. *Cold Spring Harb Perspect. Biol.*, *4*, a007922.
- Hou, K., Zhu, Z., Wang, Y., Zhang, C., Yu, S., Zhu, Q., & Yan, B. (2016). Overexpression and Biological Function of Ubiquitin-Specific Protease 42 in Gastric Cancer. *PloS one*, *11*(3), e0152997. https://doi.org/10.1371/journal.pone.0152997
- Huang, S. M., Mishina, Y. M., Liu, S., Cheung, A., Stegmeier, F., Michaud, G. A., Charlat, O., Wiellette, E., Zhang, Y., Wiessner, S., Hild, M., Shi, X., Wilson, C. J., Mickanin, C., Myer, V., Fazal, A., Tomlinson, R., Serluca, F., Shao, W., Cheng, H., … Cong, F. (2009). Tankyrase inhibition stabilizes axin and antagonizes Wnt signalling. *Nature*, *461*(7264), 614–620. https://doi.org/10.1038/nature08356
- Huang, X., Langelotz, C., Hetfeld-Pechoc, B. K., Schwenk, W., & Dubiel, W. (2009). The COP9 signalosome mediates beta-catenin degradation by deneddylation and blocks adenomatous polyposis coli destruction via USP15. *Journal of molecular biology*, *391*(4), 691–702. https://doi.org/10.1016/j.jmb.2009.06.066
- Huibregtse, J. M., Scheffner, M., Beaudenon, S., & Howley, P. M. (1995). A family of proteins structurally and functionally related to the E6-AP ubiquitin-protein ligase. *Proceedings of the National Academy of Sciences of the United States of America*, *92*(7), 2563–2567. https://doi.org/10.1073/pnas.92.7.2563 Nakielny
- Humphries, A. C., & Mlodzik, M. (2018). From instruction to output: Wnt/PCP signaling in development and cancer. *Current opinion in cell biology*, *51*, 110–116. https://doi.org/10.1016/j.ceb.2017.12.005

- Ikeda, F., & Dikic, I. (2008). Atypical ubiquitin chains: new molecular signals. 'Protein Modifications: Beyond the Usual Suspects' review series. *EMBO reports*, *9*(6), 536–542. https://doi.org/10.1038/embor.2008.93
- Inestrosa, N. C., & Arenas, E. (2010). Emerging roles of Wnts in the adult nervous system. *Nature reviews. Neuroscience*, *11*(2), 77–86. https://doi.org/10.1038/nrn2755
- Jans, D. A., Xiao, C. Y., & Lam, M. H. (2000). Nuclear targeting signal recognition: a key control point in nuclear transport?. *BioEssays : news and reviews in molecular, cellular and developmental biology*, *22*(6), 532–544. https://doi.org/10.1002/(SICI)1521-1878(200006)22:6<532::AID-BIES6>3.0.CO;2-O
- Ji, J., Loo, E., Pullarkat, S., Yang, L., & Tirado, C. A. (2014). Acute myeloid leukemia with t(7;21)(p22;q22) and 5q deletion: a case report and literature review. *Experimental hematology & oncology*, *3*, 8. https://doi.org/10.1186/2162-3619-3-8
- Ji, L., Jiang, B., Jiang, X., Charlat, O., Chen, A., Mickanin, C., Bauer, A., Xu, W., Yan, X., & Cong, F. (2017). The SIAH E3 ubiquitin ligases promote Wnt/β-catenin signaling through mediating Wnt-induced Axin degradation. *Genes & development*, *31*(9), 904–915. https://doi.org/10.1101/gad.300053.117
- Ji, L., Lu, B., Zamponi, R., Charlat, O., Aversa, R., Yang, Z., Sigoillot, F., Zhu, X., Hu, T., Reece-Hoyes, J. S., Russ, C., Michaud, G., Tchorz, J. S., Jiang, X., & Cong, F. (2019). USP7 inhibits Wnt/β-catenin signaling through promoting stabilization of Axin. *Nature communications*, *10*(1), 4184. https://doi.org/10.1038/s41467-019-12143-3
- Jiang, X., Hao, H. X., Growney, J. D., Woolfenden, S., Bottiglio, C., Ng, N., Lu, B., Hsieh, M. H., Bagdasarian, L., Meyer, R., Smith, T. R., Avello, M., Charlat, O., Xie, Y., Porter, J. A., Pan, S., Liu, J., McLaughlin, M. E., & Cong, F. (2013). Inactivating mutations of RNF43 confer Wnt dependency in pancreatic ductal adenocarcinoma. *Proceedings of the National Academy of Sciences of the United States of America*, *110*(31), 12649–12654. https://doi.org/10.1073/pnas.1307218110
- Jiang, X., Charlat, O., Zamponi, R., Yang, Y., & Cong, F. (2015). Dishevelled promotes Wnt receptor degradation through recruitment of ZNRF3/RNF43 E3 ubiquitin ligases. *Molecular cell*, *58*(3), 522–533. https://doi.org/10.1016/j.molcel.2015.03.015
- Kadowaki, T., Wilder, E., Klingensmith, J., Zachary, K., & Perrimon, N. (1996). The segment polarity gene porcupine encodes a putative multitransmembrane protein involved in Wingless processing. *Genes & development*, *10*(24), 3116–3128. https://doi.org/10.1101/gad.10.24.3116

- Kaffman, A., & O'Shea, E. K. (1999). Regulation of nuclear localization: a key to a door. *Annual review of cell and developmental biology*, *15*, 291–339. https://doi.org/10.1146/annurev.cellbio.15.1.291
- Kamitani, T., Kito, K., Nguyen, H. P., & Yeh, E. T. (1997). Characterization of NEDD8, a developmentally down-regulated ubiquitin-like protein. *The Journal of biological chemistry*, *272*(45), 28557–28562. https://doi.org/10.1074/jbc.272.45.28557
- Kim, Y. K., Kim, Y. S., Yoo, K. J., Lee, H. J., Lee, D. R., Yeo, C. Y., & Baek, K. H. (2007). The expression of Usp42 during embryogenesis and spermatogenesis in mouse. *Gene expression patterns : GEP*, *7*(1-2), 143–148. https://doi.org/10.1016/j.modgep.2006.06.006
- Kazanskaya, O., Glinka, A., del Barco Barrantes, I., Stannek, P., Niehrs, C., & Wu, W. (2004). R-Spondin2 is a secreted activator of Wnt/beta-catenin signaling and is required for Xenopus myogenesis. *Developmental cell*, *7*(4), 525–534. https://doi.org/10.1016/j.devcel.2004.07.019
- Kazanskaya, O., Ohkawara, B., Heroult, M., Wu, W., Maltry, N., Augustin, H. G., & Niehrs, C. (2008). The Wnt signaling regulator R-spondin 3 promotes angioblast and vascular development. *Development (Cambridge, England)*, *135*(22), 3655–3664. https://doi.org/10.1242/dev.027284
- Kim, H. T., Kim, K. P., Lledias, F., Kisselev, A. F., Scaglione, K. M., Skowyra, D., Gygi, S. P., & Goldberg, A. L. (2007). Certain pairs of ubiquitin-conjugating enzymes (E2s) and ubiquitin-protein ligases (E3s) synthesize nondegradable forked ubiquitin chains containing all possible isopeptide linkages. *The Journal of biological chemistry*, *282*(24), 17375–17386. https://doi.org/10.1074/jbc.M609659200
- Kim, J., Alavi Naini, F., Sun, Y., & Ma, L. (2018). Ubiquitin-specific peptidase 2a (USP2a) deubiquitinates and stabilizes β-catenin. *American journal of cancer research*, *8*(9), 1823–1836.
- Ko, R., Park, J. H., Ha, H., Choi, Y., & Lee, S. Y. (2015). Glycogen synthase kinase 3β ubiquitination by TRAF6 regulates TLR3-mediated pro-inflammatory cytokine production. *Nature communications*, *6*, 6765. https://doi.org/10.1038/ncomms7765
- Koo, B. K., Spit, M., Jordens, I., Low, T. Y., Stange, D. E., van de Wetering, M., van Es, J. H., Mohammed, S., Heck, A. J., Maurice, M. M., & Clevers, H. (2012). Tumour suppressor RNF43 is a stem-cell E3 ligase that induces endocytosis of Wnt receptors. *Nature*, *488*(7413), 665–669.
- Koo, B. K., van Es, J. H., van den Born, M., & Clevers, H. (2015). Porcupine inhibitor suppresses paracrine Wnt-driven growth of Rnf43;Znrf3-mutant neoplasia. *Proceedings of the National Academy of Sciences of the United States of America*, *112*(24), 7548–7550. https://doi.org/10.1073/pnas.1508113112

- Kosinski, C., Li, V. S., Chan, A. S., Zhang, J., Ho, C., Tsui, W. Y., Chan, T. L., Mifflin, R. C., Powell, D. W., Yuen, S. T., Leung, S. Y., & Chen, X. (2007). Gene expression patterns of human colon tops and basal crypts and BMP antagonists as intestinal stem cell niche factors. *Proceedings of the National Academy of Sciences of the United States of America*, *104*(39), 15418–15423. https://doi.org/10.1073/pnas.0707210104
- Koval, A., & Katanaev, V. L. (2011). Wnt3a stimulation elicits G-protein-coupled receptor properties of mammalian Frizzled proteins. *The Biochemical journal*, *433*(3), 435–440. https://doi.org/10.1042/BJ20101878
- Krönke, J., Fink, E. C., Hollenbach, P. W., MacBeth, K. J., Hurst, S. N., Udeshi, N. D., Chamberlain, P. P., Mani, D. R., Man, H. W., Gandhi, A. K., Svinkina, T., Schneider, R. K., McConkey, M., Järås, M., Griffiths, E., Wetzler, M., Bullinger, L., Cathers, B. E., Carr, S. A., Chopra, R., … Ebert, B. L. (2015). Lenalidomide induces ubiquitination and degradation of CK1α in del(5q) MDS. *Nature*, *523*(7559), 183–188. https://doi.org/10.1038/nature14610
- Kühl, M., Sheldahl, L. C., Malbon, C. C., & Moon, R. T. (2000). Ca(2+)/calmodulin-dependent protein kinase II is stimulated by Wnt and Frizzled homologs and promotes ventral cell fates in Xenopus. *The Journal of biological chemistry*, *275*(17), 12701–12711. https://doi.org/10.1074/jbc.275.17.12701
- Kurayoshi, M., Oue, N., Yamamoto, H., Kishida, M., Inoue, A., Asahara, T., Yasui, W., & Kikuchi, A. (2006). Expression of Wnt-5a is correlated with aggressiveness of gastric cancer by stimulating cell migration and invasion. *Cancer research*, *66*(21), 10439–10448. https://doi.org/10.1158/0008-5472.CAN-06-2359
- Lee, H., Cheong, S. M., Han, W., Koo, Y., Jo, S. B., Cho, G. S., Yang, J. S., Kim, S., & Han, J. K. (2018). Head formation requires Dishevelled degradation that is mediated by March2 in concert with Dapper1. *Development (Cambridge, England)*, *145*(7), dev143107. https://doi.org/10.1242/dev.143107
- Lee, H. K., Lee, E. W., Seo, J., Jeong, M., Lee, S. H., Kim, S. Y., Jho, E. H., Choi, C. H., Chung, J. Y., & Song, J. (2018). Ubiquitylation and degradation of adenomatous polyposis coli by MKRN1 enhances Wnt/β-catenin signaling. *Oncogene*, *37*(31), 4273–4286. https://doi.org/10.1038/s41388-018-0267-3
- Lee, H., Seidl, C., Sun, R., Glinka, A., & Niehrs, C. (2020). R-spondins are BMP receptor antagonists in Xenopus early embryonic development. *Nature communications*, *11*(1), 5570. https://doi.org/10.1038/s41467-020-19373-w
- Liu, C., Kato, Y., Zhang, Z., Do, V.M., Yankner, B.A., He, X. (1999). β-Trcp couples β-catenin phosphorylation-degradation and regulates *Xenopus* axis formation. PNAS, 96(11), 6273-6278. https://doi.org/10.1073/pnas.96.11.6273
- Liu, W., Dong, X., Mai, M., Seelan, R. S., Taniguchi, K., Krishnadath, K. K., Halling, K. C., Cunningham, J. M., Boardman, L. A., Qian, C., Christensen, E., Schmidt, S. S., Roche, P. C., Smith, D. I., & Thibodeau, S. N. (2000). Mutations in AXIN2 cause

colorectal cancer with defective mismatch repair by activating beta-catenin/TCF signalling. *Nature genetics*, *26*(2), 146–147. https://doi.org/10.1038/79859

- Liu, C., Li, Y., Semenov, M., Han, C., Baeg, G. H., Tan, Y., Zhang, Z., Lin, X., & He, X. (2002). Control of beta-catenin phosphorylation/degradation by a dual-kinase mechanism. *Cell*, *108*(6), 837–847. https://doi.org/10.1016/s0092-8674(02)00685-2
- Liu, S., Wang, T., Shi, Y., Bai, L., Wang, S., Guo, D., Zhang, Y., Qi, Y., Chen, C., Zhang, J., Zhang, Y., Liu, Q., Yang, Q., Wang, Y., & Liu, H. (2021). USP42 drives nuclear speckle mRNA splicing via directing dynamic phase separation to promote tumorigenesis. *Cell death and differentiation*, *28*(8), 2482–2498. https://doi.org/10.1038/s41418-021-00763-6
- Loregger, A., Grandl, M., Mejías-Luque, R., Allgäuer, M., Degenhart, K., Haselmann, V., Oikonomou, C., Hatzis, P., Janssen, K. P., Nitsche, U., Gradl, D., van den Broek, O., Destree, O., Ulm, K., Neumaier, M., Kalali, B., Jung, A., Varela, I., Schmid, R. M., Rad, R., … Gerhard, M. (2015). The E3 ligase RNF43 inhibits Wnt signaling downstream of mutated β-catenin by sequestering TCF4 to the nuclear membrane. *Science signaling*, *8*(393), ra90. https://doi.org/10.1126/scisignal.aac6757
- Lu, J., Wu, T., Zhang, B. *et al.* Types of nuclear localization signals and mechanisms of protein import into the nucleus. *Cell Commun Signal* **19,** 60 (2021). https://doi.org/10.1186/s12964-021-00741-y
- Ma, P., Yang, X., Kong, Q., Li, C., Yang, S., Li, Y., & Mao, B. (2014). The ubiquitin ligase RNF220 enhances canonical Wnt signaling through USP7-mediated deubiquitination of β-catenin. *Molecular and cellular biology*, *34*(23), 4355–4366. https://doi.org/10.1128/MCB.00731-14
- MacDonald, B. T., Tamai, K. & He, X. Wnt/b-Catenin Signaling: Components, Mechanisms, and Diseases. Dev. Cell 17, 9–26 (2009).
- Madan, B., Walker, M. P., Young, R., Quick, L., Orgel, K. A., Ryan, M., Gupta, P., Henrich, I. C., Ferrer, M., Marine, S., Roberts, B. S., Arthur, W. T., Berndt, J. D., Oliveira, A. M., Moon, R. T., Virshup, D. M., Chou, M. M., & Major, M. B. (2016). USP6 oncogene promotes Wnt signaling by deubiquitylating Frizzleds. *Proceedings of the National Academy of Sciences of the United States of America*, *113*(21), E2945–E2954. https://doi.org/10.1073/pnas.1605691113
- Madison, B. B., Braunstein, K., Kuizon, E., Portman, K., Qiao, X. T., & Gumucio, D. L. (2005). Epithelial hedgehog signals pattern the intestinal crypt-villus axis. *Development (Cambridge, England)*, *132*(2), 279–289. https://doi.org/10.1242/dev.01576
- Mah, A. T., Yan, K. S., & Kuo, C. J. (2016). Wnt pathway regulation of intestinal stem cells. *The Journal of physiology*, *594*(17), 4837–4847. https://doi.org/10.1113/JP271754

- Massink, M.P., Cre ́ ton, M.A., Spanevello, F., Fennis, W.M., Cune, M.S., Savelberg, S.M., Nijman, I.J., Maurice, M.M., van den Boogaard, M.J., and van Haaften, G. (2015). Loss-of-function mutations in the WNT co-receptor LRP6 cause autosomal-dominant oligodontia. Am. J. Hum. Genet. *97*, 621–626
- Matsui, M., Sakasai, R., Abe, M., Kimura, Y., Kajita, S., Torii, W., Katsuki, Y., Ishiai, M., Iwabuchi, K., Takata, M., & Nishi, R. (2020). USP42 enhances homologous recombination repair by promoting R-loop resolution with a DNA-RNA helicase DHX9. *Oncogenesis*, *9*(6), 60. https://doi.org/10.1038/s41389-020-00244-4
- Matsumoto, A., Shimada, Y., Nakano, M., Oyanagi, H., Tajima, Y., Nakano, M., . . . , Wakai, T. (2020). RNF43 mutation is associated with aggressive tumor biology along with BRAF V600E mutation in right- sided colorectal cancer. *Oncology Reports*, *43*, 1853–1862.
- McCarthy, N., Manieri, E., Storm, E. E., Saadatpour, A., Luoma, A. M., Kapoor, V. N., Madha, S., Gaynor, L. T., Cox, C., Keerthivasan, S., Wucherpfennig, K., Yuan, G. C., de Sauvage, F. J., Turley, S. J., & Shivdasani, R. A. (2020). Distinct Mesenchymal Cell Populations Generate the Essential Intestinal BMP Signaling Gradient. *Cell stem cell*, *26*(3), 391–402.e5. https://doi.org/10.1016/j.stem.2020.01.008
- Merenda, A., Andersson-Rolf, A., Mustata, R. C., Li, T., Kim, H., & Koo, B. K. (2017). A Protocol for Multiple Gene Knockout in Mouse Small Intestinal Organoids Using a CRISPR-concatemer. *Journal of visualized experiments : JoVE*, (125), 55916. https://doi.org/10.3791/55916
- Merlos-Suárez, A., Barriga, F. M., Jung, P., Iglesias, M., Céspedes, M. V., Rossell, D., Sevillano, M., Hernando-Momblona, X., da Silva-Diz, V., Muñoz, P., Clevers, H., Sancho, E., Mangues, R., & Batlle, E. (2011). The intestinal stem cell signature identifies colorectal cancer stem cells and predicts disease relapse. *Cell stem cell*, *8*(5), 511–524. https://doi.org/10.1016/j.stem.2011.02.020
- Morin, P. J., Sparks, A. B., Korinek, V., Barker, N., Clevers, H., Vogelstein, B., & Kinzler, K. W. (1997). Activation of beta-catenin-Tcf signaling in colon cancer by mutations in beta-catenin or APC. *Science (New York, N.Y.)*, *275*(5307), 1787–1790. https://doi.org/10.1126/science.275.5307.1787
- Mukai, A., Yamamoto-Hino, M., Awano, W., Watanabe, W., Komada, M., & Goto, S. (2010). Balanced ubiquitylation and deubiquitylation of Frizzled regulate cellular responsiveness to Wg/Wnt. *The EMBO journal*, *29*(13), 2114–2125. https://doi.org/10.1038/emboj.2010.100
- Najdi, R., Proffitt, K., Sprowl, S., Kaur, S., Yu, J., Covey, T. M., Virshup, D. M., & Waterman, M. L. (2012). A uniform human Wnt expression library reveals a shared secretory pathway and unique signaling activities. *Differentiation; research in biological diversity*, *84*(2), 203–213. https://doi.org/10.1016/j.diff.2012.06.004

- Nakielny, S., & Dreyfuss, G. (1999). Transport of proteins and RNAs in and out of the nucleus. *Cell*, *99*(7), 677–690. https://doi.org/10.1016/s0092-8674(00)81666-9
- Nanki, K., Toshimitsu, K., Takano, A., Fujii, M., Shimokawa, M., Ohta, Y., Matano, M., Seino, T., Nishikori, S., Ishikawa, K., Kawasaki, K., Togasaki, K., Takahashi, S., Sukawa, Y., Ishida, H., Sugimoto, S., Kawakubo, H., Kim, J., Kitagawa, Y., Sekine, S., … Sato, T. (2018). Divergent Routes toward Wnt and R-spondin Niche Independency during Human Gastric Carcinogenesis. *Cell*, *174*(4), 856–869.e17. https://doi.org/10.1016/j.cell.2018.07.027
- Neumeyer, V., Grandl, M., Dietl, A., Brutau-Abia, A., Allgäuer, M., Kalali, B., Zhang, Y., Pan, K. F., Steiger, K., Vieth, M., Anton, M., Mejías-Luque, R., & Gerhard, M. (2019). Loss of endogenous RNF43 function enhances proliferation and tumour growth of intestinal and gastric cells. *Carcinogenesis*, *40*(4), 551–559. https://doi.org/10.1093/carcin/bgy152
- Niehrs, C. The complex world of WNT receptor signalling. Nat. Rev. Mol. Cell Biol. 13, 767–79 (2012)
- Nielsen, C. P., Jernigan, K. K., Diggins, N. L., Webb, D. J., & MacGurn, J. A. (2019). USP9X Deubiquitylates DVL2 to Regulate WNT Pathway Specification. *Cell reports*, *28*(4), 1074–1089.e5. https://doi.org/10.1016/j.celrep.2019.06.083
- Niida, A., Hiroko, T., Kasai, M., Furukawa, Y., Nakamura, Y., Suzuki, Y., Sugano, S., & Akiyama, T. (2004). DKK1, a negative regulator of Wnt signaling, is a target of the beta-catenin/TCF pathway. *Oncogene*, *23*(52), 8520–8526. https://doi.org/10.1038/sj.onc.1207892
- Nishisho, I., Nakamura, Y., Miyoshi, Y., Miki, Y., Ando, H., Horii, A., Koyama, K., Utsunomiya, J., Baba, S., & Hedge, P. (1991). Mutations of chromosome 5q21 genes in FAP and colorectal cancer patients. *Science (New York, N.Y.)*, *253*(5020), 665–669. https://doi.org/10.1126/science.1651563
- Niu, J., Yu, G., Wang, X., Xia, W., Wang, Y., Hoi, K. K., Mei, F., Xiao, L., Chan, J. R., & Fancy, S. (2021). Oligodendroglial ring finger protein Rnf43 is an essential injury-specific regulator of oligodendrocyte maturation. *Neuron*, *109*(19), 3104–3118.e6. https://doi.org/10.1016/j.neuron.2021.07.018
- Nomachi, A., Nishita, M., Inaba, D., Enomoto, M., Hamasaki, M., & Minami, Y. (2008). Receptor tyrosine kinase Ror2 mediates Wnt5a-induced polarized cell migration by activating c-Jun N-terminal kinase via actin-binding protein filamin A. *The Journal of biological chemistry*, *283*(41), 27973–27981.
- Nusse, R. & Varmus, H. (1982). Many tumors induced by mouse mammary tumor virus contain a provirus integrated in the same region of the host chromosome. Cell 31, 99– 109.
- Nüsslein-Volhard, C., Wieschaus, E. (1980). Mutations affecting segment number and polarity in *Drosophila*.*Nature* **287,** 795–801. https://doi.org/10.1038/287795a0

- Ozkan, E., Yu, H., & Deisenhofer, J. (2005). Mechanistic insight into the allosteric activation of a ubiquitin-conjugating enzyme by RING-type ubiquitin ligases. *Proceedings of the National Academy of Sciences of the United States of America*, *102*(52), 18890–18895. https://doi.org/10.1073/pnas.0509418102
- Park, S., Cui, J., Yu, W., Wu, L., Carmon, K. S., & Liu, Q. J. (2018). Differential activities and mechanisms of the four R-spondins in potentiating Wnt/β-catenin signaling. *The Journal of biological chemistry*, *293*(25), 9759–9769. https://doi.org/10.1074/jbc.RA118.002743
- Paulsson, K., Békássy, A. N., Olofsson, T., Mitelman, F., Johansson, B., & Panagopoulos, I. (2006). A novel and cytogenetically cryptic t(7;21)(p22;q22) in acute myeloid leukemia results in fusion of RUNX1 with the ubiquitin-specific protease gene USP42. *Leukemia*, *20*(2), 224–229. https://doi.org/10.1038/sj.leu.2404076
- Peng, W. C., de Lau, W., Madoori, P. K., Forneris, F., Granneman, J. C., Clevers, H., & Gros, P. (2013). Structures of Wnt-antagonist ZNRF3 and its complex with R-spondin 1 and implications for signaling. *PloS one*, *8*(12), e83110. https://doi.org/10.1371/journal.pone.0083110
- Perrody, E., Abrami, L., Feldman, M., Kunz, B., Urbé, S., & van der Goot, F. G. (2016). Ubiquitin-dependent folding of the Wnt signaling coreceptor LRP6. *eLife*, *5*, e19083. https://doi.org/10.7554/eLife.19083
- Pickart, C.M.; Eddins, M.J. Ubiquitin: Structures, functions, mechanisms. *Biochim. Biophys. Acta* **2004**, *1695*, 55–72.
- Planas-Paz, L., Orsini, V., Boulter, L., Calabrese, D., Pikiolek, M., Nigsch, F., Xie, Y., Roma, G., Donovan, A., Marti, P., Beckmann, N., Dill, M. T., Carbone, W., Bergling, S., Isken, A., Mueller, M., Kinzel, B., Yang, Y., Mao, X., Nicholson, T. B., … Tchorz, J. S. (2016). The RSPO-LGR4/5-ZNRF3/RNF43 module controls liver zonation and size. *Nature cell biology*, *18*(5), 467–479. https://doi.org/10.1038/ncb3337
- Qin, X., Sufi, J., Vlckova, P., Kyriakidou, P., Acton, S. E., Li, V., Nitz, M., & Tape, C. J. (2020). Cell-type-specific signaling networks in heterocellular organoids. *Nature methods*, *17*(3), 335–342. https://doi.org/10.1038/s41592-020-0737-8
- Qiu, W., Yang, Z., Fan, Y., & Zheng, Q. (2016). ZNRF3 is downregulated in papillary thyroid carcinoma and suppresses the proliferation and invasion of papillary thyroid cancer cells. *Tumour biology : the journal of the International Society for Oncodevelopmental Biology and Medicine*, *37*(9), 12665–12672. https://doi.org/10.1007/s13277-016-5250-4
- Radaszkiewicz, T., & Bryja, V. (2020). Protease associated domain of RNF43 is not necessary for the suppression of Wnt/β-catenin signaling in human cells. *Cell communication and signaling : CCS*, *18*(1), 91. https://doi.org/10.1186/s12964-020-00559-0
- Radaszkiewicz, T., Nosková, M., Gömöryová, K., Vondálová Blanářová, O., Radaszkiewicz, K. A., Picková, M., Víchová, R., Gybeľ, T., Kaiser, K., Demková, L.,

Kučerová, L., Bárta, T., Potěšil, D., Zdráhal, Z., Souček, K., & Bryja, V. (2021). RNF43 inhibits WNT5A-driven signaling and suppresses melanoma invasion and resistance to the targeted therapy. *eLife*, *10*, e65759. https://doi.org/10.7554/eLife.65759

- Abdul Rehman, S. A., Kristariyanto, Y. A., Choi, S. Y., Nkosi, P. J., Weidlich, S., Labib, K., Hofmann, K., & Kulathu, Y. (2016). MINDY-1 Is a Member of an Evolutionarily Conserved and Structurally Distinct New Family of Deubiquitinating Enzymes. *Molecular cell*, *63*(1), 146–155. https://doi.org/10.1016/j.molcel.2016.05.009
- Rokavec, M., Kaller, M., Horst, D., & Hermeking, H. (2017). Pan-cancer EMT-signature identifies RBM47 down-regulation during colorectal cancer progression. *Scientific reports*, *7*(1), 4687. https://doi.org/10.1038/s41598-017-04234-2
- Salem, M. E., Battaglin, F., Goldberg, R. M., Puccini, A., Shields, A. F., Arguello, D., Korn, W. M., Marshall, J. L., Grothey, A., & Lenz, H. J. (2020). Molecular Analyses of Left- and Right-Sided Tumors in Adolescents and Young Adults with Colorectal Cancer. *The oncologist*, *25*(5), 404–413. https://doi.org/10.1634/theoncologist.2019-0552
- Satoh, S. et al. AXIN1 mutations in hepatocellular carcinomas, and growth suppression in cancer cells by virus-mediated transfer of AXIN1. *Nat. Genet.* **24**, 245–250 (2000).
- Scheffner, M., Nuber, U., & Huibregtse, J. M. (1995). Protein ubiquitination involving an E1-E2-E3 enzyme ubiquitin thioester cascade. *Nature*, *373*(6509), 81–83. https://doi.org/10.1038/373081a0
- Schmid, P., Lorenz, A., Hameister, H., Montenarh, M (1991). Expression of p53 during mouse embryogenesis. *Development*, 113 (3): 857–865. doi: https://doi.org/10.1242/dev.113.3.857
- Schneider, C., O'Leary, C.E. & Locksley, R.M. (2019). Regulation of immune responses by tuft cells. *Nat Rev Immunol* **19,** 584–593
- https://doi.org/10.1038/s41577-019-0176-x
- Schnell, J. D., & Hicke, L. (2003). Non-traditional functions of ubiquitin and ubiquitin-binding proteins. *The Journal of biological chemistry*, *278*(38), 35857–35860. https://doi.org/10.1074/jbc.R300018200
- Seshagiri, S., Stawiski, E. W., Durinck, S., Modrusan, Z., Storm, E. E., Conboy, C. B., Chaudhuri, S., Guan, Y., Janakiraman, V., Jaiswal, B. S., Guillory, J., Ha, C., Dijkgraaf, G. J., Stinson, J., Gnad, F., Huntley, M. A., Degenhardt, J. D., Haverty, P. M., Bourgon, R., Wang, W., … de Sauvage, F. J. (2012). Recurrent R-spondin fusions in colon cancer. *Nature*, *488*(7413), 660–664. https://doi.org/10.1038/nature11282
- Sharma, J., Mulherkar, S., Mukherjee, D., & Jana, N. R. (2012). Malin regulates Wnt signaling pathway through degradation of dishevelled2. *The Journal of*

biological chemistry, *287*(9), 6830–6839. https://doi.org/10.1074/jbc.M111.315135

- Sheldahl, L. C., Park, M., Malbon, C. C., & Moon, R. T. (1999). Protein kinase C is differentially stimulated by Wnt and Frizzled homologs in a G-protein-dependent manner. *Current biology : CB*, *9*(13), 695–698. https://doi.org/10.1016/s0960-9822(99)80310-8

- Shi, J., Liu, Y., Xu, X., Zhang, W., Yu, T., Jia, J., & Liu, C. (2015). Deubiquitinase USP47/UBP64E Regulates β-Catenin Ubiquitination and Degradation and Plays a Positive Role in Wnt Signaling. *Molecular and cellular biology*, *35*(19), 3301–3311. https://doi.org/10.1128/MCB.00373-15
- Shyer, A. E., Huycke, T. R., Lee, C., Mahadevan, L., & Tabin, C. J. (2015). Bending gradients: how the intestinal stem cell gets its home. *Cell*, *161*(3), 569–580. https://doi.org/10.1016/j.cell.2015.03.041
- Slusarski, D. C., Yang-Snyder, J., Busa, W. B., & Moon, R. T. (1997). Modulation of embryonic intracellular Ca2+ signaling by Wnt-5A. *Developmental biology*, *182*(1), 114–120. https://doi.org/10.1006/dbio.1996.8463
- Slusarski, D. C., Corces, V. G., & Moon, R. T. (1997). Interaction of Wnt and a Frizzled homologue triggers G-protein-linked phosphatidylinositol signalling. *Nature*, *390*(6658), 410–413. https://doi.org/10.1038/37138
- Spit, M., Koo, B. K., & Maurice, M. M. (2018). Tales from the crypt: intestinal niche signals in tissue renewal, plasticity and cancer. *Open biology*, *8*(9), 180120. https://doi.org/10.1098/rsob.180120
- Spit, M., Fenderico, N., Jordens, I., Radaszkiewicz, T., Lindeboom, R. G., Bugter, J. M., Cristobal, A., Ootes, L., van Osch, M., Janssen, E., Boonekamp, K. E., Hanakova, K., Potesil, D., Zdrahal, Z., Boj, S. F., Medema, J. P., Bryja, V., Koo, B. K., Vermeulen, M., & Maurice, M. M. (2020). RNF43 truncations trap CK1 to drive niche-independent self-renewal in cancer. *The EMBO journal*, *39*(18), e103932. https://doi.org/10.15252/embj.2019103932
- Sprangers, J., Zaalberg, I. C., & Maurice, M. M. (2021). Organoid-based modeling of intestinal development, regeneration, and repair. *Cell death and differentiation*, *28*(1), 95–107. https://doi.org/10.1038/s41418-020-00665-z
- Stanganello, E., & Scholpp, S. (2016). Role of cytonemes in Wnt transport. *Journal of cell science*, *129*(4), 665–672. https://doi.org/10.1242/jcs.182469
- Sun, T., Annunziato, S., Bergling, S., Sheng, C., Orsini, V., Forcella, P., Pikiolek, M., Kancherla, V., Holwerda, S., Imanci, D., Wu, F., Meylan, L. C., Puehringer, L. F., Waldt, A., Oertli, M., Schuierer, S., Terracciano, L. M., Reinker, S., Ruffner, H., Bouwmeester, T., … Tchorz, J. S. (2021). ZNRF3 and RNF43 cooperate to safeguard metabolic liver zonation and hepatocyte proliferation. *Cell stem cell*, *28*(10), 1822–1837.e10. https://doi.org/10.1016/j.stem.2021.05.013

- Szenker-Ravi, E., Altunoglu, U., Leushacke, M., Bosso-Lefèvre, C., Khatoo, M., Thi Tran, H., Naert, T., Noelanders, R., Hajamohideen, A., Beneteau, C., de Sousa, S. B., Karaman, B., Latypova, X., Başaran, S., Yücel, E. B., Tan, T. T., Vlaminck, L., Nayak, S. S., Shukla, A., Girisha, K. M., … Reversade, B. (2018). RSPO2 inhibition of RNF43 and ZNRF3 governs limb development independently of LGR4/5/6. *Nature*, *557*(7706), 564–569. https://doi.org/10.1038/s41586-018-0118-y
- Takada, R., Satomi, Y., Kurata, T., Ueno, N., Norioka, S., Kondoh, H., Takao, T., & Takada, S. (2006). Monounsaturated fatty acid modification of Wnt protein: its role in Wnt secretion. *Developmental cell*, *11*(6), 791–801. https://doi.org/10.1016/j.devcel.2006.10.003
- Tanaka, K., Kitagawa, Y., & Kadowaki, T. (2002). Drosophila segment polarity gene product porcupine stimulates the posttranslational N-glycosylation of wingless in the endoplasmic reticulum. *The Journal of biological chemistry*, *277*(15), 12816–12823. https://doi.org/10.1074/jbc.M200187200
- Takahashi, H., Yamanaka, S., Kuwada, S., Higaki, K., Kido, K., Sato, Y., Fukai, S., Tokunaga, F., & Sawasaki, T. (2020). A Human DUB Protein Array for Clarification of Linkage Specificity of Polyubiquitin Chain and Application to Evaluation of Its Inhibitors. *Biomedicines*, *8*(6), 152. https://doi.org/10.3390/biomedicines8060152
- Tauriello, D. V., Haegebarth, A., Kuper, I., Edelmann, M. J., Henraat, M., Canninga-van Dijk, M. R., Kessler, B. M., Clevers, H., & Maurice, M. M. (2010). Loss of the tumor suppressor CYLD enhances Wnt/beta-catenin signaling through K63-linked ubiquitination of Dvl. *Molecular cell*, *37*(5), 607–619. https://doi.org/10.1016/j.molcel.2010.01.035
- Tian, H., Biehs, B., Chiu, C., Siebel, C. W., Wu, Y., Costa, M., de Sauvage, F. J., & Klein, O. D. (2015). Opposing activities of Notch and Wnt signaling regulate intestinal stem cells and gut homeostasis. *Cell reports*, *11*(1), 33–42. https://doi.org/10.1016/j.celrep.2015.03.007
- Tsukiyama, T., Zou, J., Kim, J., Ogamino, S., Shino, Y., Masuda, T., Merenda, A., Matsumoto, M., Fujioka, Y., Hirose, T., Terai, S., Takahashi, H., Ishitani, T., Nakayama, K. I., Ohba, Y., Koo, B. K., & Hatakeyama, S. (2020). A phospho-switch controls RNF43-mediated degradation of Wnt receptors to suppress tumorigenesis. *Nature communications*, *11*(1), 4586. https://doi.org/10.1038/s41467-020-18257-3
- van der Flier, L. G., & Clevers, H. (2009). Stem cells, self-renewal, and differentiation in the intestinal epithelium. *Annual review of physiology*, *71*, 241–260. https://doi.org/10.1146/annurev.physiol.010908.163145
- van Wijk, S. J., Müller, S., & Dikic, I. (2011). Shared and unique properties of ubiquitin and SUMO interaction networks in DNA repair. *Genes & development*, *25*(17), 1763–1769. https://doi.org/10.1101/gad.17593511

- Voloshanenko, O., Erdmann, G., Dubash, T. D., Augustin, I., Metzig, M., Moffa, G., Hundsrucker, C., Kerr, G., Sandmann, T., Anchang, B., Demir, K., Boehm, C., Leible, S., Ball, C. R., Glimm, H., Spang, R., & Boutros, M. (2013). Wnt secretion is required to maintain high levels of Wnt activity in colon cancer cells. *Nature communications*, *4*, 2610. https://doi.org/10.1038/ncomms3610
- Voloshanenko, O., Gmach, P., Winter, J., Kranz, D., & Boutros, M. (2017). Mapping of Wnt-Frizzled interactions by multiplex CRISPR targeting of receptor gene families. *FASEB journal : official publication of the Federation of American Societies for Experimental Biology*, *31*(11), 4832–4844.
- Wang, K., Yuen, S. T., Xu, J., Lee, S. P., Yan, H. H., Shi, S. T., Siu, H. C., Deng, S., Chu, K. M., Law, S., Chan, K. H., Chan, A. S., Tsui, W. Y., Ho, S. L., Chan, A. K., Man, J. L., Foglizzo, V., Ng, M. K., Chan, A. S., Ching, Y. P., … Leung, S. Y. (2014). Whole-genome sequencing and comprehensive molecular profiling identify new driver mutations in gastric cancer. *Nature genetics*, *46*(6), 573–582. https://doi.org/10.1038/ng.2983
- Wang, G., Fu, Y., Yang, X., Luo, X., Wang, J., Gong, J., & Hu, J. (2016). Brg-1 targeting of novel miR550a-5p/RNF43/Wnt signaling axis regulates colorectal cancer metastasis. *Oncogene*, *35*(5), 651–661. https://doi.org/10.1038/onc.2015.124
- Weeraratna, A. T., Jiang, Y., Hostetter, G., Rosenblatt, K., Duray, P., Bittner, M., & Trent, J. M. (2002). Wnt5a signaling directly affects cell motility and invasion of metastatic melanoma. *Cancer cell*, *1*(3), 279–288. https://doi.org/10.1016/s1535-6108(02)00045-4
- Wei, W., Li, M., Wang, J., Nie, F., & Li, L. (2012). The E3 ubiquitin ligase ITCH negatively regulates canonical Wnt signaling by targeting dishevelled protein. *Molecular and cellular biology*, *32*(19), 3903–3912. https://doi.org/10.1128/MCB.00251-12
- Wenzel, D. M., Lissounov, A., Brzovic, P. S., & Klevit, R. E. (2011). UBCH7 reactivity profile reveals parkin and HHARI to be RING/HECT hybrids. *Nature*, *474*(7349), 105–108. https://doi.org/10.1038/nature09966
- Willert, K., Brown, J.D., Danenberg, E., Duncan, A.W., Weissman, I.L., Reya, T., Yates, J.R., III, and Nusse, R. (2003). Wnt proteins are lipid-modified and can act as stem cell growth factors. Nature *423*, 448–452.
- Winston, J. T., Strack, P., Beer-Romero, P., Chu, C. Y., Elledge, S. J., & Harper, J. W. (1999). The SCFbeta-TRCP-ubiquitin ligase complex associates specifically with phosphorylated destruction motifs in IkappaBalpha and beta-catenin and stimulates IkappaBalpha ubiquitination in vitro. *Genes & development*, *13*(3), 270–283. https://doi.org/10.1101/gad.13.3.270
- Wu, C., Luo, K., Zhao, F., Yin, P., Song, Y., Deng, M., Huang, J., Chen, Y., Li, L., Lee, S., Kim, J., Zhou, Q., Tu, X., Nowsheen, S., Luo, Q., Gao, X., Lou, Z., Liu, Z., & Yuan, J. (2018). USP20 positively regulates tumorigenesis and chemoresistance through

β-catenin stabilization. *Cell death and differentiation*, *25*(10), 1855–1869. https://doi.org/10.1038/s41418-018-0138-z

- Xie, Y., Zamponi, R., Charlat, O., Ramones, M., Swalley, S., Jiang, X., Rivera, D., Tschantz, W., Lu, B., Quinn, L., Dimitri, C., Parker, J., Jeffery, D., Wilcox, S. K., Watrobka, M., LeMotte, P., Granda, B., Porter, J. A., Myer, V. E., Loew, A., … Cong, F. (2013). Interaction with both ZNRF3 and LGR4 is required for the signalling activity of R-spondin. *EMBO reports*, *14*(12), 1120–1126. https://doi.org/10.1038/embor.2013.167
- Yang, B., Zhang, S., Wang, Z., Yang, C., Ouyang, W., Zhou, F., Zhou, Y., & Xie, C. (2016). Deubiquitinase USP9X deubiquitinates β-catenin and promotes high grade glioma cell growth. *Oncotarget*, *7*(48), 79515–79525. https://doi.org/10.18632/oncotarget.12819
- Yun, S. I., Kim, H. H., Yoon, J. H., Park, W. S., Hahn, M. J., Kim, H. C., Chung, C. H., & Kim, K. K. (2015). Ubiquitin specific protease 4 positively regulates the WNT/β-catenin signaling in colorectal cancer. *Molecular oncology*, *9*(9), 1834–1851. https://doi.org/10.1016/j.molonc.2015.06.006
- Zagaria, A., Anelli, L., Coccaro, N., Tota, G., Casieri, P., Cellamare, A., Minervini, A., Minervini, C. F., Brunetti, C., Cumbo, C., Specchia, G., & Albano, F. (2014). 5'RUNX1-3'USP42 chimeric gene in acute myeloid leukemia can occur through an insertion mechanism rather than translocation and may be mediated by genomic segmental duplications. *Molecular cytogenetics*, *7*(1), 66. https://doi.org/10.1186/s13039-014-0066-7
- Zebisch, M., Xu, Y., Krastev, C., MacDonald, B. T., Chen, M., Gilbert, R. J., He, X., & Jones, E. Y. (2013). Structural and molecular basis of ZNRF3/RNF43 transmembrane ubiquitin ligase inhibition by the Wnt agonist R-spondin. *Nature communications*, *4*, 2787. https://doi.org/10.1038/ncomms3787
- Zebisch, M., Jones, E.Y. (2015). ZNRF3/RNF43 – A direct linkage of extracellular recognition and E3 ligase activity to modulate cell surface signalling. Progress in Biophysics and Molecular Biology, 118(3), 112-118. https://doi.org/10.1016/j.pbiomolbio.2015.04.006.
- Zhan, T., Rindtorff, N., & Boutros, M. (2017). Wnt signaling in cancer. *Oncogene*, *36*(11), 1461–1473. https://doi.org/10.1038/onc.2016.304
- Zhang, Y., Liu, S., Mickanin, C., Feng, Y., Charlat, O., Michaud, G. A., Schirle, M., Shi, X., Hild, M., Bauer, A., Myer, V. E., Finan, P. M., Porter, J. A., Huang, S. M., & Cong, F. (2011). RNF146 is a poly(ADP-ribose)-directed E3 ligase that regulates axin degradation and Wnt signalling. *Nature cell biology*, *13*(5), 623–629. https://doi.org/10.1038/ncb2222
- Zhang, Y., Sun, L., Gao, X., Guo, A., Diao, Y., & Zhao, Y. (2019). RNF43 ubiquitinates and degrades phosphorylated E-cadherin by c-Src to facilitate epithelial-mesenchymal transition in lung adenocarcinoma. *BMC cancer*, *19*(1), 670. https://doi.org/10.1186/s12885-019-5880-1

- Zhong, Z., & Virshup, D. M. (2020). Wnt Signaling and Drug Resistance in Cancer. *Molecular pharmacology*, *97*(2), 72–89. https://doi.org/10.1124/mol.119.117978
- Zhou, Y., Lan, J., Wang, W., Shi, Q., Lan, Y., Cheng, Z., & Guan, H. (2013). ZNRF3 acts as a tumour suppressor by the Wnt signalling pathway in human gastric adenocarcinoma. *Journal of molecular histology*, *44*(5), 555–563. https://doi.org/10.1007/s10735-013-9504-9
- Zhou, F., Li, F., Fang, P., Dai, T., Yang, B., van Dam, H., Jia, J., Zheng, M., & Zhang, L. (2016). Ubiquitin-Specific Protease 4 Antagonizes Osteoblast Differentiation Through Dishevelled. *Journal of bone and mineral research : the official journal of the American Society for Bone and Mineral Research*, *31*(10), 1888–1898. https://doi.org/10.1002/jbmr.2863

6. Acknowledgements

First of all, I would like to thank my supervisor Sergio for giving me the opportunity to work on this interesting PhD project. I have appreciated your great supervision and you helping me grow not only in a science-related way, but also personally. Thank you also for nominating Anja and me for the Schmeil Prize, which in the end both of us were awarded with. Then, I would like to thank my Thesis Advisory Committee Prof. Dr. Thomas Holstein, Prof. Dr. Michael Boutros and Junior Professor Dr. Lazaro Centanin for reading my PhD thesis and for sharing your expertise, especially in regards to publishing our manuscript in EMBO Reports.

Of course, I would like to thank all collaborators who worked together with me on publishing our manuscript and completing my PhD Thesis.
1. Anchel: Thank you for joining me on my PhD project. Without your contribution, this project wouldn't have progressed as fast as it did and I wouldn't have had the opportunity to focus on all the exciting organoid experiments.
2. Ana García del Arco for helping to generate the USP42 truncation mutants. Also many thanks to you and Anja B for the fun times we had in the beginning of my PhD and your support during my struggles. I think we did a great job establishing the lab and its traditions.
3. Anchel, Jonathan Landry, Laura Villacorta and Vladimir Benes (Genomics Core Facility, EMBL) for performing the bulk RNAseq analysis.
4. Marlene Tietje and Vanesa Fernández-Sáiz (TUM) for performing the surface biotinylation assays.
5. Nico and Ulrike (Nikon Imaging Center, Heidelberg) for helping me image the organoids.
6. The NCT Heidelberg for performing the stainings and imaging of the tissue microarray.
6. H Bastians, M Boutros, KC Garcia, T Holstein, CY Janda, BK Koo, C Niehrs, MM Maurice, S Özbek, G Pereira and KH Vousden for sharing input and materials with us.

Special thanks go to:

Oksana Voloshanenko (Boutros lab) for generating the HEK293T USP42 KO cell line. Cheng and Bahtiyar (Pereira lab) for helping me to establish the organoid work and USP42 KO cell lines. Minseong and Jessica (Niehrs lab) for input on the regulation of ZNRF3 and the mouse work.

Next, I would like to thank my colleagues and friends for their endless support and for creating a healthy working environment. Apart from work, I really liked our many social events, the small cake and coffee breaks, as well as the social lunches/dinners. Thanks to you guys, I have really enjoyed my time here in the Acebrón lab.

Furthermore, I am grateful for all the support I received from the whole 6th floor of the COS, meaning the Holstein lab, Özbek lab and the Guse lab. Also, I had a very fun time during our social events.

Also, I would like to thank the people from HBIGS for guiding me through my time as a PhD student. By attending this PhD program I have met many interesting new people. And thank you for your patience!

Finally, I would like to thank my mom, who always supported me throughout my time as a PhD student.

♡